Mitigating Oxidative Stress in Childhood Cerebral Adrenoleukodystrophy -An Investigation of N-acetylcysteine Pharmacology

A Dissertation
SUBMITTED TO THE FACULTY OF
UNIVERSITY OF MINNESOTA
BY

Jie Zhou

IN PARTIAL FULFILLMENT OF THE REQUIREMENTS
FOR THE DEGREE OF
DOCTOR OF PHILOSOPHY

James Cloyd, PharmD, Adviser
Henning Schroeder, PhD, Co-advisor

February 2014

Acknowledgements

I would like to thank all the childhood cerebral adrenoleukodystrophy patients who are involved in the studies. Their willingness to participate in the clinical trial will hopefully lead to better outcomes. And I want to thank Dr. S.M. Ghandour (INSERM, France) for the 158N and 158JP cell lines.

I would also like to acknowledge my advisers and committee members for their support, to Dr. James Cloyd, Dr. Henning Schroeder, Dr. Reena Kartha, Dr. Paul Orchard and Dr. William Oetting. They gave me guidance all through the projects and led me through this hard journey.

I would also like to acknowledge my dear colleagues from the Center for Orphan Drug Research (CODR), Dr. Lisa Coles, Usha Mishra, Mary Holmay, and Laurie Hovde; our collaborators from the Bone Marrow Transplantation group, Dr. Troy Lund, Dr. Gerald Raymond, Dr. Weston Miller, Nardina Nash, Lisa Basso, as well as Dr. Deborah Ferrington's group, Dr. Marcia Terluk and Abrar Rageh.

Without support and help from them, I would have never finished these projects. I would also like to acknowledge the department of Experimental Clinical Pharmacology for excellent educations and guidance all through the program, in particular Dr. Richard Brundage.

In addition, I want to acknowledge the funding from University of Minnesota Office of Vice President of Research for the Grant-in-aid award, the Academic Health Center Faculty Development Grant, and the doctoral dissertation fellowship (DDF) provided by Graduate School, University of Minnesota that supported these studies.

Dedication

This thesis is dedicated to my husband and my son, my parents and parents-in-law for their great support for me to study abroad and complete the PhD studies. This thesis is also dedicated to patients with adrenoleukodystrophy and other neurodegenerative disorders with hopes that results from this study can lead to effective therapies.

Abstract

Adrenoleukodystrophy (ALD) is an X-linked genetic disorder which affects the adrenal glands, peripheral neuronal system, the spinal cord and white matter of central nervous system (CNS). It is a progressive neurology disorder with incidence of 1 in 17,000 newborns. ALD is caused by mutations in the *ABCD1* gene, which encodes the peroxisomal membrane transporter for transporting very long chain fatty acids (VLCFAs) into peroxisomes for degradation. As a result, VLCFAs accumulate in the plasma and tissues of ALD patients. Elevated VLCFAs along with *ABCD1* gene mutations are used for the diagnosis of ALD.

ALD has various clinical phenotypes. Childhood cerebral adrenoleukodystrophy (CCALD) is the cerebral form of ALD that affects young boys (4~10 years of age), causing progressive, debilitating effects on the CNS leading to death within a few years.

The pathophysiology of CCALD is only partially understood, but it is known that VLCFAs accumulate in the plasma, brain and other tissues in CCALD patients, which can cause oxidative stress and downstream neurodegeneration. Recently, oxidative stress, the accumulation of free radicals (reactive molecules), has been shown to cause CNS neurodegeneration and play a major role in CCALD pathophysiology.

Currently, the most successful treatment for CCALD is hematopoietic stem cell transplantation (HSCT), which halts disease progression and extends life when CCALD is treated early. But it is much less effective for late-stage CCALD. Based on evidence that oxidative stress plays a role in the disease, the Blood and Marrow transplantation group at University of Minnesota has utilized N-acetylcysteine (NAC) as adjunctive therapy together with HSCT in late-stage CCALD. This combinatorial approach has improved survival rate from 36% to 84% compared to HSCT only in a cohort study (Miller et al., 2011). However, NAC's mechanisms of action are still unclear in CCALD patients.

As an FDA-approved drug, NAC is used as an antidote for acetaminophen overdose and as a mucolytic agent to reduce symptoms associated with cystic fibrosis. It has gained renewed attention as a potential therapy for a number of conditions including pulmonary, neurological, psychiatric, and cardiovascular diseases. With a long history of clinical use, several mechanisms including antioxidative and anti-inflammatory activities have been proposed as the basis for its therapeutic effects. However, the exact molecular mechanism by which NAC improves the survival rate of CCALD patients is still unclear. And this missing piece of information, which is the basis for my research work, is required to further optimize the therapy.

In my thesis, four research projects were designed and implemented to address the pharmacology of NAC in CCALD related biological models. The first study was to

investigate the downstream signaling molecules induced by NAC in the plasma of CCALD patients. Heme oxygenase-1 (HO-1) and ferritin were examined in CCALD patients before and after NAC exposure. Based on the clinical study results that the expression of HO-1 and downstream ferritin were induced by NAC, the second study was further designed in oligodendrocytes, which are CNS glial cells and closely related to demyelination and neurodegeneration, to investigate the cytoprotective role of HO-1 induced by NAC. Moreover, we also tried to delineate the role of accumulation of VLCFAs in CCALD and its relationship with oxidative stress and mitochondria. The third study was designed in oligodendrocytes to investigate whether mitochondria and oxidative stress status are affected by pathophysiological concentrations of VLCFAs and if so, whether NAC could be used to reverse this condition. Finally, the fourth pharmacokinetic/pharmacodynamics study was designed and implemented in wild-type mice to address the relationship between NAC concentration and pharmacodynamic endpoints *in vivo*. This study is also critical to determine the biotransformation of NAC *in vivo*.

The results from my studies indicate HO-1 as the newly discovered downstream mediators for NAC action. Studies also show for the first time that depletion of mitochondrial glutathione (mtGSH) is the pathological cause for CCALD, and that targeting mitochondrial dysfunction can be a potential effective intervention for CCALD patients. In addition, GSH levels, redox ratio, HO-1 and ferritin levels can serve as biomarkers or pharmacodynamic endpoints to evaluate NAC efficacy.

In the long term, characterization of NAC mechanisms of action will help to optimize therapy in CCALD patients. In addition, the information generated from my studies on the efficacy of NAC in CCALD is also applicable to other neurodegenerative disorders sharing similar pathologies such as Gaucher's disease, multiple Sclerosis, Alzheimer's disease etc.

Table of Contents

List of Tables

List of Figures

List of Abbreviations

ALD: Adrenoleukodystrophy

AMN: Adrenomyeloneuropathy

aGVHD: acute graft-versus-host disease

BSO: L-buthionine-(S,R)-sulfoximine

BBB: Blood-brain-barrier

CCALD: Childhood cerebral adrenoleukodystrophy

CrMP: Chromium mesoporphyrin IX chloride

CO: Carbon monoxide

CNS: Central nervous system

FACS: Fluorescence-activated cell sorting

GSH: Glutathione

HO-1: Heme oxygenase-1

HSCT: hematopoietic stem cell transplantation

JP: Jimpy

mtGSH: Mitochondrial glutathione

NAC: N-acetylcysteine

N: Normal

NCA: Non-compartmental analysis

PK: Pharmacokinetic

PD: Pharmacodynamic

ROS: Reactive oxygen species

RNS: Reactive nitrogen species

Redox: Reduction-oxidation

TAC: Total antioxidant capacity

VLCFAs: very long chain fatty acids

WT: wild type

CHAPTER 1

INTRODUCTION

1.1 Neurodegenerative disorders and oxidative stress

Neurodegenerative disorders are a heterogeneous group of diseases characterized by selective loss of neurons and progressive neuronal dysfunction. Prototype examples of neurodegenerative disorders with central nervous system (CNS) dysfunction include Parkinson's disease, Alzheimer's disease, Huntington's disease, multiple sclerosis, Gaucher's disease and Adrenoleukodystrophy (ALD) etc. Despite the heterogeneity in clinical manifestations and genetic origins, this group of neurodegenerative diseases may share common pathological mechanisms, resulting in neuronal cell death. Accumulations of insoluble biomolecules such as misfolded proteins or very long chain fatty acids (VLCFAs), mitochondria dysfunction and oxidative stress, as well as neuroinflammation (Lin and Beal, 2006, Skovronsky et al., 2006, Frank-Cannon et al., 2009) were demonstrated over the past few years as the common motifs in neurodegenerative disorders. Among all others, oxidative stress was thought to be the early event during the neurodegenerative process (Frank-Cannon et al., 2009). The relationship between neurodegeneration and oxidative stress, as well as antioxidant therapeutic strategies will be discussed in this section.

1.1.1 Neurodegenerative disorder: epidemiology, pathology and current treatment options

Epidemiology and influence

Neurodegenerative disorders account for a significant proportion of morbidity and mortality of U.S. populations, e.g. the average incidence of Parkinson's disease was estimated as 13.4 per 100,000 per year (Van Den Eeden et al., 2003), and it is expected 1 out 45 Americans will be affected by Alzheimer's Disease by 2040 (Reitz and Mayeux, 2010). Moreover, these disorders cost the U.S. country billions of dollars a year, e.g. an estimate of over $100 billion per year is attributed to the direct cost on Alzheimer's disease alone (Meek et al., 1998). In addition, there is tremendous physical and emotional burden on the society. Thus an investigation for efficient therapies to treat neurodegenerative disorder is quite necessary. Given that neurodegenerative disorders share the common characteristic of progressive loss of functional neuron cells, investigating mechanisms causing neuronal cell death is critical to provide valuable insights for therapeutics discovery and development. In this thesis, I will focus on deciphering the toxicological mechanisms in ALD resulting in cell death and examining the efficacy of potential antioxidants. This piece of information hopefully can be applied to other neurodegenerative disorders with similar pathologies.

Pathology

Two major known risk factors associated with neurodegenerative disorders are genetic polymorphisms and environmental factors. Genetic mutations are identified in certain patient populations, e.g. Gaucher's disease is caused by mutations in the glucocerebrosidase gene that encodes the critical lysosomal enzyme for degradation of glucocerebroside (Bennett and Mohan, 2013); and mutations in amyloid precursor protein

are closely related to familial forms of Alzheimer's disease (Maltsev et al., 2013). Many of the neurodegenerative diseases are rare and caused by genetic mutations. However, environmental factors such as aging and oxidative stress are also crucial in neurodegenerative disease progression. In addition, other possible environmental factors include gender, social factors, psychological factors, inflammation, infection, tumors, chemical exposure, endocrine levels or physiological conditions. These environmental factors could influence the time for disease onset, severity of the disease and speed of disease progression. Environmental factors have been demonstrated to play an important role in neurodegenerative disorders (Brown et al., 2005). It is quite possible that both environmental and genetic risk factors synergistically accelerate the neurodegeneration process (Peng et al., 2010).

Treatment challenges

Many neurodegenerative diseases are associated with dysfunction in CNS. Although it seems necessary to deliver drugs into the brain, challenges of drug delivery arise due to blood-brain-barrier (BBB). BBB is a tightly regulated barrier across the CNS. It is composed of a layer of endothelial cells with tight junctions surrounding by astrocytes. Only necessary nutrients come across the brain, through passive diffusion in the case of non-polar small molecule, or through selective transporters. For example, glucose is transported through the BBB via GLUT family transporters (Pardridge et al., 1990). However, the tight junctions of BBB prevent the penetration of most hydrophilic drug

molecules. In addition, BBB is equipped with active transporters such as P-glycoprotein (PgP), acting in the reverse direction to export selective molecules. Optimal drug molecules (or its active metabolites) for neurodegenerative disorders are expected to have the potential to come across the BBB and elicit its efficacy at the site of brain. And, reports have shown that the structure of BBB is still intact in neurodegenerative disorders such as Parkinson's and Alzheimer's disorders (Desai et al., 2007). In such scenarios, the efficacy of the drug molecule is directly linked to the active metabolite concentration in the brain rather than in the plasma. Pharamcokinetic/ pharmacodynamic (PK/PD) modeling, a mathematical model describing the relationship between plasma concentrations and efficacy in the brain, could greatly facilitate the understanding of drug mechanisms.

Another major challenge is the unclear disease pathology, as well as lack of reliable evaluation parameters for neurodegenerative diseases. Clinical performance including various scales of disease evaluation is the golden standard for clinical trial evaluation. However, these scales are within a limited range and usually insensitive to the modest changes in early phase of disease progression (Stocchi and Olanow, 2013). Therefore, simple, inexpensive, reliable, rapidly obtainable, well-defined biomarkers are necessary to facilitate diagnosis, prognosis, therapy, disease monitoring and drug development (Feigin, 2004). In addition, the US Food and Drug Administration (FDA) could possibly accept biomarkers as clinical endpoints in drug application as long as the biomarkers are "reasonably likely, based on epidemiologic, therapeutic, pathophysiologic, or other

evidence, to predict clinical benefit" (Biomarkers-Definitions-Working-Group, 2001). Based on these promising applications of biomarkers, a lot of efforts have been made to achieve reliable biomarkers to evaluate the efficacy of drug candidates and disease progression. For example, the project of "Parkinson's Progression Markers Initiative (PPMI)" is in progress to identify biomarkers related to Parkinson's disease (PPMI, 2011). Other biomarkers related to ALD have also been reported for drug monitoring and treatment of disease (Orchard et al., 2011). GSH level is also reported to be a valuable biomarker for NAC efficacy in Parkinson's and Gaucher's patients (Holmay et al., 2013). Validated biomarkers, of which the change can be detected early and parallel to disease progression, are quite important in finding new treatments to neurodegenerative disorders.

1.1.2 Oxidative stress in neurodegenerative disorder

Free radicals related to oxidative stress

Oxidative stress arises from imbalanced reduction-oxidation (redox) regulation in biological systems. Oxidative stress involves free radicals such as reactive oxygen species (ROS) and reactive nitrogen species (RNS). 95% of ROS is produced through the mitochondrial respiratory chain as byproducts of O_2 consumption and ATP generation (Emerit et al., 2004). ROS species mainly include super oxide anion (O^{2-}) and H_2O_2, and RNS species originate from the gaseous messenger nitric oxide (NO). NO reacts rapidly

with O^{2-} to form peroxynitrite ($ONOO^-$), which is a highly reactive oxidant. ROS and RNS are produced in large amounts in disease conditions and are thought to be highly related to neuronal cell death in neurodegenerative diseases (Calabrese et al., 2005).

Endogenous antioxidants in brain

The brain utilizes an antioxidant system to defend against oxidative stress as well as possible related detrimental effects. This complicated self-defense system includes enzymes such as superoxide dismutases, glutathione peroxidase, glutathione reductase, glutathione S-transferase, catalase and peroxiredoxins; small molecule antioxidants such as GSH, cysteine, ascorbate, α-tocopherol and ubiquinol; or metal-binding related protective proteins such as metallothionein, heme oxygenase-1 and ferritin (Halliwell, 2001). Levels of these endogenous antioxidants are closely modulated in biological systems to neutralize oxidative stress.

A scheme for oxidative stress

The balance between endogenous free radicals and antioxidants determines the redox status in biological systems (Figure 1-1). In normal conditions where the balance is well kept, minimal oxidative stress related damage is caused; while in disease conditions where the balance is tipped towards free radicals, increased oxidative stress related damage is observed which could further lead to disease progression. Normally the biological system can balance the production of free radicals and levels of endogenous

antioxidants to maintain redox equilibrium. However, under disease conditions when the biological system is unable to adjust the production of free radicals and endogenous antioxidants appropriately, oxidative stress can be caused by either increased free radicals or decreased endogenous antioxidants.

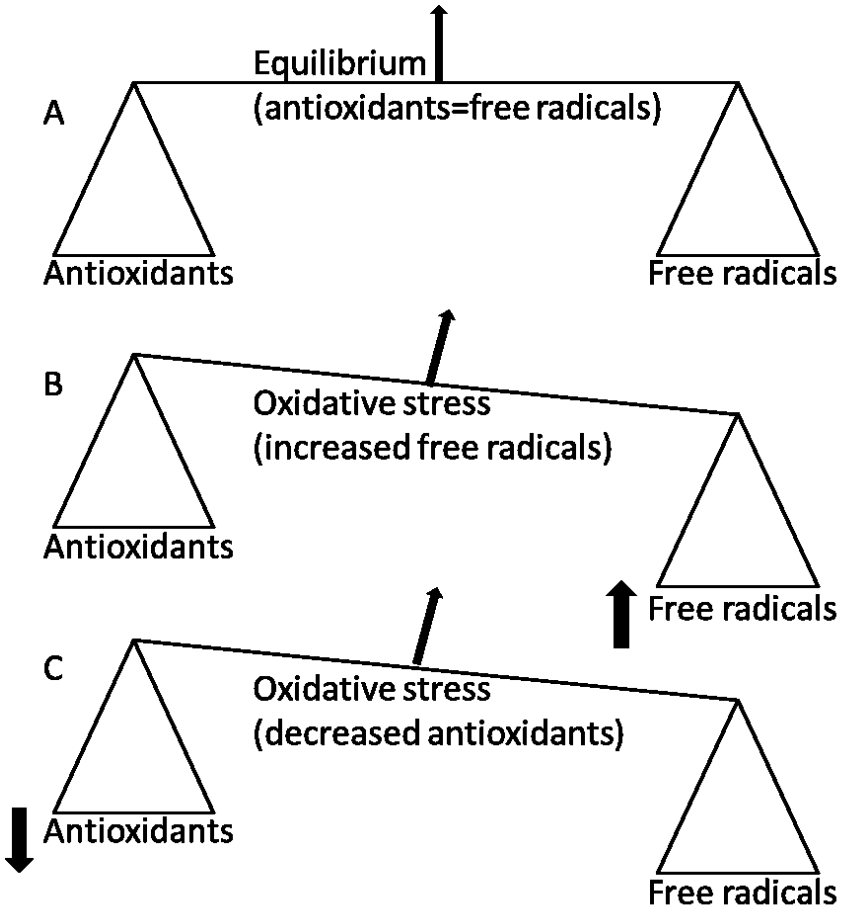

Figure 1-1 *Oxidative stress is caused by either increased free radicals or decreased antioxidants (adapted from (Scandalios, 2005)).*

Damage caused by oxidative stress and related biomarkers

Oxidative stress could damage macromolecules and cause detrimental effects on the cells. Free radicals can lead to elevated lipid peroxidation, DNA oxidation and protein nitration (Shukla et al., 2011a). Accordingly, several biomarkers for evaluation of oxidative stress were reported and validated *in vitro* and *in vivo*, including lipid peroxidation biomarkers of 4-hydroxynonenal and malondialdehyde, protein oxidation and nitration biomarkers of protein carbonyl groups and 3-nitrotyrosine, carbohydrates oxidation biomarkers of advanced glycation end products (AGE) and Receptor for AGE (RAGE), DNA/RNA oxidation biomarkers of 8-hydroxyguanosine and 8-hydroxy-2'deoxyguanosine (Sultana et al., 2013), depletion of GSH levels indicating decreased endogenous antioxidants (Petrillo et al., 2013b). These biomarkers and more others under investigation are useful to monitor oxidative stress and evaluate drug efficacy in neurodegenerative disease.

In addition, oxidative stress is closely related to programmed cell death, which is referred to as “apoptosis”. Apoptosis is a main reason for the neuronal cell death in neurodegenerative disorders, the intrinsic pathway of which is also closely related to oxidative stress. Elevated oxidative stress activates the mitochondrial permeability transition pore (mtPTP) and results in collapse of mitochondrial inner membrane potential and mitochondrial dysfunction. ATP production is reduced and apoptogenic mitochondrial mediators are released including “cytochrome c, procapases 2, 3, and 9, apoptosis-initiating factor, and caspase activated DNase” etc. (Emerit et al., 2004). The

cell subsequently undergoes apoptosis pathway. Mitochondria induced apoptosis, or the intrinsic pathway as opposed to extrinsic pathways (Elmore, 2007), accounts for the most common cause of cell death in neurodegenerative disorders.

The brain is more highly metabolic active but with much less cell regeneration, compared to other organs. Therefore brain is believed to be more sensitive to oxidative stress (Andersen, 2004). In addition, oxidative stress biomarkers were reported to increase within the same region of brain undergoing selective neurodegeneration. For example, lipid oxidation biomarkers have been reported to increase in the cortex and hippocampus of Alzheimer's patients and the substantia nigra of Parkinson's patients, co-localizing with neurodegenerative regions (Dexter et al., 1989, Butterfield et al., 2002). Dysregulation of GSH homeostasis in brain is also reported in a number of neurodegenerative diseases including multiple sclerosis (Choi et al., 2011a), Parkinson's disease (Sian et al., 1994), Alzheimer's disease (Lovell et al., 1998), Huntington's disease, amyotrophic lateral sclerosis, and Friedreich's ataxia (Johnson et al., 2012). Interestingly, 40% reduction in GSH levels were found in substantia nigra region of brains from Parkinson's patients compared to age-matched controls (Sian et al., 1994). In particular, the depletion of GSH was found to parallel the severity of Parkinson's disease (Riederer et al., 1989). Results from these studies showed that oxidative stress paralleled the progression of neurodegeneration. Co-localization of oxidative stress markers and neuronal cell death might also indicate the cause and effect relationship between oxidative stress and neuronal cell death.

Cause and effect relationship between oxidative stress and neurodegeneration

Despite evidence of close relationships between oxidative stress and neurodegeneration, whether oxidative stress is the cause or consequence of neurodegeneration is still under investigation. Also, the relationship between oxidative stress and other pathologic process such as inflammation is unclear. These unanswered questions are the key to decipher the mechanism of neuronal cell death and neurodegeneration. A wide range of studies in recent literatures focused on investigation of the close relationship between oxidative stress and neurodegeneration. E.g., oxidative stress biomarkers were reported to be one of the earliest detectable biochemical changes in Parkinson's patients, even earlier than markers for dopamine loss or dopaminergic neurodegeneration (Riederer et al., 1989). Chinta *et al.* showed that depletion of GSH within the substantia nigra region resulted in nigrostriatal neurodegeneration in mice, providing *in-vivo* evidence of a causal relationship between oxidative stress and Parkinson's disease (Chinta et al., 2007). Based on these proofs, Singh *et al*. proposed a three-hit hypothesis for ALD, assuming oxidative stress as the first hit which causes subsequent inflammation, leading to loss of cell function and cell death as well as disease progression (Singh and Pujol, 2010). Similarly, Zhu *et al.* proposed a two-hit hypothesis where oxidative stress plays an important role in the early progression of Alzheimer's disease (Zhu et al., 2007). An improved understanding of the relationship between oxidative stress and neurodegenerative

disorder may provide possible efficient therapies towards the treatment of other types of neurodegenerative disorders.

1.1.3 Antioxidant therapy in neurodegenerative diseases

Recently it was found that endogenous antioxidants were depleted under conditions of neurodegeneration and that oxidative stress contributes to the progression of neurodegeneration (Fourcade et al., 2008, Matsuzawa et al., 2008). Supplementing exogenous antioxidants seems to be a reasonable therapy to mitigate oxidative stress and improve the redox status. Antioxidant therapy in neurodegeneration is being vigorously investigated, including antioxidants of superoxide dismutase, NAC, GSH, α-tocopherol and Coenzyme Q_{10} (Table 1-1).

Study	Drug tested	Subjects studied □	Results
(Wengenack et al., 1997)	Superoxide dismutase	Rat with global cerebral ischemia and neurodegeneration	Decreased hippocampal CA1 neuron loss
(Holmay et al., 2013)	N-acetylcysteine	Parkinson's, Gaucher's patients and healthy volunteers	Increased brain GSH levels
(Adair et al., 2001)	N-acetylcysteine	Probable Alzheimer's patients clinical trial	No significant changes on most cognitive evaluations but a trend for NAC superiority is observed
(Sechi et al., 1996)	Glutathione	Parkinson's patients clinical trial	Improvement in neurological symptoms
(Sano et al., 1997)	α-tocopherol	Alzheimer's patients clinical trial	α-tocopherol and selegiline synergistically improve neurological symptoms
(Parkinson-study-group, 1993)	α-tocopherol	Parkinson's patients clinical trial	Ineffective in preventing the progression of disease in early stage
(Shults et al., 1998)	Coenzyme Q_{10}	Parkinson's patients clinical trial	CoQ_{10} did not change the disease rating scale but improve complex I activity

Table 1-1 *Selected studies of antioxidant therapy in neurodegeneration*

Exogenous antioxidants as therapy for neurodegeneration can be classified into two major groups, enzymatic and non-enzymatic molecules. Enzymatic molecules include superoxide dismutase, catalase and glutathione peroxidase and their mimetics etc. Non-enzymatic antioxidants include direct free radical scavenging molecules such as tocopherols, GSH, and indirect acting molecules that reduce cellular metal concentrations, increase endogenous antioxidants and target to relieve metabolic burden on cellular organelles, e.g., mitochondria such as ion chelators, NAC and Coenzyme Q_{10}.

In one open label study in early-stage, asymptomatic Parkinson's patients, 600mg twice daily GSH was administered intravenously in 9 patients for 30 days. Results indicated that patients improved significantly after treatment compared to baseline and washout periods (Sechi et al., 1996). However, the idea of direct GSH dosing requires careful examination since whether reduced GSH can be transported across the BBB is still controversial and under investigation (Cornford et al., 1978, Kannan et al., 1990, Kannan et al., 2000). According to these reports, very limited GSH is transported across the BBB.

In addition, other antioxidants are also widely investigated in neurodegenerative diseases. α-tocopherol (Vitamin E) was shown to be as good as selegiline in a large scale controlled trial to slow the progression of Alzheimer's disease. In addition, a treatment group with both α-tocopherol and selegiline showed synergistic effects (Sano et al., 1997). However, in one large-scale randomized control trial, tocopherol was shown to be ineffective in preventing the progression in early Parkinson's patients (Parkinson-study-

group, 1993). Despite several successful clinical trials and encouraging cell and animal studies, antioxidant therapy was shown to have varying degree of success (Table 1-1). The inconclusive results suggest a better understanding of the roles for antioxidants in neurodegenerative disorders is required. And rationale dosing regimens and study designs are also crucial elements of a successful clinical trial.

1.2 Adrenoleukodystrophy

1.2.1 Definition, cause, clinical manifestation, pathology and current treatment options

ALD is an X-linked genetic disorder which affects the adrenal glands, peripheral neuronal system, the spinal cord and white matter of the CNS. It is a progressive neurology disorder with incidence of 1 in 17,000 newborns. ALD has been shown to be caused by mutations in the *ABCD*1 gene, which encodes a member of the ATP binding cassette transporter protein family, and believed to function as a peroxisomal membrane transporter of very long chain fatty acid (VLCFA) (Kemp et al., 2012). Degradation of VLCFAs requires them to be transported into peroxisomes to facilitate β-oxidation. Mutations in ABCD1 transporter impair regular degradation of VLCFAs and cause intracellular accumulation (Figure 1-2). Igarashi *et al.* reported observation of increased levels of VLCFAs such as hexacosanoic acid (C:26:0) in the brain and adrenal tissues of ALD patients (Igarashi et al., 1976).

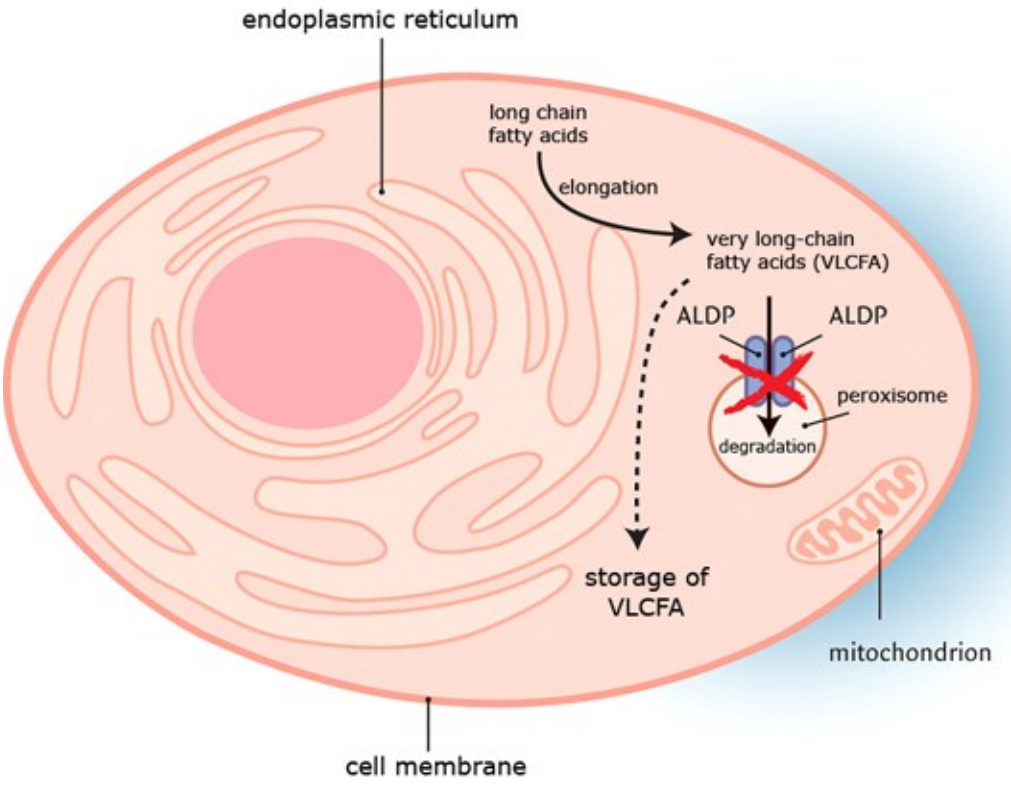

Figure 1-2 Mutations in ABCD1 gene cause adrenoleukodystrophy. Mutations in ABCD1 gene cause dysfunctional adrenoleukodystrophy protein (ALDP), and impair the transport of VLCFAs into peroxisomes which consequently prevents the degradation of VLCFAs. As a result, intracellular VLCFAs accumulate and cause detrimental effects. VLCFAs mainly come from the elongation reactions which take place at the endoplasmic reticulum, catalyzing the elongation of very long-chain fatty acids enzymes (ELOVL). (Figure adapted from: (Engelen et al., 2008))

1.2.2 Diagnosis, clinical phenotypes and disease progression stages

ALD is an X-linked genetic disorder which affects males, while females may be carriers of the mutated gene. ALD has several different clinical phenotypes. The two major forms are childhood cerebral ALD (CCALD), usually affecting boys 4-10 years of age, and adrenomyeloneuropathy (AMN) typically affecting patients in early adulthood. Approximately 35-40% of the total patient population develops CCALD, which is the most severe phenotype. CCALD is characterized by impairment of CNS, generally rapidly progressive development and primarily affecting pediatric patient population. Death typically occurs within 2-4 years of symptoms onset in CCALD without interventions (Berger et al., 2013).

Diagnostic tools for general ALD include genetic and biochemistry assays. *ABCD1* gene mutation analysis is useful in ALD diagnosis. However, more than 1400 different mutations have been identified in *ABCD1* so far (Kemp et al., 2001) and almost 50% of all mutations are non-recurrent, meaning they are specific to certain individual patient. And no clear correlations between a specific genetic mutation and clinical phenotypes/disease stages have been discovered. The characteristic biochemistry assay for ALD is the measurement of VLCFAs levels. VCLFAs levels are represented by C26:0 concentration, the ratio of C24:0/C22:0, and the ratio of C26:0/C22:0 in plasma, all of which are highly specific and sensitive. 99.9% of ALD patients were found to have elevated VLCFAs compared to control group (Valianpour et al., 2003). This test can also identify female carriers whose levels typically fall between control and ALD males. Interestingly, plasma levels of VLCFAs do not correlate with forms of disease or stages

of disease progression (Ofman et al., 2010) while concentrations of VLCFAs in white matter of brain tissues (myelin sheath) correlate with severity of ALD phenotypes (Asheuer et al., 2005).

Diagnosis and disease monitoring are quite important in the treatment of ALD, especially for the most severe form CCALD, in order to implement effective treatments. Often it is quite difficult to diagnose CCALD in the early stage, except those with known genetic family history. Patients are usually asymptomatic before 4 years old, and presentation of mild behavior symptoms occurs around 4 to 8 years old, usually followed by aggressively rapid CNS dysfunction, total disability and death within 2 years of time. Those early symptoms of learning and behavioral deficits are often mistaken as attention deficit disorder or hyperactivity until ALD specialists get involved. The diagnosis of CCALD usually takes long time. And patients may already come to the late stage.

Brain Magnetic Resonance Imaging (MRI) provides the first diagnostic lead in detecting the cerebral neurological symptoms in CCALD patients. MRI patterns in CCALD patients could facilitate the prediction of disease progression or selection of treatment strategies (Loes et al., 2003). The Loes score (0-34), a point rating system developed based on MRI severity, was established to help better define the ALD disease in conjunction with other clinical parameters (Loes et al., 1994). Males with ALD were suggested to undergo MRI every 6 months during childhood and yearly for adulthood to watch for cerebral manifestation. (Peters et al., 2004)

1.2.3 The role of oxidative stress in ALD

Although the pathology of ALD is only partially understood, accumulation of intracellular VLCFA, along with other environmental factors such as oxidative stress and inflammation, is thought to trigger subsequent neuronal cell death, demyelination and neurodegeneration (Powers et al., 2005, Galea et al., 2012).

Both an increase in free radicals and a decrease in endogenous antioxidants can lead to oxidative stress. Evidence of oxidative stress as a hallmark of ALD has been shown in recent studies. Vargas *et al.* evaluated oxidative stress biomarkers in plasma, erythrocytes and fibroblasts from ALD patients. Results showed that biomarkers of free radicals and lipid peroxidation were elevated in ALD patients compared to control, while total antioxidant capacity was decreased suggesting deficient capacity to rapidly handle oxidative stress (Vargas et al., 2004). Petrillo *et al.* observed decreased total and reduced GSH in lymphocytes of ALD patients as well as high levels of oxidized GSH forms (Petrillo et al., 2013b). Various clinical phenotypes of ALD including adult form of AMN, CCALD and heterogeneous female carriers were also examined in detail (Deon et al., 2007, Deon et al., 2008). In these studies, plasma levels of oxidative stress markers from both symptomatic and asymptomatic patients showed significant increase in lipid peroxidation, indicating oxidative stress as a hallmark for ALD disease. In addition, levels of total antioxidants were decreased in symptomatic patients while asymptomatic

patients stayed unchanged compared to control. From these studies, Deon *et al.* showed that the depletion of antioxidants exposed patients/carriers with ALD gene mutations with increased free radicals. However, asymptomatic patients/carriers do not present clinical symptoms with sufficient antioxidants while patients with depletion of antioxidants fail to defend against increased free radicals.

Studies in ALD mouse models (*Abcd1* knockout mice) provided another proof for the involvement of oxidative stress in pathogenesis of ALD. Increased ROS formation and elevation of other oxidative stress markers were observed in early phase of disease progression before manifestation of axonal degeneration in *Abcd1* knockout mice (Fourcade et al., 2008). In addition, the same group showed that a combination of antioxidants containing α-tocopherol, NAC and α-lipoic acid reversed oxidative damage and axonal degeneration in *Abcd1* knockout mice (Lopez-Erauskin et al., 2011a). Results indicated that oxidative stress was not only a hallmark of ALD but also the leading cause for disease progression.

1.2.4 Treatment options and hematopoietic stem cell transplantation (HSCT)

Treatment options for ALD are fairly limited. Adrenal steroid replacement therapy could account for the dysfunctional adrenal glands but has no effect on neurology system or disease progression (Moser, 2006). The use of Lorenzo's oil as well as dietary restriction could efficiently lower the plasma levels of VLCFAs back to normal levels by week 10

of clinical trial (Aubourg et al., 1993). And Lorenzo's oil was shown to reduce the risk to develop MRI abnormities which was correlated to reduced VLCFAs levels in 89 asymptomatic patients (Moser et al., 2005b). However, no detectable clinical changes were observed in AMN patients following a mean interval of 33 months (Aubourg et al., 1993). In addition, Lorenzo's oil was found to have no effect on MRI progression in c-ALD with CNS manifestation (Duchesne et al., 1995). These inconsistent reported results might be due to the fact that most of them are single-armed studies without well-controlled group. In addition, gene therapy was also investigated for ALD, with promising preliminary results in small group of patients (Cartier and Aubourg, 2010, Cartier et al., 2010, Biffi et al., 2011).

Hematopoietic stem cell transplantation (HSCT) has been demonstrated to be the most successful therapy for CCALD, which was shown to halt disease progression in multiple clinical trials and displayed consistent efficacy during the early stage of ALD (Peters et al., 2004). However, survival rates for patients receiving HSCT highly depend on the neurologic clinical stages at the time of the procedure. 5-year survival for patients receiving HSCT during late stage CCALD, defined as MRI severity score (Loes score from MRI images) more than 9 and with more than one neurological deficit, was reported to be 45%, while the survival rate was 92% for early stage patients (Peters et al., 2004). The prognosis is poor for late-stage CCALD due to extensive demyelination in the brain white matters.

The low survival rate of performing HSCT in advanced CCALD patients prompted the Blood and Marrow Transplantation Group at University of Minnesota to add NAC adjuvant therapy to HSCT. Late-stage CCALD patients were given large doses of intravenous NAC infusion (70 mg/kg infusion over 1 hour every 6 hours), beginning after the administration of chemotherapy through 100 days post-transplantation. Significantly greater survival rate was observed in the NAC treatment group (84%) compared to untreated group (36%). Although historical controls were used in the comparison, the results were quite encouraging and suggesting the beneficial effects of antioxidants in HSCT for late-stage CCALD (Tolar et al., 2007, Miller et al., 2011). Although NAC adjuvant therapy appears to increase survival, the mechanism of action for NAC is not clear, and the rationale for NAC dosing (70mg/kg every 6 hours for over approximately 100 days) is not clear either.

Although HSCT procedures and NAC adjuvant therapy increase the survival rates in CCALD patients, the symptoms of neurodegeneration in CNS are not improved in these patients (Miller et al., 2011).

1.3 N-acetylcysteine

1.3.1 History and status, indications and therapeutic applications

NAC is a thiol-containing antioxidant, available both as FDA-approved products and dietary supplements. NAC is indicated as an inhaled agent for mucolysis in cystic fibrosis

(Mucomyst®) and intravenously as an antidote for acetaminophen overdose (Acetadote®) (Heard and Green, 2012b, Rushworth and Megson, 2013a). Recently, NAC has gained renewed attention as a potential therapy for a number of conditions including pulmonary (Sadowska et al., 2006), neurological (Adair et al., 2001, Berman et al., 2011), psychiatric (Dean et al., 2011a), and cardiovascular (Marian et al., 2006, Mahmoud and Ammar, 2011), metabolic deficiency (Atkuri et al., 2007) disorders and diseases. Although NAC has a long history of clinical use, its biotransformation and distribution as well as mechanisms of action are not fully understood.

1.3.2 Physical-chemical properties

NAC is a derivative of the naturally occurring amino acid L-cysteine, with an acetyl group attached to its nitrogen atom. The chemical formula of NAC is $C_5H_9NO_3S$, with a molecular weight of 163.2 g/mol. NAC is a white crystalline powder, with melting point around 104° ~110°C (Package insert for Acetadote, 2004). Its structure is shown in Figure 1-3.

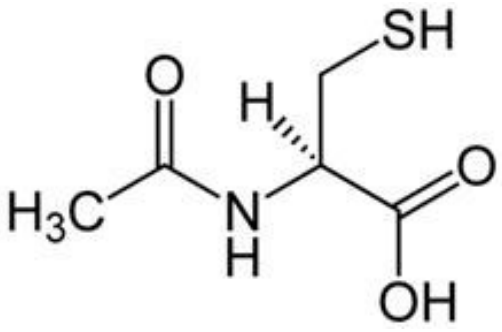

Figure 1-3 Chemical structure of NAC

Acetadote®, the sterile NAC solution, contains 20% w/v (200 mg/mL) NAC. The pH of the solution is around 6.0~7.5. This condensed solution is diluted in compatible diluents before use. It also has a slight unpleasant odor.

1.3.3 Pharmacokinetics

Absorption and disposition

The bioavailability of oral NAC is reported to be low (~4-10%) in healthy adults (Borgstrom et al., 1986, Olsson et al., 1988). Interestingly, a meta-analysis found little difference in outcomes between oral and intravenous formulation of NAC in treating acetaminophen overdose (Buckley et al., 1999). This is probably because NAC or its metabolite cysteine during the first-pass metabolism can both be converted to GSH. Volume of distribution at steady state in healthy volunteers was reported as 0.47 L/Kg. The protein binding for NAC was reported to be 83% (Package insert for Acetadote, 2004). The distribution of oral NAC into peripheral tissues such as liver, kidney, skin, thymus, spleen, eye, and serum is fairly quick and within 1 hour in rats (Arfsten et al., 2007). Clinical pharmacokinetic information of NAC transportation into the Blood-Brain-Barrier (BBB) or placenta is not adequate, although there is evidence of NAC crossing the BBB in animal studies (Neuwelt et al., 2001, Farr et al., 2003). The transportation of NAC across BBB requires more investigation. Moreover, NAC was found to increasingly enter into the brain following inflammation in the brain induced by LPS (Erickson et al.,

2012). In addition, placental transfer of NAC in 4 pregnant women following treatment of acetaminophen overdose was also observed (Horowitz et al., 1997).

Metabolism and biotransformation

NAC forms cysteine, disulfides and conjugates with other thiols *in vivo*. Reported forms include N, N'-diacetylcysteine, N-acetylcysteine-cysteine, N-acetylcysteine-glutathione, N-acetylcysteine-protein etc. (Package insert for Acetadote, 2004).

NAC, cysteine, and GSH are present *in vivo* in both the reduced (active) and oxidized (inactive) forms. The fate of NAC in the body follows several different pathways. The first one is the formation of cysteine via acyclase enzyme directly (Dringen and Hamprecht, 1999). Once deacetylated, cysteine, the rate-limiting substrate is available for cellular GSH synthesis. GSH may then be actively transported out of the cell where it is metabolized by a transpeptidase in extracellular fluid. However, cysteine is rapidly oxidized in plasma and extracellular fluid to cystine (oxidized form of cysteine) among other disulfide compounds. There are also other pathways that NAC exchanges thiol with cystine and releases free reduced form cysteine for GSH synthesis, or that NAC directly exchanges thiol with oxidized form of GSH and releases reduced GSH.

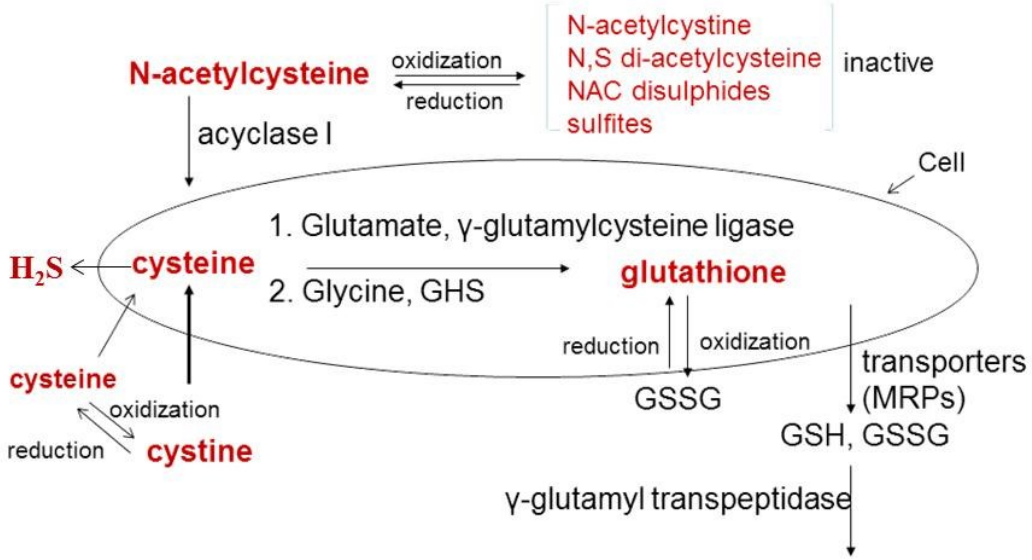

Figure 1-4 Biotransformation of NAC. The formation of cysteine, GSH and H_2S from NAC and transportation into cells are shown. (Figure adapted with the permission of Coles L.)

NAC is also a plausible precursor for hydrogen sulfide (H_2S) (Kartha et al., 2012). The two enzymes Cystathionine β-synthase (CBS) and cystathionine γ-lyase (CSE) are responsible for H_2S synthesis from cysteine. H_2S is a gasotransmitter similar to Nitric oxide (NO) and Carbon monoxide (CO). Recently, H_2S has been widely studied in various disease conditions and has been found to elicit neuroprotective signaling pathways (Hu et al., 2011). H_2S is further metabolized to thiosulfate which is more stable and easier to detect (Hildebrandt and Grieshaber, 2008).

Elimination

Published NAC pharmacokinetic studies report widely varied results which appear dependent on the method of analysis (Olsson et al., 1988). Borgstromet al. reported an elimination half-life of 2.27 h after IV administration in healthy adult volunteers, whereas others have observed a mean half-life of approximately 6 h (Borgstrom et al., 1986, Holdiness, 1991). The elimination rate of NAC in pediatric population is possibly different from adults. A study in pre-term newborn infants reported a mean elimination half-life of 11 h following IV administration (Ahola et al., 1999). Renal clearance is reported to be approximately 30% of the total Clearance (Package insert for Acetadote, 2004).

1.3.4 Pharmacology

NAC is a thiol-containing compound that increases the biosynthesis of GSH, a potent endogenous antioxidant. GSH is a crucial antioxidant in cells that protects against damage from free radicals (Wu et al., 2004a). In addition, mitochondrial GSH is receiving more and more attention due to its influence in oxidative stress related pathological conditions. Mitochondrial GSH has emerged as the major defense mechanism to maintain mitochondrial function (Mari et al., 2009).

In addition, NAC has other pharmacological properties that play key roles in mitigating oxidative stress and inflammation. These include acting as direct free radical scavengers, regulators of tissue protective genes and proteins, as well as chelator and anti-

inflammatory agent, methyl donor in the conversion of homocysteine to methionine, glutamate transport facilitator, and protein modifier (Zafarullah et al., 2003, Dodd et al., 2008). In particular, NAC regulates tissue protective genes that reduce damage inflicted by reactive oxygen species (ROS). One example of a cytoprotective protein that is inducible by thiol-containing biomolecules is hemeoxygenase-1 (HO-1). This enzyme catalyzes the oxidative metabolism of heme to form equimolar amounts of biliverdin, carbon monoxide (CO) and free iron, all of which have antioxidative effects (Abraham and Kappas, 2008). HO-1 and its downstream products are considered to be mediators of cytoprotective effects that might be of particular significant defending system against oxidative stress.

1.3.5 Side effects and adverse responses

The severity of NAC side effects ranges from nausea to death. The most common side effect of NAC is the rotten egg odor related nausea. And some of its adverse responses are referred to as “anaphylactoid”, which shares similar clinical manifestations as anaphylaxis, but does not involve IgE-mediated immunological responses. The patterns of side effects are quite different with oral and intravenous administration of NAC. Gastrointestinal effects such as nausea and vomiting are more common in oral administration and anaphylactoid reactions are more common in intravenous administration (Bebarta et al., 2010).

The frequency of anaphylactoid is reported in a wide range, as 2-6% (Bebarta et al., 2010), 9.3% (Whyte et al., 2007), 14.9% (Waring et al., 2008) and 48% (Lynch and Robertson, 2004) in patients with acetaminophen overdose. The most frequent reported side effects are cutaneous anaphylactoid reactions include rash, urticaria, pruritus and angioedema (Sandilands and Bateman, 2009) and other adverse responses include bronchospasm and hypotension. In extreme cases, cardiac arrest was reported (Cassidy et al., 2008) as well as fatal anaphylactoid reaction in a patient with asthma (Appelboam et al., 2002). Despite these potential concerns, the toxicity observed with intravenous NAC in the ALD population has proven to be minimal.

CHAPTER 2

RESEARCH RATIONALE, SCOPE

AND GENERAL APPROACHES

2.1 Hypothesis and specific aims

Oxidative stress plays an important role in neurodegenerative disorders such as ALD and antioxidant therapy including NAC may be potential efficient therapy. The focus of my research is to characterize the role of oxidative stress in ALD, and investigate the pharmacology of NAC in *in-vitro, in-vivo* and clinical models.

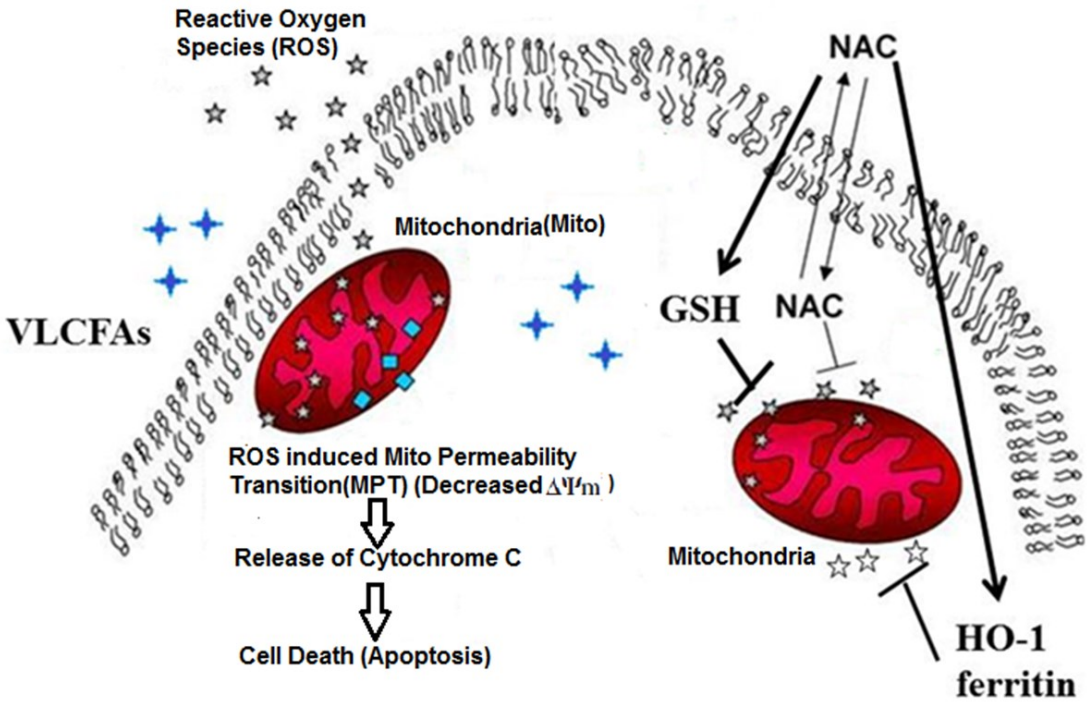

Figure 2-1 Hypothesis for research; increased ROS, mitochondrial dysfunction and subsequent cell death are caused by accumulation of VLCFAs in CCALD, and addition of NAC reverses the oxidative stress status and improves cell survival through supplementing mitochondrial GSH and induction of HO-1.

The hypothesis is that increased ROS is caused by accumulation of VLCFAs which further leads to mitochondrial dysfunction and cell death, and NAC reduces oxidative stress and improves cell survival through generation of antioxidants (e.g., GSH), regulation of cytoprotective proteins (e.g., HO-1) and restoration of mitochondrial function (Figure 2-1).

Based on this hypothesis, four specific aims were formed and pursued in four projects:
Specific Aim 1: To characterize the expression of antioxidant proteins (HO-1, ferritin) following NAC exposure in CCALD patients;
Specific Aim 2: To investigate the cytoprotective role of NAC *in vitro;*
Specific Aim 3: To determine the PK/PD relationship following NAC exposure *in vivo;*
Specific Aim 4: To examine the effects of NAC on mitochondrial function *in vitro.*

2.2 General approaches for research

2.2.1 Disease-related pharmacological models

Disease-related pharmacological models could greatly facilitate the validation of hypothesis and test of potential therapies. In order to investigate the pathology of ALD and the potential mechanisms of action of NAC, different *in-vitro, in-vivo* and clinical models were used in my research.

In-vitro models

It's widely known that CCALD is characterized with abnormal concentrations of VLCFAs which accumulate in the brain white matter and cause neurodegeneration. Oligodendrocyte is the major cell type in the white matter of brain, thus oligodendrocyte cells challenged with similar concentrations of VLCFAs as in patients are established as the *in-vitro* model for ALD. Oxidative stress is also considered as a crucial component in ALD disease pathology. Oligodendrocyte cells challenged with H_2O_2 are also used as an *in-vitro* cell model to mimic oxidative stress. Oligodendrocytes with genetic mutation and previous proof of endogenous oxidative stress are also explored. Meanwhile, fibroblast cells derived from ALD patients are also considered as a valuable *in-vitro* model (Fourcade et al., 2008) and used for part of the proof-of-concept studies.

In-vivo models

Abcd1 knock-out mice are used widely as an effective tool for ALD research (Lopez-Erauskin et al., 2011a). By generating null mutations on the *Abcd1* gene, mouse displays similar impaired VLCFAs degradation in peroxisomes and accumulation of VLCFAs in the plasma and tissues. However, this mouse model has been widely criticized for the absence of cerebral neurodegeneration symptoms. No obvious myelin pathology is observed in the brain tissues of *Abcd1* knock-out mouse model. And it turns out *Abcd1* mutations and VLCFAs accumulations are not enough to cause neurodegeneration in

mouse. Interestingly, although without presentation of brain and spinal cord neurodegeneration similar to CCALD, *Abcd1* knock-out mice present peripheral neuropathy symptoms similar to the adult form AMN.

In recognizing the defects of *Abcd1* knock-out mice in the research of CCALD, *pex5* gene, an essential peroxisome biogenesis factor, is selectively inactivated in oligodendrocytes in *Pex5* knock-out mice. This mutation leads to widespread axonal degeneration and cerebral demyelination, similar to clinical symptoms in CCALD patients (Kassmann et al., 2007). The fact that oligodendrocyte-specific peroxisomal dysfunction leads to cerebral symptoms, indicates that oligodendrocytes play an important role in preventing axon degeneration and demyelination.

At this initial stage of research, wild-type mice were used to obtain preliminary PK/PD data in preparation for further studies in *Abcd1* knock-out mice or *Pex5* knock-out mice.

Clinical samples

CCALD is one major subtype among ALD patients. The Bone Marrow Transplantation (BMT) Group located at University of Minnesota is one of the major centers performing transplants for patients with CCALD (Miller et al., 2011). In collaboration with the BMT group, plasma samples from CCALD patients were collected and used for antioxidant protein identification and measurement.

2.2.2 Pharmacokinetic-pharmacodynamic modeling

Pharmacokinetics (PK) refers to the study of time course of drug absorption, distribution, metabolism and excretion, describing changes in plasma concentrations of target molecules over time. Pharmacodynamics (PD) is defined as the study of time course of pharmacological responses elicited by target molecules (Meibohm and Derendorf, 1997). For example, the study of tumor growth curve in patients after chemotherapies is considered as PD study while the study of drug concentrations used during chemotherapy is considered as PK study.

The aim of PK/PD modeling is to establish the relationship between drug concentrations and drug effects following drug administration. Mathematical equations are used as efficient tools to describe and establish the PK/PD models. PK/PD modeling is useful tool at various stages of pre-clinical and clinical development, contributing to drug candidate selection and optimization, design of first-in-human study as well as clinical development (Lave et al., 2007). Successful PK/PD models help clinicians to adjust doses in clinical practice and facilitate new drug development. They are quite useful tools in:

1) Description of drug exposure-response time profile;
2) Understanding of detailed drug mechanisms and/or making judgments among different hypothesis of mechanisms of action;

3) Prediction of drug expose-response under new dosing regimens, physiological conditions (e.g., disease conditions or during drug-drug interaction), or different experimental systems (e.g., *in vitro-in vivo* correlations).

4) Identification and quantification of system variables which could play a role in PK/PD relationships (e.g. creatinine clearance, weight, age, sex etc.)

5) Explanation of the observed variability of responses in patients' population (e.g., separation of the total variability into between-subject variability and intra-individual variability).

PK/PD models

PK/PD models can be generally classified as empirical models, mechanism-based models and physiological models (Mager et al., 2003).

1) Empirical models are solely based on the best-fit mathematical equations for PK/PD profile without considering the underlying mechanisms of action.

2) Mechanism-based models incorporate the underlying drug mechanisms of action into the mathematical models which could be applied towards other drugs from the same category, e.g., receptor-occupancy models.

3) Physiological models are established based on physiological information of biological systems. Blood flow rates are used to link between particular organs while partition ratios measured experimentally are used to define the properties of organs.

One type of models above or a combination of them is often used in PK/PD modeling and data analysis. In particular, mechanism-based models are widely used and applied towards different phases of drug development. Basic components of mechanism-based PD models for drug action are summarized as Figure 2-2 (Jusko et al., 1995, Mager et al., 2003).

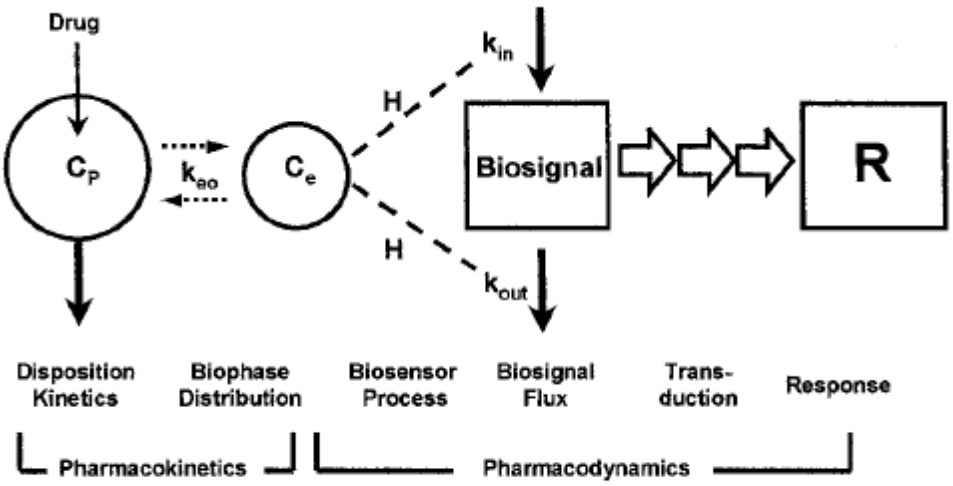

Figure 2-2 Basic components of PD models of drug action. Cp is defined as the plasma concentration of drugs; Ce is defined as the concentration at the site of action, or referred as the effect compartment; Keo is the first-order rate constant that links the plasma concentration and the effect compartment concentration; H refers to the biosensor process which involves the direct interaction between the drug concentration at the site of action and the biological process; Kin and Kout are defined as rate of production and loss of the endogenous mediators within the biosignal flux; R(response) is the pharmacological effect, or the PD endpoint measured during the study. Figure adapted from (Jusko et al., 1995).

The PD endpoint (response) could be linked to the plasma concentration of the drug in various ways. Biophase distribution model describes the linkage between plasma concentration and the concentration at the site of action (effect compartment). Direct measurement of the effect compartment concentration is preferable but not realistic for most of studies. Biophase distribution model enables modeling of the delay in response due to the rate-limiting distribution. In addition, drugs could possibly elicit pharmacological effect indirectly through certain endogenous biological mediator (biological flux). Drugs could increase or decrease the levels of the endogenous mediator, through stimulating/ inhibiting the rate of synthesis, or inhibiting/stimulating the rate of clearance. Further, the endogenous mediators could elicit more biological responses through signal transduction which can be modeled quite differently depending on the mechanism of action.

Population PK/PD modeling

Population PK/PD modeling is to study PK/PD models in a population, where data from all individuals are evaluated simultaneously with a nonlinear mixed-effects model. The term "nonlinear" means that the dependent variables (e.g., drug concentration or drug effect in PK/PD) can be expressed with nonlinear functions of model parameters and independent variables (e.g., time). "Mixed-effects model" quantifies the influence of fixed-effect parameters and random-effect parameters simultaneously on the dependent variable. Fixed-effect parameters refer to the average population value or average

relationship with measurable patients' factors (e.g., average population clearance, or weight that do not vary across individuals). Random-effect parameters describe the unexplained between-individual and within-individual random variability in a model, sometimes inter-occasional variability is also considered. This population method enables one to investigate the variability observed in PK and PD outcomes among individuals and within individuals at different occasions (Mould and Upton, 2013).

The primary goal of population PK/PD is to find average population values and determine the sources of variability in a population. With enough information, one could possibly relate the drug concentration/drug effect with dosing regimens (e.g., dose, interval, route of administration) and patient characteristics (e.g., age, weight, renal clearance, ethic, genetic), predicting the outcomes of a new regimen or for another patient population.

In population PK/PD modeling, structural model of nonlinear parameter function is established with PK model, PD model and disease progression model; statistical model describes the variability around the structural model, including the information of intra- and inter- individual variability; covariate model identifies the patients' individual demographic factors which influence the parameters (e.g., $Vi = V \times EXP(BWi/70)$, Vi is individual volume of distribution, V is the population average, BWi is the individual body weight (Cella et al., 2012)).

2.3 My roles in projects

Four projects as well as my role in each project were listed below:

Project 1: Investigation of cytoprotective biomarker (HO-1) in NAC pharmacology in CCALD patients;

- Authored abstract and poster (American Society for Clinical Pharmacology and Therapeutics Annual Meeting, Washington, 2012), presentations and manuscript;
- Contributed in assay validation, standardized the detection methods, authored standard operation protocols;
- Carried out all the experiments and data analysis.

Project 2: Investigation of mechanisms of action of NAC in oxidative-stress cell models of oligodendrocytes;

- Authored grant application, abstract and poster (Chemistry Biology Interface Training Grant Symposium, MN, 2011), presentations and manuscript;
- Contributed in the study design, standardized the sampling/detection methods, authored standard operation protocols;
- Carried out all the experiments and data analysis.

Project 3: Investigation of the role of mitochondrial function in ALD pathology and mechanisms of action of NAC in VLCFAs challenged oligodendrocytes

- Authored grant application, abstract and poster (Mitochondrial Medicine symposium, CA, 2013), presentations and manuscript;
- Collaborated and communicated between PIs from two different labs, contributed in the study design, purchased materials and standardized the sampling/detection methods, authored standard operation protocols;
- Carried out all the experiments and data analysis.

Project 4: Investigation of PK/PD properties of single *i.v.* dose of NAC in mice

- Authored grant application (not funded though), presentations and manuscript;
- Collaborated and communicated between PIs from three different labs, contributed in the study design, purchased materials and standardized the sampling/detection methods, managed the logistics of sample collection and analysis, authored standard operation protocols;
- Carried out the quantification analysis of samples;
- Performed non-compartmental and compartmental PK analysis and PK/PD modeling.

CHAPTER 3

NAC THERAPY INCREASED PLASMA CONCENTRATIONS OF HEME OXYGENASE-1 IN CCALD PATIENTS

3.1 Introduction

NAC is used as adjuvant therapy along with HSCT in late-stage CCALD, resulting in increased survival from 36% to 84% (Miller et al., 2011). These patients received high dose of NAC for a long period of time. However, the underlying mechanism is unknown. NAC is a thiol-containing antioxidant that scavenges free radicals, chelates metal ions, facilitates GSH biosynthesis (Zafarullah et al., 2003), contributes to the synthesis of gasotransmitter hydrogen sulfide (Kartha et al., 2012) as well as regulates tissue protective genes and proteins that reduce damage inflicted by reactive oxygen species (ROS) (Zafarullah et al., 2003).

An example of cytoprotective proteins induced by thiol-containing biomolecules is hemeoxygenase-1 (HO-1). HO-1 is a 32-kDa microsomal protein which catalyzes the oxidation of heme to form biliverdin, carbon monoxide (CO) and free iron. Biliverdin is then reduced by biliverdin reductase (BVR), forming a potent free radical scavenger and antioxidant biliverdin (Tenhunen et al., 1968). CO has been shown to provide neuroprotective effects through the soluble guanylate-cyclase (sGC) pathway, and also have anti-apoptotic, and anti-inflammatory actions (Brouard et al., 2000, Otterbein et al., 2000, Schallner et al., 2013). The HO-1-dependent release of free irons during heme oxidation results in the upregulation of a secondary protein, ferritin (Eisenstein et al., 1991). Ferritin functions as an endogenous antioxidative protein by rapidly sequestering free cytosolic irons, which catalyzes oxygen centered radical formation via the Fenton

reaction in cells (Juckett et al., 1995). In total, HO-1 and its downstream products are considered to be the 2nd most important in antioxidant defense system after GSH (Dulak and Jozkowicz, 2003). Their cytoprotective effects may be particular significant during conditions of oxidative stress given there are excessive free radicals and depleted antioxidants.

HO-1 is expressed extensively at low basal levels in normal tissues apart from liver and spleen (Tenhunen et al., 1968). However, HO-1 can be upregulated by a variety of pro-oxidant and stress stimuli as a sensitive oxidative stress marker. Increased HO-1 concentrations are generally considered as a signal of the biological system to restore redox homeostasis (Cuadrado and Rojo, 2008). Thus modulation of HO-1 expressions within the therapeutic range is critical to oxidative stress related disorders (Jazwa and Cuadrado, 2010).

Cysteine, GSH and H_2S, the three major metabolites of NAC (Zafarullah et al., 2003, Kartha et al., 2012), have been shown to induce HO-1 expression *in vitro* (Erdman, K., unpublished data from our lab). We reasonably hypothesized that the concentrations of HO-1 are increased in CCALD patients with exposure of NAC and its metabolites. To test this hypothesis, plasma HO-1 concentrations were measured since it was identified as a useful surrogate biomarker for HO-1 expression *in vivo* (Bao et al., 2010, Bao et al., 2012, Zager et al., 2012). In the current study, plasma concentrations of HO-1 and its downstream ferritin were measured in CCALD patients prior to and after NAC dosing.

As part of the HSCT procedure, CCALD patients received extensive preparatory regimen (Figure 3-1). The HSCT procedure and chemotherapy used could also possibly affect HO-1 and ferritin concentrations. In fact plasma ferritin levels were found to be increased considerably during the first 3 months following HSCT (Or et al., 1987). Total body irradiation (Suzuki et al., 2002), mycophenylate mofetil (MMF) and cyclosporine (CSA) (Teng et al., 2006) were also found to induce HO-1 levels *in vivo*. In contrast, Clofarabine was found to decrease HO-1 expression (Lee et al., 2012). No previous reports have addressed the influence of campath-1H and Melphalan on HO-1 expression. In this study, we also explored plasma HO-1 and ferritin levels following HSCT procedure.

3.2 Methods

3.2.1 Demographics of patients, NAC dosing and blood sampling

17 CCALD patients scheduled to undergo HSCT at the University of Minnesota Blood and Marrow Transplant (BMT) Program were included in this study. In accordance with the Declaration of Helsinki and following the provision of informed consent by patients or guardians, protocols were approved by the University of Minnesota Institutional Review Board. The inclusion/exclusion criteria require that patients were diagnosed with advanced radiographic disease (Loes score $\geq$ 10) and received the NAC adjuvant therapy

(70 mg/kg intravenously every 6 hours from -11 day till -8 day prior to HSCT, and day 1 till day 100 post-HSCT procedures) as part of the protocol. The HSCT regimen also includes campath-1H, clofarabine, melphalan, total body irradiation (TBI), mycophenylate mofetil (MMF) and cyclosporine (CSA) as shown in Figure 3-1.

Plasma samples were drawn from patients prior to NAC therapy (-12day, PRE-NAC) and post NAC therapy (-8 days, POST-NAC-1; +7 days, POST-NAC-2; +21days, POST-NAC-3) as shown in Figure 3-1. Few sampling points were not obtainable in some of the patients. We obtained PRE-NAC and POST-NAC1 samples from 11 patients. Data from these 11 patients were taken for further analysis.

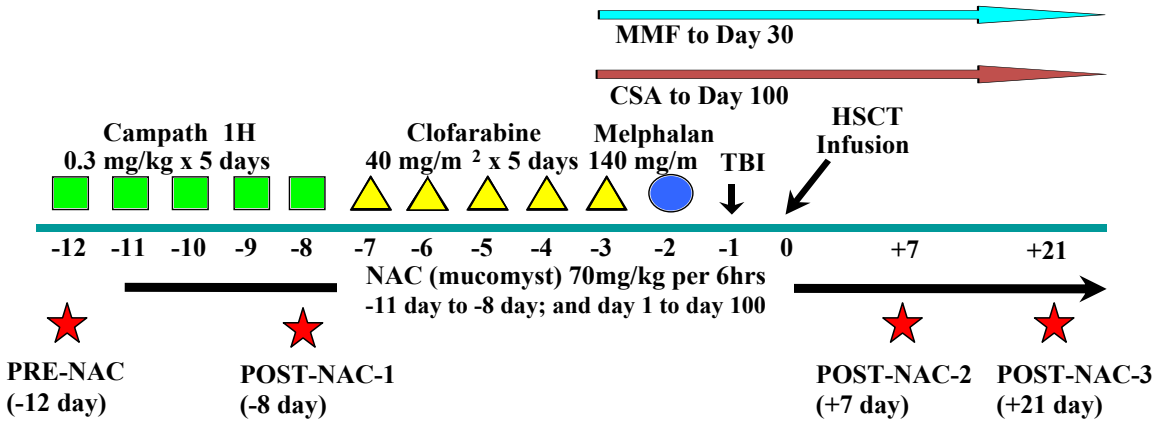

Figure 3-1 HSCT procedures with NAC adjuvant therapy for CCALD patients. In addition to preparative drugs used in the protocol, NAC was administered intravenously at 70 mg/kg every 6 hours from -11 day till -8 day prior to HSCT, and day 1 till day 100

post-HSCT. Plasma samples were drawn at 4 time points including -12 day (PRE-NAC), -8 day (POST-NAC-1), +7 day (POST-NAC-2) and +21days (POST-NAC-3).

3.2.2 Determination of plasma HO-1 concentrations

Plasma HO-1 levels were determined using commercial HO-1 ELISA kit (Enzo Life Sciences, MI, USA). Briefly, plasma samples were first centrifuged at 13000 rpm for 10mins, and diluted subsequently with rat HO-1 diluents (Enzo Life Sciences, MI, USA) at a ratio of 1:2. The subsequent assay procedures were performed as per the manufacture's protocol. Normal human plasma (Biological Specialty Corporation, PA, USA) and normal human plasma spiked with 10ng/ml HO-1 standard (Enzo Life Sciences, MI, USA) were used as control samples. The two control samples were run in parallel with each set of test samples. After the assay, the data was analyzed using a 4-parameter algorithm to calculate the plasma HO-1 concentrations.

3.2.3 Determination of plasma ferritin concentrations

Plasma ferritin concentrations were determined using commercial ferritin ELISA kit (Abnova, Taiwan). Plasma samples were first centrifuged at 13000 rpm for 10mins, and diluted using diluent provided by the kit. PRE-NAC and POST-NAC-1 samples were diluted at ratio of 1:2 while POST-NAC-2 and POST-NAC-3 samples were diluted at ratio of 1:20. The subsequent assay procedures were performed as per the manufacture's

protocol. Normal human plasma (Biological Specialty Corporation, PA,USA) and normal human plasma spiked with 50ng/ml and 250ng/ml ferritin were taken as control samples. The three control samples were run in parallel with each set of test samples. After the assay, the data was analyzed using 4-parameter algorithm to calculate the plasma ferritin concentrations.

3.2.4 *In-vitro* cell culture

Around 10^4 primary human non-transformed fibroblast cells (derived from non-CCALD human controls) were seeded on 24-well plates (Corning, NY, USA) in DMEM glucose media supplemented with 10% FBS and 1% antibiotics. Cells were incubated overnight in 37 °C incubator with 5% CO_2. For experimental set up, cells were cultured overnight to get 80% confluence before being exposed to NAC (10µM-100µM) for 4 hours. HO-1 mRNA expression was quantified using real-time PCR (SYBR green method) and protein expression by ELISA.

3.2.5 Real time PCR

Real time PCR

Approximately 105 primary human fibroblast cells were trypsinized and harvested from 24-well plate. Cell pellets were collected and stored at -80 °C freezer. Total RNA was extracted from frozen pellets using RNeasy Plus Mini kit (Qiagen, CA, USA) according

to the manufacture's protocol. Quality of total RNA was assessed using non-denaturing agarose gel (1% agarose) electrophoresis to examine RNA degradation. Further, the concentration of total RNA was quantified using Take3™ plate (BioTek, VT,USA) and Synergy 2 spectrophotometer (BioTek, VT,USA), the readings of which provided quick spectrophotometric quantification of total RNA. Approximately 1μg of total RNA was used for reverse transcription using qScript cDNA synthesis kit (Quanta, MD, USA) in Mastercycler (Eppendorf, Germany). cDNA was amplified using SYBR green method (Clontech, CA, USA) following manufacturer's protocol in MyiQ single color real-time PCR detection system (Bio-Rad, CA, USA). Real-time PCR results were analyzed by IQ5 optical system software (version 2.0, Bio-Rad) provided with the MyiQ system. Hypoxanthine phosphoribosyl transferase 1 gene (HPRT) was used as the normalization control for each sample.

Primers for HO-1: FP, 5'-ATT GCC AGT GCC ACC AAG TTC AAG-3'; RP, 5'-ACG CAG TCT TGG CCT CTT CTA TCA-3'; Primers for HPRT: FP, 5'-GGT GAA AAG GAC CCC ACG AA- 3'; RP, 5'- AGT CAA GGG CAT ATC CTA CA-3'.

3.2.6 Determination of HO-1 concentrations in cell lysates

To quantify the HO-1 protein concentrations in vitro, cell lysates were harvested on 24-well plates treated with different concentrations of NAC. HO-1 concentrations in cell lysate were analyzed using HO-1 ELISA kit (Enzo Life Sciences, MI, USA). Total

protein concentrations were analyzed by Bradford protein assay (Bio-RAD, CA) according to manufacturer's protocol and used as normalization parameter across treatments.

3.2.7 Statistical Analysis

Results are expressed as means ± standard error. For multiple comparisons, one-way ANOVA and Dunnett's test were used. In addition, t-test was used to compare between two groups. The statistical methods are specified in each section of the results. A p-value <0.05 was considered significant.

3.3 Results

3.3.1 Demographics of CCALD patients

Demographic and clinical characteristics of the study subjects are summarized as below. All patients were diagnosed with advanced radiographic disease (Loes score ≥ 10) at the time of enrollment. All 17 CCALD patients enrolled were male and the median age of ALD patients at the time of HSCT was 8.2 years old (range from 4.4 to 14.5 years). The median weight of ALD patients at the time of HSCT was 24.4 kg (range from 17.3kg to 41.5 kg). The intravenous dose for NAC was 70mg/kg/6hrs for all patients.

3.3.2 NAC increases plasma concentrations of HO-1 and ferritin in CCALD patients prior to HSCT

11 patients with samples prior to NAC therapy (-12 day, PRE-NAC) and post NAC but before HSCT (-8 day, POST-NAC-1) were taken for analysis. In these patients, NAC was dosed during the pre-conditioning period for 4 days (-11 day till -8 day). Analysis of plasma samples from CCALD patients prior to and 4 days after treatment with NAC showed significant increases in the antioxidant protein, HO-1 (Figure 3-2 A). We also observed significant increase in the concentrations of ferritin, a downstream product of HO-1 activity (Figure 3-2 B). This suggests that HO-1 mediated antioxidant signaling pathway is induced following NAC therapy.

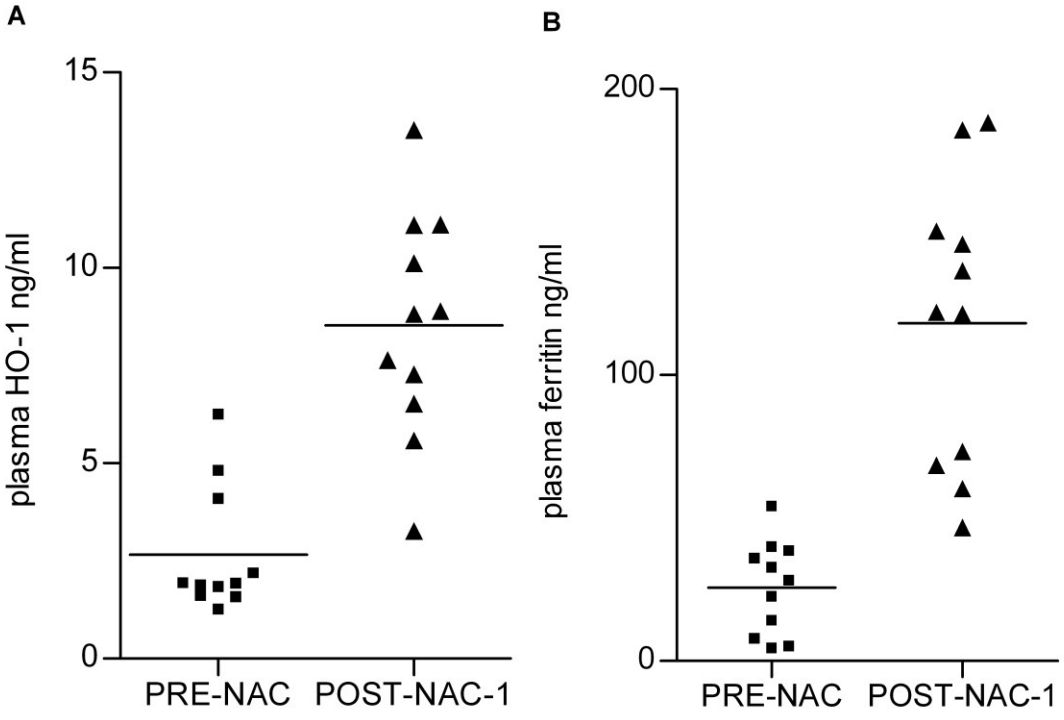

Figure 3-2 Plasma HO-1(A) and ferritin (B) levels in plasma samples from CCALD patients increased significantly before and after NAC treatment (n=11); means of each group are represented by lines; (A) $p < 0.001$, paired t-test; (B) $p<0.01$, paired t-test .

3.3.3 Plasma concentrations of HO-1 and ferritin prior to HSCT are highly correlated

If HO-1 and ferritin are in the same signaling pathway, we hypothesized that there should be a good correlation between plasma levels of these proteins. In the 11 patients with paired plasma samples collected prior to and after NAC treatment, Pearson's correlation coefficient r was found to be 0.74 ($p<0.0001$) between plasma levels of HO-1 and ferritin as shown in Figure 3-3. The significant correlation observed proves the close relationship between HO-1 and ferritin. Moreover, a clear separation was observed in the distribution of HO-1 and ferritin levels indicating the values to be higher in POST-NAC-1 samples compared to PRE-NAC samples.

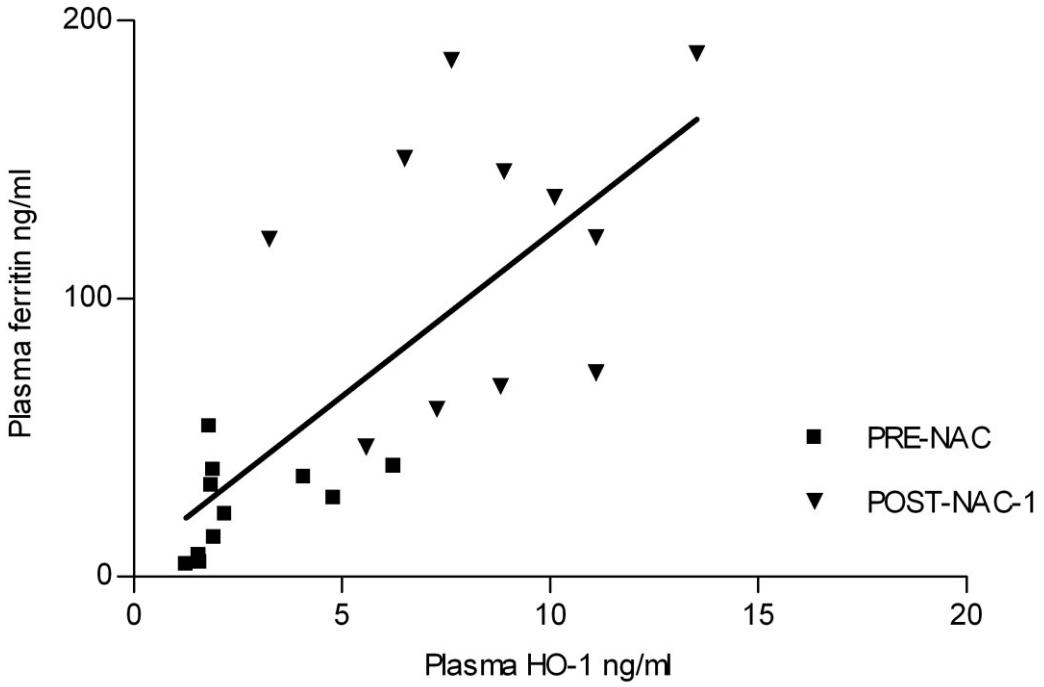

Figure 3-3 Correlation between plasma HO-1 and plasma ferritin in CCALD patients for PRE-NAC and POST-NAC-1 samples prior to HSCT (n=11). Pearson's correlation r is equal to 0.74, p value <0.0001 with two tailed t test.

3.3.4 Plasma concentrations of HO-1 and ferritin prior and after HSCT procedures

Since HSCT procedures and various chemotherapy agents are known as interfering factors, we pursued to examine the HO-1 and ferritin levels in patients all along the procedure. In total, plasma samples of four time points were analyzed: PRE-NAC (-12 day), POST-NAC-1 (-8 day), POST-NAC-2 (+7 day), POST-NAC-3 (+21 day). Among these samples, PRE-NAC and POST-NAC-1 were sampled prior to HSCT procedure

while POST-NAC-2 (+7 day) and POST-NAC-3 (+21 day) were sampled after HSCT procedure (Figure 3-4).

Interestingly, plasma HO-1 levels were observed to be induced significantly after NAC dosing ($p<0.01$, POST-NAC-1 compared to PRE-NAC, Dunnett's test following ANOVA). And HO-1 levels were sustained all through the HSCT procedure. The mean HO-1 levels for PRE-NAC, POST-NAC-1, POST-NAC-2 and POST-NAC-3 were found to be 2.7±0.3, 8.6±0.9, 9.4±1.9 and 10.3±0.8 ng/ml respectively (Figure 3-4 A).

The plasma levels of ferritin turned to be another interesting story. Ferritin levels is not only increased following the NAC administration but was also induced by HSCT procedure. The mean plasma levels of ferritin for PRE-NAC, POST-NAC-1, POST-NAC-2 and POST-NAC-3 were found to be 33.0±8.6, 135.4±21.7, 2305.0±578.9 and 5557.0±1181.0 ng/ml respectively (Figure 3-4 B). Note that PRE-NAC and POST-NAC-1 were sampled before HSCT and POST-NAC-2 and POST-NAC-3 were sampled after HSCT.

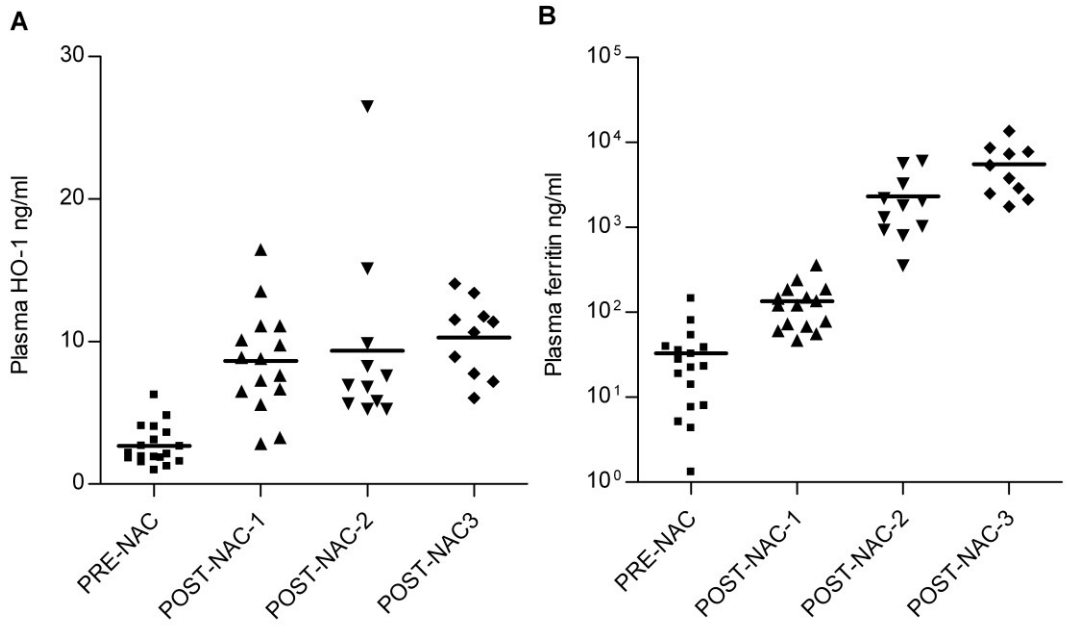

Figure 3-4 HO-1(A) and ferritin (B) levels in plasma samples from CCALD patients prior to and after HSCT procedure (n=10~17); means of each group are represented by lines; one way ANOVA was used to compare HO-1 (A) and ferritin (B) levels for all sampling time point, $p<0.0001$ (A) and $p<0.0001$ (B); Dunnett's multiple comparison test was used to compare the sampling time point during NAC treatment with PRE-NAC levels, $p<0.01$ for all other comparisons except ferritin levels between PRE-NAC and POST-NAC-1 ($p<0.05$).

3.3.5 NAC increases HO-1 mRNA and protein levels in human fibroblasts

To exclude multiple interfering factors in HSCT procedures and to investigate the sole influence of NAC on HO-1 expression, we also designed and performed *in vitro* cell studies. Human fibroblast cells derived from non-CCALD control were used. NAC

Fibroblast cells were incubated with NAC (10-100 μM) for 4 hrs. mRNA levels of HO-1 was examined using real time PCR and protein levels by ELISA. Interestingly, at all incubation concentrations and at both mRNA and protein levels, the HO-1 levels were found to be significantly higher than the baseline ($p<0.001$ for both mRNA and protein). Figure 3-5 showed a representative graph showing increased HO-1 expression following incubation with NAC.

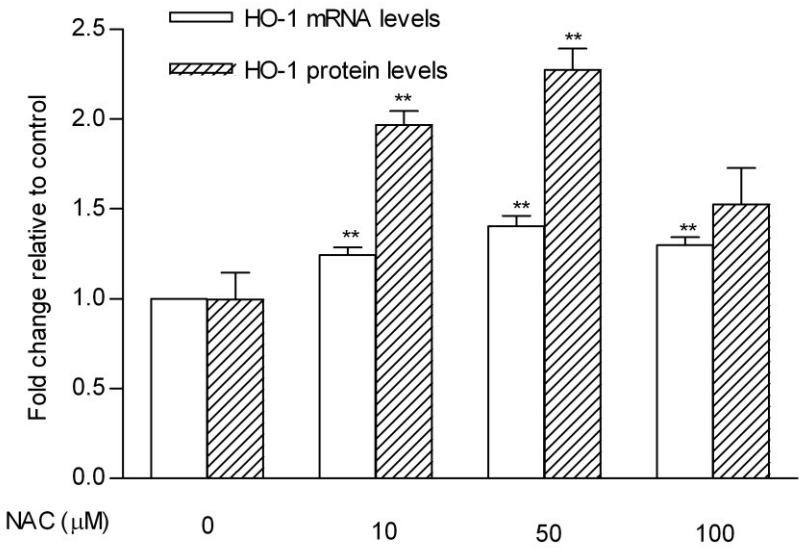

Figure 3-5 HO-1 expression (mRNA and protein levels) in human fibroblast cell line following NAC treatment (n=3). ANOVA was used to compare HO-1 mRNA and protein levels across treatments, $p<0.001$ for both comparisons. Dunnett's test was used to compare the treatments of different concentrations of NAC with control, $**p<0.01$.

3.4 Discussion

Plasma HO-1 concentrations have been measured extensively in clinical studies as surrogate biomarkers. However there was wide variation in the reported concentration of HO-1 in plasma. HO-1 levels in control patients were reported to be 1.11 (median, range 0.63-2.06) ng/ml (Bao et al., 2010), 1.34 (median, range 0.81-2.29) ng/ml (Bao et al., 2012), and 20±3 ng/ml (mean±SEM) (Zager et al., 2012) depending on different detection methods. In our study, we performed assay validation and calibration in collaboration with Enzo Life Sciences (MI, USA) before the sample analysis. Since the commercial kit was not validated for plasma, we modified the procedure, by using a different sample diluent, which increased the detection of HO-1 and gave us a more reliable measure. Using this procedure, HO-1 level in normal human plasma was found to be 4.05± 0.5. The basal plasma HO-1 level for CCALD patients without any treatment (PRE-NAC samples) was observed to be 2.7±0.3 ng/ml. However, since we did not have any age and sex matched controls, no further conclusion could be drawn. . Future studies enrolling matched controls would be quite useful to compare the basal levels of HO-1 in CCALD patients with controls.

NAC is administered at approximately 6000-9000 mg per day for CCALD patients (20-30kg weight), with each dose administered at levels similar to what is recommended for treatment for acetaminophen overdose. Thus the NAC exposure in CCALD patients in this study is way more than that dosed in patients with acetaminophen overdose. NAC is

dosed in the CCALD patients for more than 100 days while it is only typically dosed in patients with acetaminophen overdose for 72 hrs (Kociancic and Reed, 2003). In addition, this exposure is higher than what is previously reported for other chronic applications of NAC. Long-term NAC therapy is reported to be at 600 mg daily oral dose (Decramer et al., 2005) in chronic obstructive pulmonary disease and at 1200-3600mg daily oral dose (Mardikian et al., 2007) in treating cocaine-dependent patients.

Here I report for the first time increased plasma HO-1 levels in CCALD patients following high exposure of NAC. However we do acknowledge that there are multiple factors that can interfere with our observation. During the preparatory regimen of HSCT (-11 day till -8 day), NAC and Campath-1H were dosed to the CCALD patients. Thus the influence of Campath-1H on plasma HO-1 cannot be ruled out in our study due to the limitation of the study design although no previous reports have reported any relationship between HO-1 and Campath-1H. To rule out this possibility, we designed and performed the *in vitro* cell studies to examine the relationship solely between NAC and HO-1 expression as shown in Figure 3-5. Both mRNA and protein levels of HO-1 were found to be increased following the incubation of NAC at three different concentrations of 10, 50 and 100 μM. Interestingly, NAC at 50 μM *in vitro* turned out to induce maximal HO-1 expression, which is within the range of pharmacokinetic NAC plasma concentrations in CCALD patients (Holmay et al., 2012).

All through the HSCT procedure, HO-1 levels were found to be consistently high following NAC administration although several interfering factors exist for POST-NAC-2 and POST-NAC-3 time points. This can occur due to two reasons. Either, the HO-1 induction by NAC became saturated at the maximum level after the first few days or that the turn-over rate of HO-1 protein is such that we couldn't see an apparent increase in HO-1.

The induction of HO-1 can be helpful for CCALD patients undergoing HSCT in multiple ways. Firstly, HO-1 induction in the brain was shown to be closely related to neurodegenerative disorders such as Alzheimer's, Parkinson's and multiple sclerosis (Schipper, 2004). Although the expression of HO-1in the brain is normally confined to a small subset of neuronal and glial cells in the CNS, HO-1 expression in these cells is highly inducible and can exert antioxidant and anti-inflammation effects to slow down the disease progression. Secondly, induction of HO-1 is possibly beneficial to the HSCT procedure. Reports have shown that induction of HO-1 levels in liver/bowel tissues improved overall survival and reduced acute graft-versus-host disease (aGVHD) rates in mouse aGVHD models during bone marrow transplantation (Gerbitz et al., 2004, Ewing et al., 2007).

The induction of HO-1 in cells and tissues may be harmful in spite of the general understanding of cytoprotective effects of HO-1. Excessive HO-1 induction was found to associate with tissue iron sequestration and mitochondrial insufficiency (Schipper et al.,

2009b). Inhibition of HO-1 hyperactivity in glial cells prevented iron deposition which was indicated as therapeutic target in Alzheimer's disease (Schipper et al., 2009a). These results indicate that the HO-1 concentrations should be kept within reasonable therapeutic range. Our observation of saturated induction of HO-1 levels following NAC administration may be beneficial, as excessive HO-1 expression is harmful. In summary, modulation of appropriate HO-1 induction is a crucial for mitigating oxidative stress.

Ferritin, as one the downstream product of HO-1, was also induced following the administration of NAC. The concentrations of ferritin were observed to be linearly correlated with increased HO-1 before HSCT procedures. However, ferritin was also highly influenced by the HSCT procedure as shown in Figure 3-4. This observation is consistent with previous finding that ferritin is highly induced by bone marrow transplantation (Or et al., 1987).

3.5 Conclusion

In our study, the survival of CCALD patients increased with NAC adjuvant therapy. Following NAC administration, there was significant increase in HO-1 and ferritin concentrations in CCALD patients' plasma. With the observation of increase in survival and increase in HO-1 plasma concentrations, we hypothesized that HO-1 played crucial roles in mediating the cytoprotective effects of NAC in CCALD patients and this increase in HO-1 is reasonably beneficial for the CCALD patients.

In addition, our *in vitro* results suggest HO-1 as a cell signaling mediator of NAC-induced protection. These results indicate that HO-1 and ferritin contribute to the cytoprotective benefits of NAC in CCALD patients.

CHAPTER 4

N-ACETYLCYSTEINE PROVIDES CYTOPROTECTION IN MURINE OLIGODENDROCYTES THROUGH HEME OXYGENASE-1 ACTIVITY

4.1 Introduction

Oxidative stress in the CNS plays a significant role in the pathophysiology of neurodegenerative disorders. ROS produced during CNS oxidative stress can lead to damage of intracellular DNAs, proteins and lipids resulting in cell death (Shukla et al., 2011b). Oligodendrocytes are CNS cells that produce myelin sheath around neurons. They are highly vulnerable to oxidative stress, which can disrupt their maturation or cause cell death (Jana and Pahan, 2007, French et al., 2009). Death of oligodendrocytes has been considered as an early event in CNS demyelination and neurodegeneration (Zhang et al., 2013). Due to the close relationship between oxidative stress induced damage and neurodegeneration, reduction in oxidative stress is being explored as an approach to slow down progression of various neurodegenerative diseases as demonstrated in recent *in-vivo* and clinical studies (Ahmad et al., 2012, Goes et al., 2013, Jin et al., 2013).

NAC is a thiol-containing antioxidant, available both as FDA-approved products and dietary supplements. NAC is indicated as an inhaled agent for mucolysis in cystic fibrosis (Mucomyst®) and intravenously as an antidote for acetaminophen overdose (Acetadote®) (Heard and Green, 2012b, Rushworth and Megson, 2013a). Because of NAC's apparent successful clinical use in a wide range of diseases, several mechanisms have been proposed for its beneficial antioxidative and anti-inflammatory properties. These include direct free radical scavenging, metal ion chelation, and as a precursor for

synthesis of the endogenous GSH (Schroder et al., 1993, Dodd et al., 2008). In addition, one of the mechanisms of action of NAC may involve the regulation of tissue protective genes that reduce damage inflicted by reactive oxygen species (ROS) (Zafarullah et al., 2003). Among the cytoprotective proteins, HO-1is induced by thiol-containing biomolecules such as lipoic acid and NAC (Ogborne et al., 2005, Xu et al., 2013). This enzyme catalyzes the oxidative metabolism of heme to form equimolar amounts of biliverdin (which is then converted to bilirubin), carbon monoxide (CO), and free iron; all of which have anti-oxidative properties (Abraham et al., 2007, Abraham and Kappas, 2008). Thus HO-1 may contribute to the cytoprotective effects of NAC that might be of particular significance during inflammatory processes triggered by oxidative stress.

Despite previous extensive research works, the exact mechanisms by which NAC exert its cytoprotective effects on oligodendrocytes remain poorly elucidated. In this study, we have characterized the mechanisms underlying the cytoprotective properties of NAC in oligodendrocytes, under conditions of oxidative stress.

4.2 Materials and methods

4.2.1 Materials

Dulbecco's Modified Eagle Medium (DMEM) high glucose medium, fetal bovine serum (FBS), and antibiotic-antimycotic (AA), phosphate buffered saline (PBS), Trypsin-EDTA

and fluorescent CM-H_2DCFDA probe were obtained from Life Technologies, (CA, USA). 7-AAD fluorescent probe was from BD Biosciences (CA, USA). L-buthionine-(S,R)-sulfoximine (BSO), hydrogen peroxide (H_2O_2), N-acetyl-L-cysteine (NAC), sucrose, mannitol and ethylene glycol-bis(2-aminoethylether)-N,N,N′,N′-tetra acetic acid (EGTA) were purchased from Sigma-Aldrich (MO, USA). HEPES 1M solution was from Mediatech (VA, USA). Chromium mesoporphyrin IX chloride (CrMP) was obtained from Frontier Scientific (UT, USA). Acetonitrile, ammonium formate in the mobile phase were purchased from Fisher Scientific (PA, USA). Stock solutions of compounds were made in PBS. Culture medium was used to prepare working solutions. The pH of the NAC stock solution in PBS (10mM) was adjusted to 7.4 and filtered prior to making further dilutions.

4.2.2 Cell culture and experimental conditions

Immortalized murine oligodendrocyte cell lines, 158N (normal) and proteolipid protein mutant 158JP (Jimpy) were a generous gift from Dr. Ghandour (Baarine et al., 2009a). 158N and 158JP were derived from normal and Jimpy mice respectively, showing characteristics of well-differentiated oligodendrocytes. 158JP oligodendrocytes demonstrated a mutation on proteolipid protein PLP/DM20 which caused premature death of oligodendrocytes and severe CNS demyelination (Knapp et al., 2009). 158JP cells were observed to have significantly higher spontaneous ROS and superoxide anion production compared to 158N cells (Baarine et al., 2009a). Approximately 10^6 cells were

seeded on 75 cm^2 culture flasks (Corning, NY, USA) in DMEM high glucose medium supplemented with 5% FBS and 1% AA. Cells were incubated overnight in 37 °C incubator with 5% CO_2. At the onset of experiments, cells were seeded on 24-well or 96-well plates and cultured overnight to achieve 80% confluence. Cells were treated with 500μM H_2O_2 to mimic oxidative stress conditions. For all experiments, NAC, at concentrations ranging from 50μM to 500μM, was co-incubated with H_2O_2 for 24 hours. For inhibitor studies, 50μM BSO (GSH inhibitor) or 30μM CrMP (HO-1 inhibitor) was added 20 minutes prior to addition of NAC with H_2O_2. For all experiments, cells in culture medium served as negative control.

4.2.3 Cell survival assays

Cell survival following various experimental treatments was quantified using colorimetric assays on treated cells cultured in 96-well plates. CellTiter 96® Aqueous (Promega, MI, USA) and Cell Counting Kit-8 (Dojindo, Kumamoto, Japan) were used to determine cell viability following manufacturer's protocol.

4.2.4 Evaluation of intracellular ROS

Evaluation of intracellular ROS was performed by fluorescence-activated cell sorting (FACS) using fluorescent CM-H_2DCFDA probes. Briefly, after 24 hours in varying conditions, cells seeded on 24-well plates were harvested and washed twice with PBS.

The cells were then stained with 1μM CM-H_2DCFDA for 5 minutes. The samples were subsequently washed twice and resuspended in 250μl PBS containing 5μl 7-AAD fluorescent probes for analysis. During acquisition of FACS data, the live cells (negative for 7-AAD) were gated and evaluated for ROS with CM-H_2DCFDA.

Further, the fluorescence intensity of CM-H_2DCFDA was also gated uniformly to designate positive events of CM-H_2DCFDA stained cells. The percentage of positive stained CM-H_2DCFDA was used as the indicator for ROS levels in different treatment groups. To compare across different sets of experiments, ROS levels in 158N cells incubated with medium were used to normalize across different groups to achieve relative ROS levels.

4.2.5 Determination of intracellular GSH

Cells seeded on 24-well plates were subjected to different experimental conditions. At the end of incubation, the cells were washed twice with PBS and the harvested cells were lysed using lysis buffer (20mM HEPES, 1mM EGTA, 210mM mannitol and 70mM sucrose, pH 7.2). 2 ml of methanol was added into 100 μL of cell lysates and vortexed. The processed samples were centrifuged at 2500 rpm for 10 minutes at 4 ^{o}C. The organic layer was removed and evaporated under nitrogen gas at 37 ^{o}C. The samples were reconstituted in mobile phase and filtered in vials using nylon acrodisc syringe filters (Pall Life Sciences, MI, USA). Intracellular GSH was determined using liquid chromatography-mass spectrometry (HPLC-MS) (Agilent Technologies, CA, USA) with

series 1100 system consisted of a G1322A degasser, a G1311A quaternary pump, and a G1313A autosampler. The electrospray interface is connected to a single quadrupole G1946A. The HPLC-MS system was controlled and data were processed using Chemstation software (Agilent Technologies, CA, USA). The samples were analyzed using selective ion monitoring (SIM) mode and the positive ion for GSH was set at 308 (m/z). GSH separation was performed using a mobile phase consisting of 98% 20mM ammonium formate buffer at pH 3.0 and 2% acetonitrile through Agilent ZORBAX Eclipse XDB-C18 (3×150mm, 3.5μm) column. Total cellular protein concentrations were analyzed using Quick Start Bradford protein Assay Kit (Bio-Rad, CA, USA) according to manufacturer's protocol. Total GSH concentrations in each group were normalized to total protein concentrations to obtain GSH concentrations in μg/mg. GSH concentrations in cells incubated with medium served as control and were used to normalize across different groups.

4.2.6 Total antioxidant capacity assay

Total antioxidant capacity (TAC) was evaluated by a colorimetric method (Miller et al., 1993), using Antioxidant Assay Kit from Cayman Chemical (MI, USA). At the end of incubation with different experimental conditions, cells seeded on 24-well plates were washed twice with PBS, harvested using trypsin-EDTA, lysed and sonicated in ice-cold balanced buffer (5mM KH_2PO_4, 0.9% sodium chloride and 0.1% glucose, pH 7.4). The cell lysates were centrifuged and analyzed following the manufacture's protocol. TAC

was expressed as equivalent Trolox concentrations and normalized to total protein concentrations determined using the Bradford protein assay in each group. Finally, TAC levels in cells incubated with medium served as controls, which were used to normalize across different groups.

4.2.7 Statistical data analysis

For all cellular assays, results were expressed as means ± standard error. Data was analyzed using ANOVA with a Bonferroni's correction for multiple comparisons. A p-value <0.05 was considered significant. Analyses are based on data from three independent experiments using different cell passages on different days.

4.3 Results

4.3.1 N-acetylcysteine decreases ROS formation in oligodendrocytes under conditions of oxidative stress

In order to characterize the anti-oxidative properties of NAC, murine oligodendrocytes (158N) were incubated either with 500μM H_2O_2 alone or in combination with increasing concentrations of NAC (50-500 μM) for 24 hrs. The cells were then subjected to FACS analysis using CM-H_2DCFDA probe to analyze intracellular ROS levels. Incubation of 158N oligodendrocytes with H_2O_2 resulted in 5.6±0.8 fold increase in ROS levels

compared to the control. Additionally, we observed that co-incubation of the cells with both NAC and H_2O_2 prevented the increase in ROS in a concentration-dependent manner (Figure 4-1).

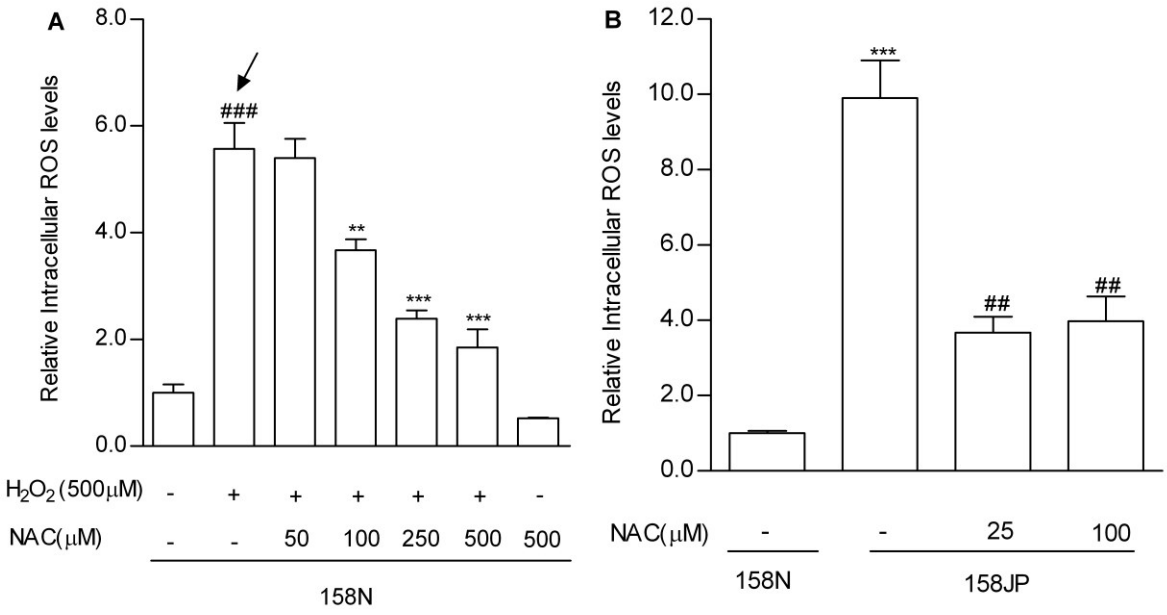

Figure 4-1 *Incubation with NAC decreased ROS in 158N (A, exogenous ROS, n=3) and 158JP (B, endogenous ROS, n=3) cells. A) Incubation of 158N cells with H_2O_2 increased ROS levels (as indicated by arrow). Addition of NAC (50-500μM) for 24hrs decreased ROS levels as measured by FACS. Medium treated 158N cells were used as control. # # # $p<0.001$ indicates significant difference between H_2O_2 and control; ** $p<0.01$, ***$p<0.001$; indicate significant difference between NAC+ H_2O_2 treatments and H_2O_2 alone. B) 158N cells and 158JP cells cultured in medium were compared side by side. ***$p<0.001$ indicate significant difference in the spontaneous ROS production between*

158N and 158JP cells. Addition of NAC (25 μM and 100 μM) for 24hrs decreased the endogenous ROS levels in 158JP cells. # # p<0.01 indicate significant difference between 158JP cells in medium and cells treated with NAC. All data were normalized to 158N control (ROS levels= percentage of stained cells in each group/percentage of stained cells in 158N control). ANOVA followed by Bonferroni test was used for statistical analysis.

In parallel, we conducted similar studies in a cell line with endogenous high ROS levels due to a mutation in proteolipid protein (158JP). These cells were observed to spontaneously generate higher ROS when compared to158N cells. The baseline ROS levels of 158JP cells were approximately 10-fold compared to 158N cells. We further characterized the effect of NAC in scavenging the endogenous ROS in these cells. The 158JP cells were incubated with NAC at 25μM and 100μM concentration for 24 hrs. Interestingly, we observed a significant decrease in baseline ROS levels (from 9.9±1.0 to 3.7±0.4) in these cells at NAC concentrations as low as 25μM (Figure 4-1 B). However, we did not observe a concentration-dependent decrease in ROS with NAC (no observed statistical difference between treatments of NAC 25μM and 100μM). The above results indicate that NAC can decrease both exogenous and endogenous ROS in oligodendrocytes.

4.3.2 Incubation with NAC improved cell survival in a concentration-dependent manner

We next investigated whether the reduction in ROS resulted in increased cell survival. For this purpose, cells were incubated with 500μM H_2O_2 alone or in combination with NAC (50-500μM) for 24hrs and then subjected to cell survival analyses. Exposure of 158N cells to 500μM H_2O_2 resulted in approximately 50% cell survival compared to control which is considered to be 100%. In contrast, the co-incubation of increasing concentrations of NAC (50-500μM) with H_2O_2 improved cell survival in a concentration-dependent manner (Figure 4-2). The survival rate in cells co-treated with 250μM NAC+ H_2O_2 was 77.3±1.3% as compared to 52.4±1.6% in cells treated with H_2O_2 alone ($p<0.001$) . This suggests that NAC plays a cytoprotective role in oligodendrocytes, preventing H_2O_2-induced cell death.

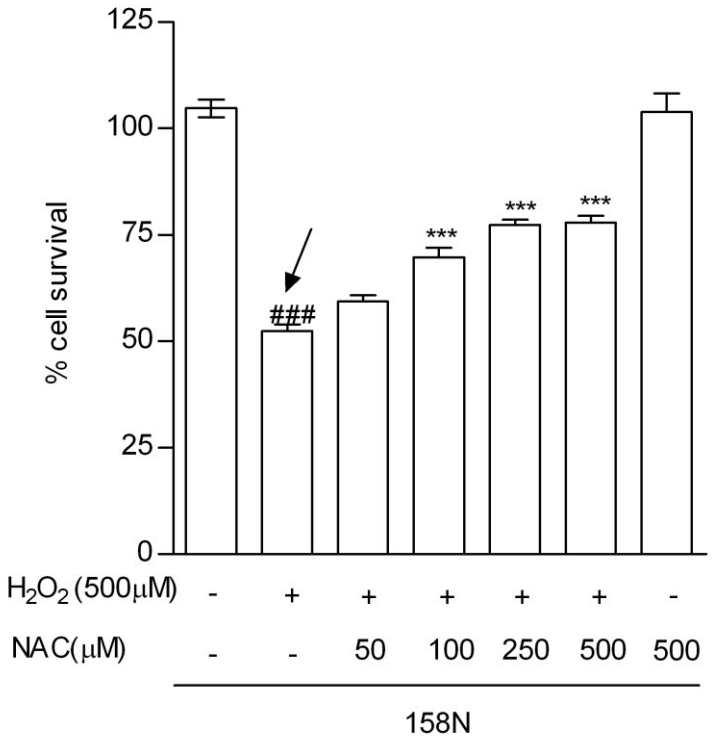

Figure 4-2 *NAC augmented cell survival under conditions of oxidative stress in a concentration dependent manner. Incubation with H_2O_2 induced cell death in 158N cells (as indicated by arrow). Addition of NAC (50-500μM) for 24hrs improved cell survival (n=6). Cells in culture medium were used as control. # # # $p<0.001$ indicate significant difference between cells treated with H_2O_2 and control; ***$p<0.001$; indicate significant difference between NAC+ H_2O_2 treatment and H_2O_2 alone. ANOVA followed by Bonferroni test was used for statistical analysis.*

4.3.3 Improved cell survival is attained by increase in intracellular total GSH levels

Next we were interested to explore the mechanism underlying the cytoprotective properties of NAC. For this we measured the total GSH levels in 158N cells under conditions of oxidative stress (500μM H_2O_2 for 24hrs) with or without the incubation of increasing concentrations of NAC (50-500μM for 24hrs). Intracellular GSH in 158N cells was found to be 24.3 ±1.3 μg/mg total protein. Further, we observed an increase in total GSH levels with increasing concentrations of NAC (Fig 4-3 A). The total GSH increased 1.7±0.02 fold with 500μM NAC relative to control. Incubation with 500μM H_2O_2 resulted in an 80% decrease of intracellular GSH (0.2 ± 0.01 fold of control). This depletion of total GSH was partially restored by co-incubation with 500μM each of NAC and H_2O_2 (0.58±0.04 fold of control). It is noteworthy that this nominal increase in GSH was sufficient to increase cell survival by ~80% (Figure 4-2).

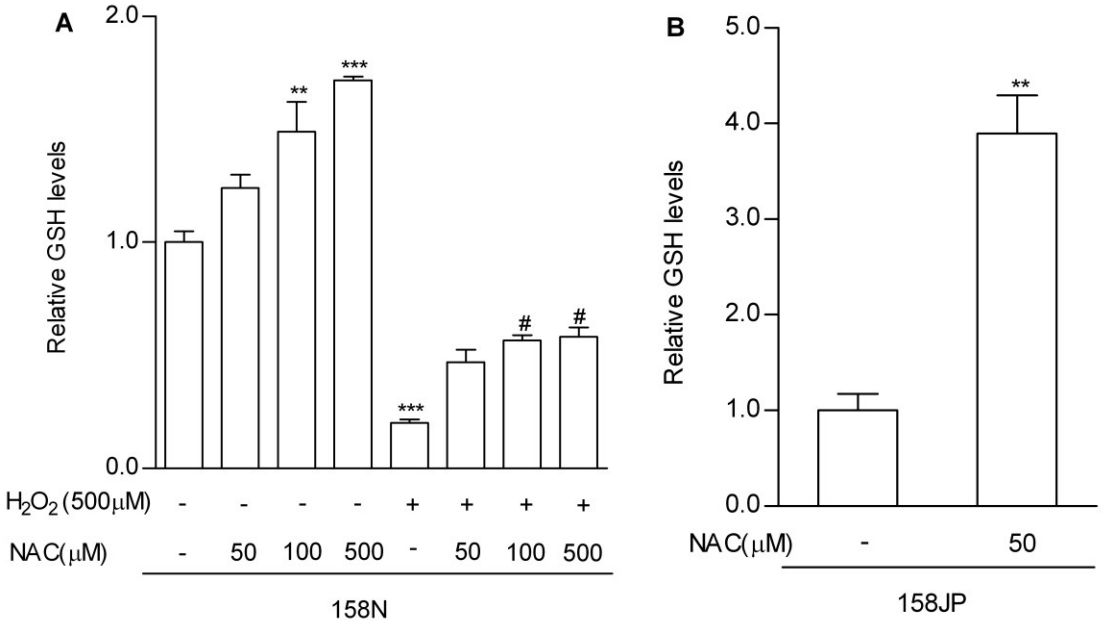

Figure 4-3 *LC-MS analysis of intracellular reduced form of GSH in 158N (A, n=3) and 158JP cells (B, n=3). A) NAC (50, 100 and 500 μM, 24hrs) increased GSH in 158N cells (**p<0.01, ***p<0.001) compared to control. Incubation of 158N cells with H_2O_2 (500 μM, 24hrs) reduced intracellular GSH levels significantly (***p<0.001). Upon NAC treatment, GSH levels were replenished significantly in a concentration-dependent manner (# p<0.05). ANOVA followed by Bonferroni test was used for statistical analysis. 3B) NAC (50μM, 24hrs) significantly increased GSH in 158JP cells (**p<0.01). Student's t-test was used for statistical analysis.*

Intracellular GSH in 158JP cells was observed to be 29.1±4.9 μg/mg total protein at baseline. Despite high intracellular ROS, the GSH level was higher in these cells compared to normal oligodendrocytes. This is consistent with previous observations

(Baarine et al., 2009a). In order to examine whether NAC can replenish GSH in cells with endogenous high ROS levels, we measured the total GSH levels in 158JP cells following incubation with a low concentration of NAC (50 μM). Remarkably, incubation with NAC increased the total GSH levels by 3.9±0.4 fold as compared to control (Figure 4-3 B).

4.3.4 Inhibition of GSH synthesis blocked cytoprotective effects of NAC

In order to further analyze the role of intracellular GSH in mediating the cytoprotective effects of NAC, we performed inhibitor studies in 158N cells using 50μM of BSO, a well-known GSH synthesis inhibitor (Drew and Miners, 1984). The 158N cells were co-incubated with H_2O_2, NAC or BSO in different combinations as indicated for 24hrs and then subjected to cell survival assays. Incubation of cells with 500μM H_2O_2 resulted in 52.0±1.6% cell death. Supplementation of 250μM NAC increased cell survival to 79.7±1.5% (Figure 3-4). Addition of BSO blocked cell survival (decreased to 71.4±1.8 %, $p<0.05$). These results indicate that inhibition of GSH synthesis reduces the cytoprotective effects of NAC.

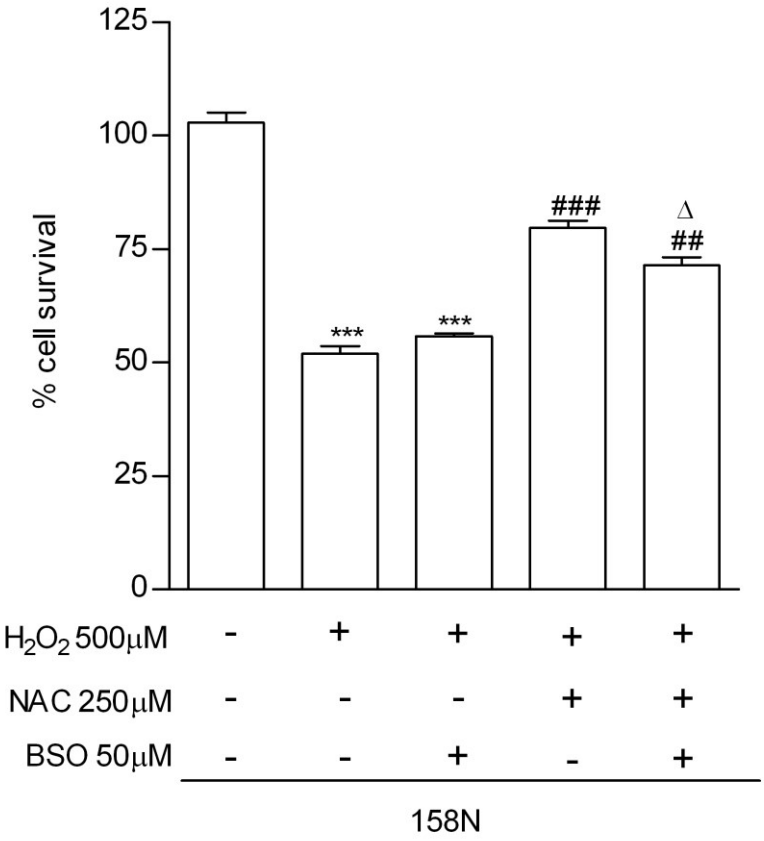

Figure 4-4 *Inhibition of GSH synthesis blocked cytoprotective effects of NAC. Cell survival assays were performed in presence of GSH synthesis inhibitor (BSO) in 158N cells (n=6). *** $p<0.001$ indicate significant cell death following H_2O_2 (500 μM, 24hrs) treatment compared to control. ### $p<0.001$ indicate the cytoprotective effects of NAC (250μM, 24hrs) compared to H_2O_2 treated group. Δ $p<0.05$ indicate significant difference in cell survival between cells treated with NAC+H_2O_2 +BSO compared to NAC+H_2O_2 co-treatment group. ## $p<0.01$ indicate that observed cell survival in presence of BSO was higher than H_2O_2 treated group. ANOVA followed by Bonferroni test was used for statistical analysis.*

4.3.5 Heme oxygenase-1 is a potential mediator of the cytoprotective effects of NAC

In order to further delineate the mechanisms by which NAC causes cytoprotection, we investigated the role of a well-known inducible cytoprotective protein, heme oxygenase-1 (HO-1) Towards this end, we performed inhibitor studies in 158N cells using chromium mesoporphyrin IX (CrMP, 30μM), a selective inhibitor of HO-1 activity (Appleton et al., 1999). The 158N cells were co-incubated for 24 hrs with H_2O_2, NAC or CrMP in different combinations as indicated and then subjected to cell survival assays. Incubation of NAC (50-500μM) with H_2O_2 (500μM) showed improved cell survival (Figure 4-5, solid grey bars) compared to H_2O_2 treated group. However, addition of CrMP resulted in a significant decrease in cell survival (Figure 4-5, checkered bars) with the survival rate being comparable to the H_2O_2 treated group. This indicates that the cytoprotective properties of NAC were abolished by CrMP treatment. Interestingly, the cytoprotective effects of NAC at 500μM was not affected by the addition of CrMP, suggesting either the incomplete inhibition of HO-1 activity or that cytoprotection by NAC at higher concentrations utilized mechanisms other than HO-1 activity.

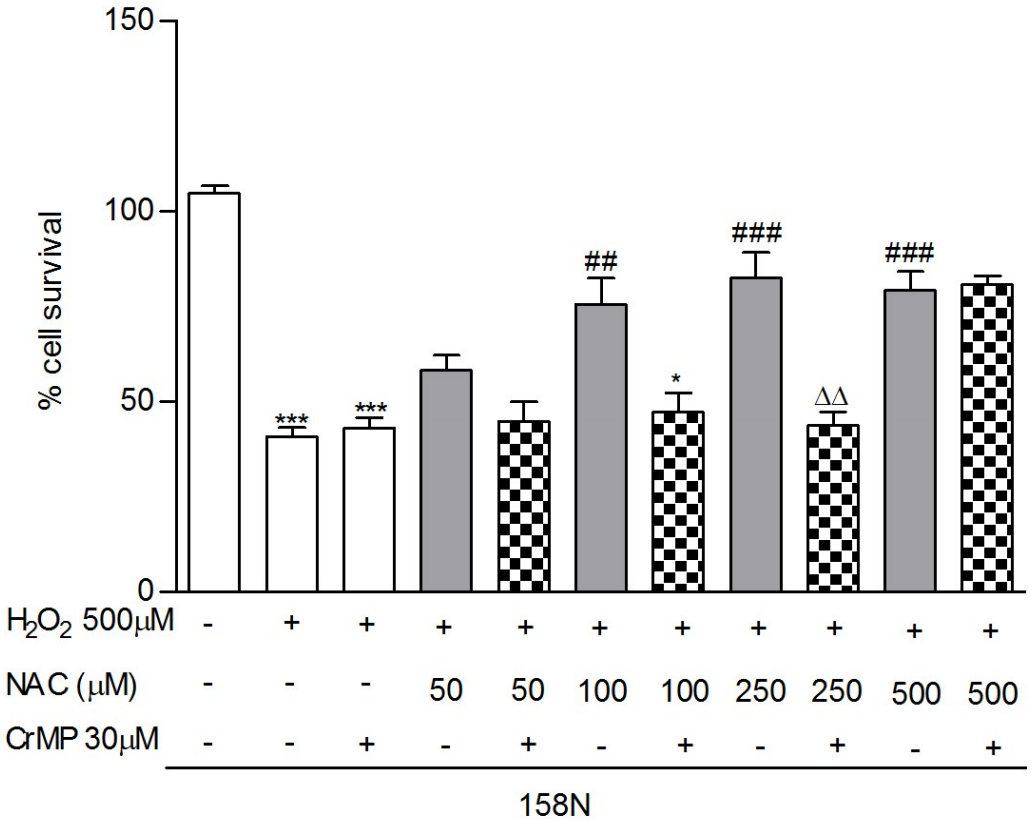

Figure 4-5 *HO-1 plays a vital role in the cytoprotective action of NAC. Cell survival assays were performed in presence of HO-1 activity inhibitor (CrMP) (n=6). *** $p<0.001$ indicate significant cell death following H_2O_2 treatment compared to control. ##$p<0.01$ and ###$p<0.001$ indicate the cytoprotective effects of NAC (50-500 μM, 24hrs, solid grey bars) compared to H_2O_2 treated group. The addition of CrMP abolished the cytoprotective effects of NAC (50-250 μM, 24hrs) as shown (checkered bars).*$p<0.05$, ΔΔ $p<0.01$ indicate significant decrease in cell survival rate after the addition of CrMP (30 μM) in NAC+ H_2O_2 co-treated group. ANOVA followed by Bonferroni test was used for statistical analysis.*

In order to further confirm that CrMP in fact inhibits the downstream antioxidant activity of HO-1, we analyzed the total antioxidant capacity (TAC) in these experimental conditions (Figure 4-6). This kit measures the combined antioxidant activities of vitamins, proteins, lipids, GSH, uric acid, etc. present in cell lysates. The baseline TAC levels in 158N cells were measured as equivalent to 0.28 ±0.01 μmol/mg total protein of Trolox. Upon incubation with NAC (100μM, 24 hrs), TAC levels were increased to 0.34±0.02μmol/mg total protein of Trolox (1.2±0.07 fold of control). In contrast, the incubation of H_2O_2 (500μM) decreased TAC levels to 0.13±0.03 μmol/mg total protein of Trolox (0.45±0.1 fold of control), indicating oxidative stress in the cells. Co-treatment of H_2O_2 (500μM) and NAC (100μM) significantly increased the TAC approximately to baseline levels (0.24±0.03 μmol/mg total protein of Trolox). However, addition of CrMP (30μM) along with NAC and H_2O_2 resulted in significant decrease in TAC to levels comparable to oxidative stress conditions. These results are in line with our observation that inhibition of HO-1 activity can effectively abolish the cytoprotective effects of NAC.

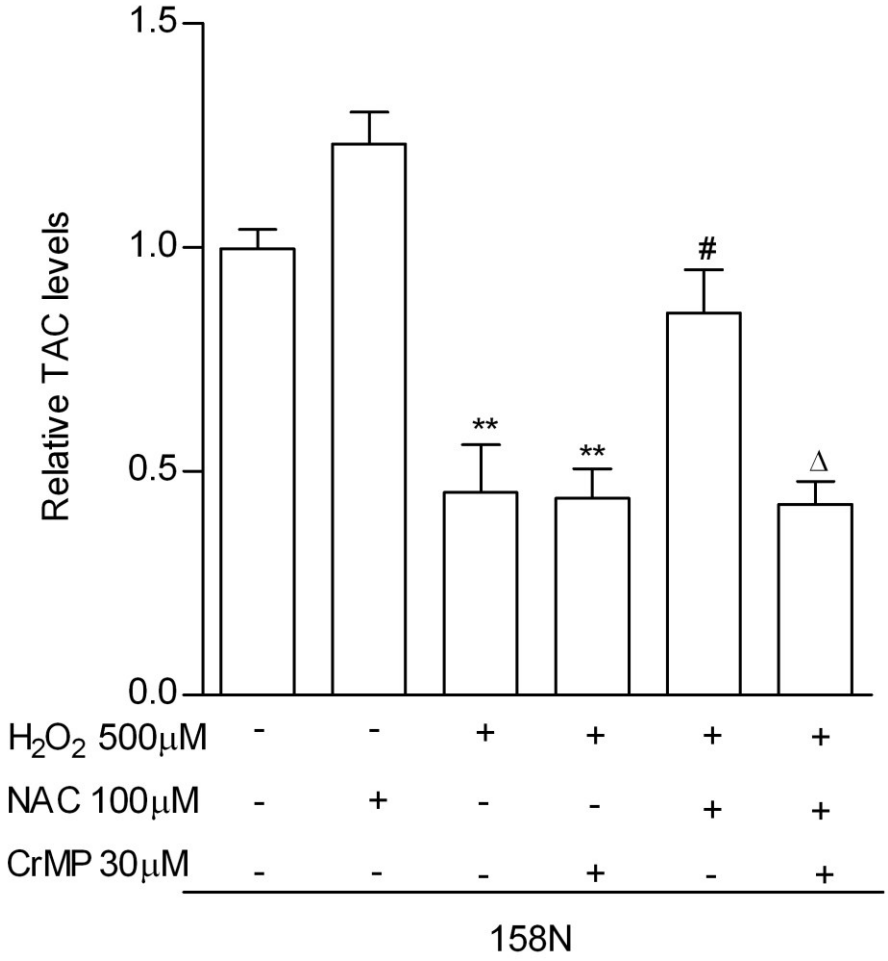

Figure 4-6 *Total antioxidant capacity (TAC) assays in presence of HO-1 activity inhibitor (CrMP) (n=3). **p<0.01 indicate that H_2O_2 treatment (500 μM, 24hrs) significantly decreased the total amount of antioxidants in cell lysates compared to control. # p<0.05 indicate that the addition of NAC (100 μM, 24hrs) increased TAC of the system compared to H_2O_2 only group. Δ p<0.05 indicate that the addition of CrMP (30 μM) inhibited the effects of NAC. ANOVA followed by Bonferroni test was used for statistical analysis.*

4.4 Discussion

In this study, we describe the mechanisms underlying the cytoprotective effect of NAC in oligodendrocytes in conditions of oxidative stress. Oxidative stress is associated with depletion of intracellular GSH resulting in decreased cell survival (Aoyama and Nakaki, 2013). NAC is a prodrug that increases biosynthesis of GSH levels, but we show for the first time that the cytoprotective properties of NAC are, in part, dependent on the activity of the antioxidant protein HO-1.

Oligodendrocytes are crucial glial cells in the CNS that are involved in the formation of myelin sheath (Harauz et al., 2004). Loss of the myelin sheath, also called demyelination, is a hallmark of several neurodegenerative diseases including multiple sclerosis and X- linked ALD. Although the precise mechanism by which demyelination occurs has not been determined, there are reports describing the presence of oxidative stress markers in demyelinating lesions of the patients' brain (Smith et al., 1999). Interestingly, oligodendrocytes are the most sensitive cell type in the brain to oxidative stress *in vitro* compared to both astrocytes and neuronal cells (Smith et al., 1999) and the death of these cells is an early event in a CNS demyelination rat model (Zhang et al., 2013). These reports indicate that mitigating oxidative stress in oligodendrocytes may have a role as therapy for neurodegenerative disorders. Antioxidants such as NAC, lipoic acid and tocopherol (Vitamin E) have been widely investigated in diseases associated with oxidative stress such as diabetes, brain injury, multiple sclerosis and X-ALD

(Gilgun-Sherki et al., 2004, Satpute et al., 2010, Lopez-Erauskin et al., 2011b, Hegazy et al., 2013, Ishaq et al., 2013). In this study, we utilized a mutated oligodendrocyte cell line, 158JP that showed endogenously high levels of spontaneous ROS as well as a normal oligodendrocyte cell line 158N, in which H_2O_2 was exogenously used to mimic oxidative stress.

NAC is an effective free radical scavenger as well as a precursor for intracellular cysteine and GSH. It helps maintain intracellular levels of the antioxidant GSH by providing the rate-limiting substrate cysteine for GSH synthesis (van Zandwijk, 1995a, Rushworth and Megson, 2013a). GSH is an endogenous non-enzymatic scavenger of free radicals, and depletion of GSH is an indicator of oxidative stress (Wu et al., 2004a). Using ^{1}H magnetic resonance spectrometry, Low GSH levels are found in brain tissues of patients with multiple sclerosis (Choi et al., 2011b). Further, impaired GSH biosynthesis is found in Parkinson's disease (Zhou and Freed, 2005b, Choi et al., 2006b). And impaired utilization of GSH is observed in Alzheimer's disease (Lovell et al., 1998). GSH levels in blood cells of X-ALD patients are also observed to be lower compared to control (Petrillo et al., 2013a). The increased interest in using NAC for a wide range of unrelated diseases necessitates the need to better understand its pharmacology. Our observation that NAC replenished GSH and consequently improved glial cell survival under conditions of oxidative stress is consistent with previously published report (Badisa et al., 2013). Further, we confirmed this observation using an inhibitor of GSH synthesis (BSO). BSO is an established specific inhibitor of glutamate cysteine ligase (GCL, the rate-limiting

enzyme in GSH synthesis) and treatment with BSO reduced levels of intracellular GSH (Dusre et al., 1989, Zaman et al., 1995).

Moreover, our study documents the critical role of HO-1 in mediating the cytoprotective effects of NAC. HO-1 has been proposed as a potent protective protein against oxidative stress in both *in-vitro* neuronal cells (Le et al., 1999) and *in-vivo* oxidative stress mouse models of ischemia (Panahian et al., 1999) and Huntington's disease (Colin-Gonzalez et al., 2013). Further, impairment of HO-1 expression or post-transcription modification plays an important role in neurodegenerative disorders including Parkinson's disease (PD) (Chien et al., 2011) and Alzheimer's disease (AD) (Barone et al., 2012). Although the exact role of HO-1 is still under debate, upregulation of HO-1 is assumed to be an early adaptive event in response to stress (Barone et al., 2013).

HO-1 is highly inducible by a variety of chemical or physical agents (Chien et al., 2011). For example, the HO-1 signaling pathway is under a feedback regulation wherein the accumulation of its substrate, heme, induces the expression of HO-1. Other inducers include heavy metals, endotoxin, heat shock, inflammatory cytokines, and prostaglandins that directly or indirectly generate ROS (Choi and Alam, 1996, Ryter and Choi, 2005). In addition to oxidative stress related inducers, HO-1 is also found to be induced and mediate the antioxidant effects of aspirin (Grosser et al., 2003, Sparatore et al., 2009) and statins (Grosser et al., 2004, Hinkelmann et al., 2010, Kim et al., 2012, Li et al., 2012). Interestingly, HO-1 is also found to mediate the antioxidant effects of a variety of

antioxidants such as α-lipoic acid (Ogborne et al., 2005, Lin et al., 2013), S-adenosyl methionine (Erdmann et al., 2008), curcumin and resveratrol (Son et al., 2013), L-methionine (Erdmann et al., 2005) and 3-O-caffeoyl-1-methylquinic acid (Kweon et al., 2004). Our results with CrMP also demonstrate HO-1 is an important mediator of the cytoprotective action of NAC in oligodendrocytes, which in turn, correlated with a decrease in total antioxidant capacity (TAC). NAC has been shown to elevate HO-1 levels through enhancement of Brahma-related gene 1 (Brg1) in cardiac tissues (Xu et al., 2013). In another study conducted in diabetic rats, it was shown that the cardiac protective effects of antioxidants NAC and allopurinol were abolished with HO-1 inhibitors, showing the important role of HO-1 as a signaling mediator (Mao et al., 2013). This is in contrast to the several studies were NAC was used to attenuate HO-1 expression (Rensing et al., 1999, Kim et al., 2013). This is because NAC is a free radical scavenger (Aruoma et al., 1989, Cotgreave, 1997). By removing free radicals, NAC can decrease HO-1 expression induced by higher ROS levels.

Previously in our lab, we have determined the HO-1 promoter activity in NIH3T3-HO-1-*luc* cells using *in vivo* bioluminescence imaging (Sparatore et al., 2009). Using the same model, treatment with NAC (50-1000μM) revealed a signal towards an increase in luciferase activity as early as 2 hours after NAC treatment, which was sustained up to 8 hours and decreased to below baseline levels by 24 hours (Erdman. K, unpublished data). Recently treatment of rat retinal ganglion cells with NAC showed an increasing trend of HO-1 expression in during normal redox conditions (~1.5 fold) (Majid et al., 2013).

These data indicate the ability of NAC to induce HO-1 expression under optimal conditions, and here we demonstrate HO-1 as a mediator of NAC action in protecting oligodendrocytes from oxidative stress damage.

4.5 Conclusions

In summary, we investigated the mechanisms by which NAC mitigates oxidative stress in oligodendrocytes. We have demonstrated that HO-1 is a signaling mediator critical for NAC action. NAC reduces ROS, supplements intracellular GSH as well as protects 158N cells thereby improving survival in conditions mimicking oxidative stress. Moreover, NAC boosted GSH levels in 158JP oligodendrocytes which have high ROS levels. Notably this antioxidant property was evident in these mutant cells at lower NAC concentrations compared to normal oligodendrocytes highlighting the therapeutic benefit of NAC in genetic conditions causing oxidative stress. In addition to its role as a free radical scavenger, our study shows other important mechanisms of NAC action, which may permit more effective use of this antioxidant in disorders with oxidative stress.

CHAPTER 5

N-ACETYLCYSTEINE REVERSES MITOCHONDRIAL TOXICITY OF VERY LONG CHAIN FATTY ACIDS IN MURINE OLIDODENDROCYTES

5.1 Introduction

Mutations in ABCD1, the peroxisomal membrane transporter of very long chain fatty acid (VLCFA), cause ALD. Since degradation of VLCFAs requires these molecules to be transported into peroxisomes to facilitate β-oxidation, mutations in ABCD1 transporter impair regular degradation of VLCFAs and cause intracellular accumulation of VLCFAs. Igarashi *et al.* for the first time reported observation of increased levels of VLCFAs such as hexacosanoic acid (C26:0) in the brain and adrenal tissues of ALD patients (Igarashi et al., 1976). However, the detailed pathogenesis is largely unknown. CCALD is one type of ALD with manifestations of demyelination and CNS neurodegeneration affecting boys at 4-10 years old (Steinberg et al., 1993). Currently only limited therapeutic interventions are available to CCALD patients. Thus better understanding of the contribution of VLCFAs in CCALD disease pathology could greatly facilitate the research towards therapies.

It is known that degradation of long-chain fatty acids requires the collaboration of mitochondria in addition to peroxisomes (Hashimoto et al., 1999). Recently, growing evidence indicates a close relationship between VLCFAs accumulation and mitochondrial dysfunction: the rate of peroxisomal VLCFA β-oxidation is affected by mitochondrial dysfunction (McGuinness et al., 2003) and decreased mitochondria function parameters were observed in ALD *in vitro* and *in vivo* models (Fourcade et al., 2008, Hein et al., 2008, Fourcade et al., 2013, Lopez-Erauskin et al., 2013). Mitochondria

are involved in scavenging free radicals and store antioxidants such as GSH and harbor detoxifying enzymes (Schrader and Yoon, 2007). It plays a central role in initiating and regulating programmed cell death or apoptosis (Wang and Youle, 2009). Thus even if the primary cause of a pathology is unrelated to mitochondria, mitochondrial dysfunction is a significant secondary factor in determining clinical outcomes (Smith and Murphy, 2011). Among the arsenal of protective mechanisms, mtGSH has emerged as the main line of defense by the maintenance of optimal redox environment within the organelle (Fernandez-Checa et al., 1998). As shown in various pathological conditions, loss of mtGSH pre-disposed the cell towards oxidant-induced injuries including cerebral ischemia (Anderson and Sims, 2002) and hypoxia (Lluis et al., 2005). Thus strategies aimed at the restoration of mtGSH could possibly de-sensitize the cells to VLCFAs and in turn improve cell survival.

Research into the restoration of mitochondrial function has been widely reported using antioxidants (Fedotcheva et al., 2012, Singh et al., 2012, Nguyen et al., 2013). NAC is a well-known antioxidant, precursor for the crucial intracellular antioxidant GSH (van Zandwijk, 1995b) that protects against damage from free radicals (Wu et al., 2004b). NAC was shown to effectively suppress lipid peroxidation induced mitochondrial injury in primary neuronal cells (Arakawa et al., 2006). And it was shown to play a protective role through targeting mitochondria in neurodegenerative disorders such as Alzheimer's disease (Robinson et al., 2011) and Parkinson's disease (Bagh et al., 2008).

In this study, we investigated the mitochondrial toxicity induced by VLCFAs and focused specifically on its influence on the change of mtGSH in 158N cells. Further, an effort was made to test the possible therapeutic effects of NAC on reversing the toxicity of VLCFAs.

5.2 Materials and methods

5.2.1 Materials

Dulbecco's Modified Eagle Medium (DMEM) high glucose media, fetal bovine serum (FBS), and antibiotic-antimycotic (AA), phosphate buffered saline (PBS), Trypsin-EDTA and fluorescent CM-H_2DCFDA probes and MitoSOX^{TM} probes were obtained from Life Technologies, (CA, USA) and 7-AAD was from BD Biosciences (CA, USA).

Hexacosanoic acid (C26:0), acrolein, N-acetyl-L-cysteine (NAC), sucrose, mannitol and ethylene glycol-bis (2-aminoethylether)-N, N, N′, N′-tetraacetic acid (EGTA) were purchased from Sigma-Aldrich (MO, USA). HEPES 1M solution was from Mediatech (VA, USA). Hexacosanoic acid was dissolved in ethanol (heated to 37 °C) at 2.5mM as stock solution. The following validated kits were used: Cell Counting Kit-8 from Dojindo (Kumamoto, Japan), JC-1 Mitochondrial Membrane Potential Assay Kit and Glutathione Assay Kit from Cayman Chemical (MI, USA), Mitochondria Isolation Kit for Cultured Cells from (Thermo Scientific, IL, USA), Quick Start Bradford Protein Assay from Bio-Rad (CA, USA) and ATPlite™ Luminescence Assay System from PerkinElmer (MA,

USA). Stock Solutions of all chemicals were made and culture medium was used to prepare working solutions. The pH of the NAC stock solution (10mM) was adjusted to 7.4 and filtered prior to making further dilutions.

5.2.2 Cell culture and treatments

An immortalized murine oligodendrocyte cell line, 158N (normal) was a generous gift from Dr. Ghandour (Baarine et al., 2009b). Around 10^6 cells were seeded on 75 cm^2 culture flasks (Corning, NY, USA) in DMEM high glucose media supplemented with 5% FBS and 1% AA. Cells were incubated overnight in 37 °C incubator with 5% CO_2. For experimental set up, cells were seeded on 75 cm^2 culture flasks; 24-well or 96-well plates and cultured overnight to get 80% confluence. Cells were challenged for 24hrs with 1-100 µM Hexacosanoic acid (C26:0), to mimic disease conditions. NAC, at concentrations ranging from 50µM to 500µM, was co-incubated with C26:0 for 24 hours to examine the therapeutic effects of NAC.

5.2.3 Cell survival assays

Cell survival following various experimental treatments was quantified using colorimetric assays on treated cells cultured in 96-well plates. Cell Counting Kit-8 from Dojindo was used to determine the cell viability following manufacturer's protocol.

5.2.4 Evaluation of intracellular ROS

Evaluation of intracellular ROS was performed by Fluorescence Assisted Cell Sorting (FACS) using fluorescent CM-H_2DCFDA probe. Briefly, after 24 hours of experimental treatments, cells seeded on 24-well plates were harvested and washed twice with PBS. The cells were then stained with 1μM CM-H_2DCFDA for 5min. The samples were subsequently washed twice and resuspended in 250 μl PBS containing 5μl 7-AAD for analysis. During acquisition of FACS data, the live cells (negative for 7-AAD) were gated and evaluated for ROS with CM-H_2DCFDA. Further, the fluorescence intensity of CM-H_2DCFDA was also gated uniformly to designate positive events of CM-H_2DCFDA stained cells. The % gated for positive stained CM-H_2DCFDA was used as the indicator for ROS levels in different treatment groups.

5.2.5 Determination of intracellular GSH

Cells seeded on 24-well plates were subjected to different experimental conditions. At the end of incubation, the cells were washed twice with PBS and the harvested cells were lysed using lysis buffer (20mM HEPES, 1mM EGTA, 210mMmannitol and 70mM sucrose, pH7.2). Intracellular GSH was analyzed by Glutathione Assay Kit from Cayman Chemical. Total protein levels were analyzed by Quick Start Bradford Protein Assay Kit from Bio-Rad. All manufacture's protocols were followed. Total GSH levels in each group were normalized to total protein levels to obtain GSH concentrations in μg/mg.

GSH levels in cells incubated with culture medium served as control and were used to normalize across different groups.

5.2.6 Mitochondrial inner membrane potential

Mitochondrial inner membrane potential was measured by JC-1 (Mitochondrial Membrane Potential Assay Kit) according to manufacturer's protocol and measured by both fluorescence microplate reader SpectraMax from Molecular Devices (CA, USA) and fluorescence microscope Zeiss Axiovert 200M(Germany). (J- aggregates (red): excitation/emission= 560/595nm; JC-1 monomers(green): excitation/emission= 485/535nm)

Following treatments, digital images were taken by an inverted fluorescence microscope fitted with a matched Axiocam 4 mega-pixel camera. Images were captured using 20× objective lens (N.A. 0.3) to characterize the JC-1 monomers inside the mitochondria. In addition, fluorescence microplate reader was also used to quantify the J-aggregates as well as JC-1 monomers in 96-well cell culture plates following treatments. The fluorescence ratio of JC-1 aggregates and JC-1 monomers was calculated for each well.

5.2.7 Mitochondrial superoxide levels

MitoSOX red reagent was used to quantify superoxide anion produced from mitochondria. MitoSOX permeates live-cells, target to mitochondria and exhibit red fluorescence once oxidized by superoxide. MitoSOX stained cells were measured by fluorescence microscopy.

Following treatments, digital images were taken by an inverted fluorescence microscope (Zeiss Axiovert 200M) fitted with a matched Axiocam 4 mega-pixel camera. Images were captured using 20× objective lens (N.A. 0.3). The excitation/emission spectra for MitoSOX were set up at 510/580nm as manufacture's protocol.

5.2.8 Mitochondrial GSH (mtGSH) levels

Mitochondria were isolated using Mitochondria Isolation Kit for Cultured Cells following experimental treatments. Isolated mitochondria were further lysed with buffer (20mM HEPES, 1mM EGTA, 210mMmannitol and 70mM sucrose, pH7.2). Subsequently mtGSH levels were measured using GSH assay kit the same way as the determination of the intracellular GSH. Total protein levels were measured and acquired mtGSH levels were expressed in μg/mg total protein. mtGSH levels in cells treated with culture medium served as control and were used to normalize across different groups.

5.2.9 ATP production analysis

ATPlite™ Luminescence Assay System was used to detect ATP production as per manufacturer's protocol on 24-well cell culture plates post experimental treatments.

5.2.10 Statistical analysis

For all cellular assays, results were expressed as means ± standard error. Data was analyzed using ANOVA with a Bonferroni's correction for multiple comparisons or Dunnett's test in case of performing multiple comparisons towards the control. A p-value <0.05 was considered significant. Analyses are based on data from three independent experiments using different cell passages on different days.

5.3 Results

5.3.1 VLCFAs reduce cell survival and ATP production

Murine oligodendrocyte cells (158N) were exposed to increasing concentrations of hexacosanoic acids (C26:0) (range from 1-100 μM) for a period of 24hrs. Ethanol treated cells were used as vehicle control. Cell viability and intracellular ATP production were measured following C26:0 treatments. The survival of oligodendrocytes was not significantly influenced by incubation with C26:0 at concentrations less than 25μM (Figure 5-1 A). However, the cell survival rates were significantly lower at 25μM (84±3%) and 50 μM (60±8%) C26:0, compared to vehicle control (Dunnett's test,

p<0.01). Moreover, we observed a concentration- dependent decrease in ATP production following treatment with C26:0 (Figure 5-1 B), suggesting there might be potential toxicity of VLCFAs on mitochondria where most of the ATP is produced. The concentration of C26:0 at 25μM seemed to be quite interesting in that though cell death at this concentration was ~15%, ATP production was found to be significantly lower compared to vehicle controls (Dunnett's test, p< 0.05). Combined together, the lower toxicity limit was found to be 25 μM for C26:0 on both cell survival and ATP production.

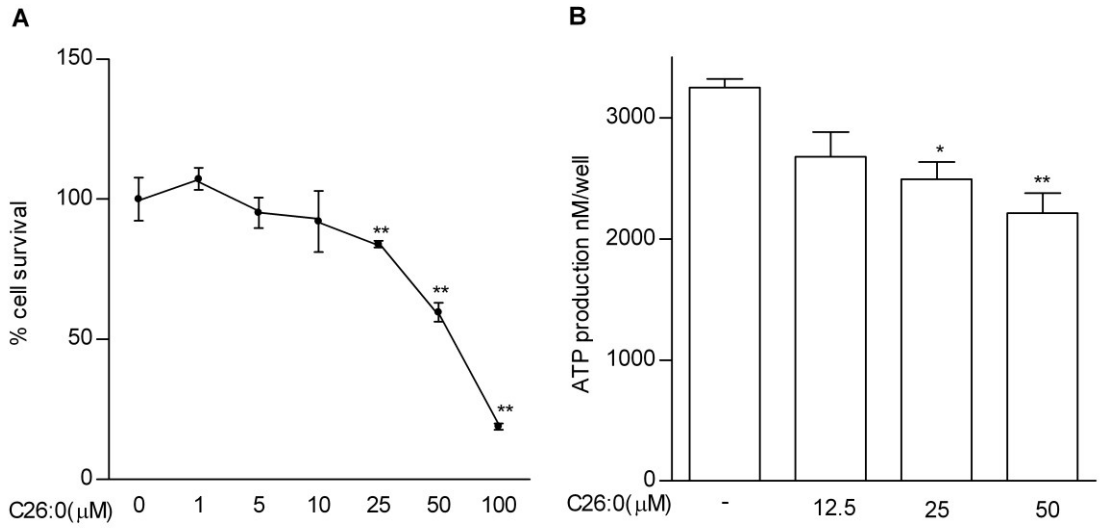

Figure 5-1 *C26:0 reduced cell survival (A) and ATP production (B) in a concentration dependent manner. A) Percentage of viable 158N cells after incubation with C26:0 (0-100 μM) for 24 hrs are shown (Fig 1A, n=6). At concentrations of C26:0 equal to and higher than 25 μM, significant cell death was observed, ** p<0.01, ANOVA followed by Dunnett's test. 1% and 2% ethanol were both used as control and no difference was observed between controls (data not shown). B) ATP production was also evaluated after incubation with C26:0 (0-50 μM) for 24 hrs (Fig 1B, n=6). At concentrations of C26:0*

*equal to and higher than 25 µM, significant decrease in ATP production compared to ethanol control was observed, *p<0.05, ** p<0.01, ANOVA followed by Dunnett's test.*

5.3.2 VLCFAs do not cause significant changes in cellular oxidative stress

In order to evaluate the effect of VLCFAs on oxidative stress, we analyzed ROS (as measured by H_2DCFDA) and intracellular GSH (total) levels in oligodendrocytes following treatment with C26:0 at the threshold concentration 25 µM for 24 hrs. Although the trend of increased ROS formation was observed, the increase was not significant compared to vehicle treated controls (Figure 5-2, t test, p=0.17). Importantly, 25 µM C26:0 did not cause any depletion in total GSH (Figure 5-3 A, t test, p=0.99) as compared to vehicle controls.

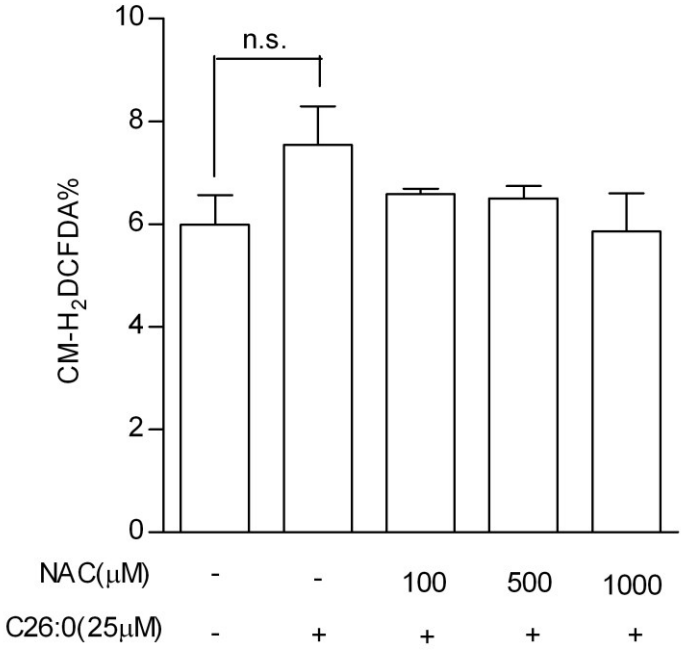

Figure 5-2 *ROS levels in 158N cells after incubation with C26:0 and NAC for 24 hrs were measured (n=3) and 25μM C26:0 did not change cellular ROS levels as measured by H_2DCFDA. No statistical significance was observed between ethanol control and 25 μM C26:0 treatment (t test, p =0.17). Additional co-incubation of NAC (100-1000 μM) did not change cellualr ROS levels either.*

5.3.3 VLCFAs deplete mtGSH, affect mitochondrial redox balance and induce mitochondrial depolarization

Although low levels of VLCFAs did not affect the cellular oxidative stress, there was ~16% cell death and ~23% decrease of ATP production on exposure to 25 μM C26:0 for 24 hrs. To further understand how C26:0 exerts its toxicity on cells, several key parameters describing mitochondrial redox status and function were measured including levels of mtGSH, superoxide anions and mitochondrial inner membrane potential (ΔΨm). Interestingly, although VLCFAs did not cause any depletion in total GSH (Figure 5-3 A, t test, p=0.99), we observed a significant depletion to ~0.2 fold of control in the levels of mtGSH (Figure 5-3 B, t test, $p<0.01$), indicating that VLCFAs have a major influence on the mitochondrial antioxidant defense system. This observation of depletion in mtGSH without any change in total GSH may also indicate possible translocation of intracellular total GSH from mitochondria to cytosol induced by C26:0 treatments.

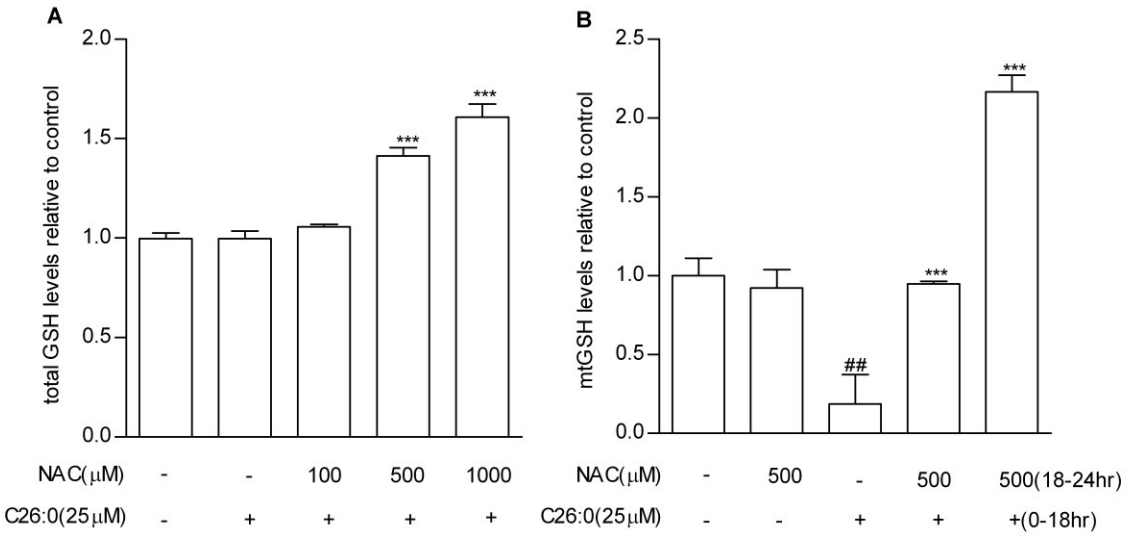

Figure 5-3 *Total intracellualr GSH (A) and mtGSH levels (B) in 158N cells were measured after incubation with C26:0 and NAC for 24 hrs (n=3). A) No statistical significance in total GSH was observed between control and C26:0 (25μM) (t test, p=0.99). Additional co-incubation of NAC (100-1000 μM) increased total GSH in a concentration dependent manner (A; ***p<0.001, ANOVA followed by Dunnett's test); B) Significant decrease in mtGSH was observed between control and C26:0 (25μM) (t test, p <0.01). Additional co-incubation of NAC (500 μM) restored mtGSH depleted by C26:0 (B; ***p<0.001 indicates significant increase in mtGSH with co-incubation of NAC compared to C26:0(25μM) treatment only; ANOVA followed by Bonferroni test). Moreover, mtGSH was increased to 2.2±0.1 fold of control when performing pre-treatment with C26:0 (25μM) for 18hrs followed by NAC (500 μM) only for 6hrs. 1% Ethanol treated cells served as control.*

Next we proceeded to examine the influence of C26:0 treatments on levels of superoxide anion. Superoxide anion (O_2^-) is produced mainly in mitochondria as the first free radical to drive further ROS production in mitochondria (Kirkinezos and Moraes, 2001).

MitoSOX red reagent that specifically target mitochondria was used to quantify superoxide anion. As shown in Figure 5-4, panel C, Treatment of 25 µM C26:0 for 24hrs greatly increased the superoxide anion levels as shown by the excited MitoSOX fluorescence (red). Solvent (1% ethanol) does not affect the mitoSOX fluorescence (data not shown). A concentration-dependent toxicity of C26:0 was also observed (Figure 5-4, panel B to C). These results indicate that VLCFAs increased the superoxide anion levels within mitochondria; however, the increase could be due to either accelerated superoxide anion production or impaired antioxidant defense system.

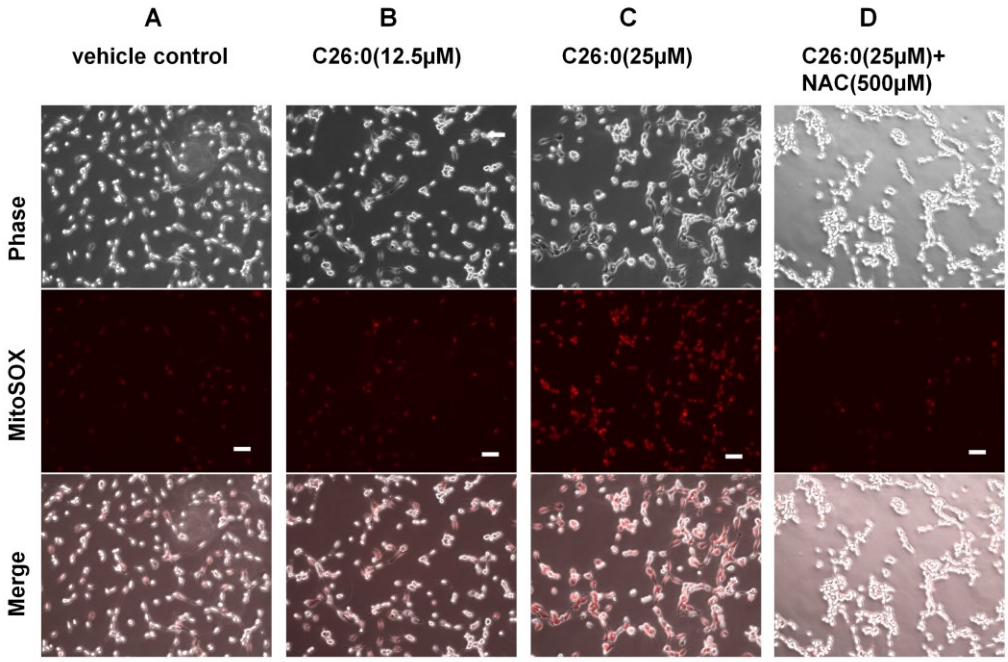

Figure 5-4 *C26:0 increased mitochondrial superoxide levels and NAC decreased the levels. Representative images of 158N cells showing increase in MitoSOX fluorescence (red) following treatment with C26:0 (0-25μM) for 24 hrs. Additional co-incubation of NAC (500 μM) notably decreased MitoSOX fluorescence indicating decreased levels of mitochondrial superoxide formation. No difference in MitoSOX fluorescence was observed bwtween vehicle control (1% Ethanol) and media control (data not shown).Scale bars represent 50 μm.*

To further characterize toxic effects of C26:0 on mitochondrial function, we measured another crucial parameter, mitochondrial inner membrane potential. JC-1 is a lipophilic fluorescent dye that acts as the mitochondrial inner membrane potential ($\Delta\Psi_m$) indicator. In healthy cells with high $\Delta\Psi_m$, JC-1 spontaneously formed J-aggregates with red fluorescence while in unhealthy cells with low $\Delta\Psi_m$, JC-1 remained in the monomeric form with green fluorescence. We monitored the green monomeric JC-1 dye specifically for tracking the unhealthy cells with low $\Delta\Psi_m$ by fluorescence microscopy. We observed that percentage of low $\Delta\Psi_m$ cells increased in a concentration-dependent fashion with increasing C26:0 (Fig 5-5, panel A to D). Accordingly, when we measured the ratio of healthy and unhealthy cells by fluorescent plate reader, we also observed decrease in the $\Delta\Psi_m$ (Fig 5-6). These results indicate that VLCFAs adversely affect the mitochondrial inner membrane potential.

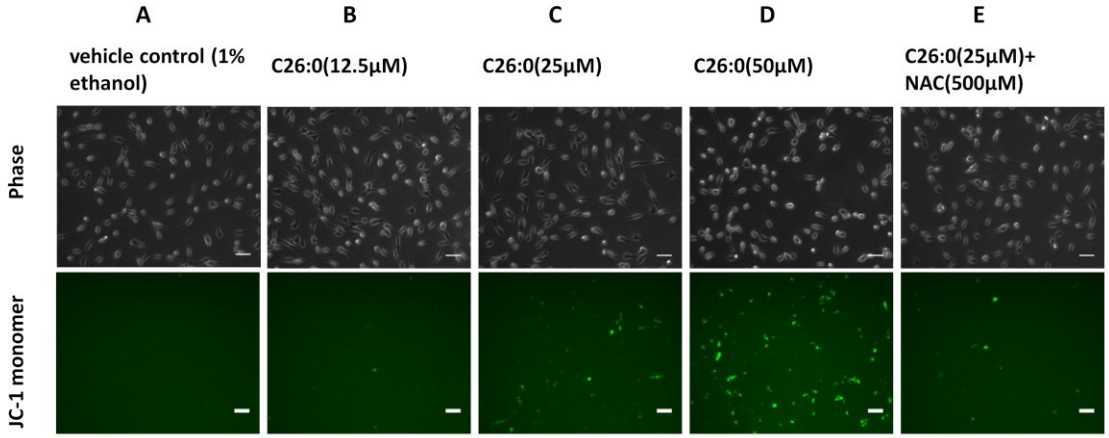

Figure 5-5 *C26:0 decreased mitochondrial inner membrane potential (ΔΨm) and NAC alleviated this effect. A): Representative images of 158N cells showing increase in JC-1 monomers (green fluorescence in dead cells) following C26:0 (0-50 µM) incubation for 24 hrs. Additional co-incubation of NAC decreased green fluorescence, indicating restoration of ΔΨm. Scale bars represent 50 µm.*

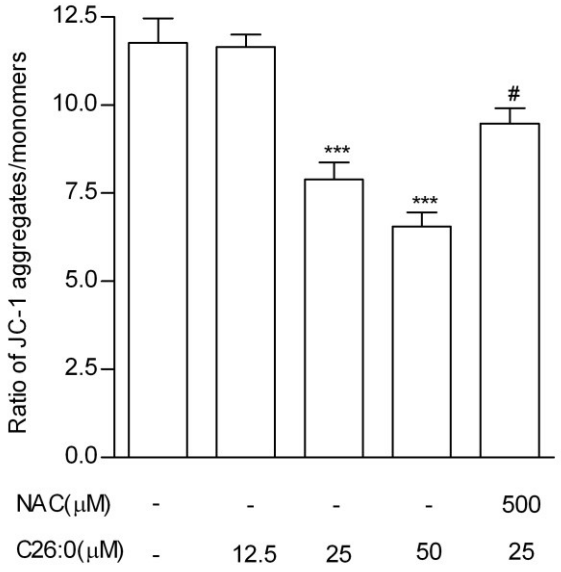

Figure 5-6 Bar plot indicated quantification of JC-1 fluorescence in 96-well plates. The ΔΨm decreased significantly following incubation with C26:0 (25μM and 50μM) compared to control ($p<0.001$, ANOVA followed by Dunnett's test). This mitochondrial toxicity was reversed by NAC (# $p<0.05$, ANOVA followed by Bonferroni test).

5.3.4 Effect of NAC treatment on VLCFA induced mitochondrial toxicity

We were interested to examine whether the mitochondrial specific effects of VLCFAs can be reversed by treatment with NAC. For this we co-incubated158N oligodendrocytes with 500μM NAC and 25 μM C26:0 for 24 hrs and performed similar analysis as mentioned in previous section.

NAC replenishes mtGSH

We analyzed both intracellular total GSH and mtGSH levels in 158N oligodendrocytes incubated with C26:0 (25 μM) and NAC (500 μM). We observed that NAC was able to replenish the mtGSH levels back to normal levels during co-incubation while intracellular total GSH was observed to increase simultaneously (Figure 5-3, A and B). In particular, pretreatment with C26:0 (25μM, 18hrs) followed by NAC (500μM, 6hrs) was found to induce the mtGSH levels to 2.2±0.1 fold of control, indicating NAC as a potent antioxidant to replenish mtGSH during depletion (Figure 5-3 B). These results suggest that replenishment of mtGSH is one potential mechanism by which NAC provides cellular protection.

NAC Reverses C26:0 Induced Increase in Mitochondrial Superoxide

In a parallel set of experiments, we evaluated the levels of superoxide anions within mitochondria after the co-incubation of NAC and C26:0 (Figure 5-4, panel C to D). C26:0 increased mitochondrial superoxide formation in oligodendrocytes in a concentration-dependent manner and addition of 500 μM NAC notably decreased MitoSOX fluorescence. Results indicate that treatment with NAC could effectively decrease superoxide anion levels in mitochondria.

NAC Alleviates C26:0 Induced Decrease in Mitochondrial Inner Membrane Potential (ΔΨm)

Previously, we observed C26:0 induced mitochondrial depolarization in 158N cells. The percentage of unhealthy cells increased (Figure 5-5, panel A to D) and mitochondrial inner membrane potential (ΔΨm) decreased (Figure 5-6). Subsequently, we evaluated the therapeutic effects of NAC in cells incubated with C26:0. Surprisingly, 500 μM NAC was shown to effectively decrease the percentage of unhealthy cells (Figure 5-5, panel E), as well as increase $\Delta\Psi_m$ (Figure 5-6). These results indicate that NAC could reverse the toxic effect of VLCFAs on mitochondrial inner membrane potential.

5.3.5 VLCFAs Increase the Sensitivity to Chemical Oxidants in 158N Oligodendrocytes

Although C26:0 at threshold toxicity concentration (25 μM) was observed to deplete mtGSH, increase levels of superoxide anions, as well as impair mitochondrial inner membrane potential, it did not demonstrate any significant effects on intracellular ROS and total GSH levels, causing moderate cell death. We hypothesized that the induced mitochondrial toxicity by pre-treatment of C26:0 would sensitize the cells towards death when encountering further chemical oxidants. Acrolein, the major reactive oxidant metabolite for the commonly used chemotherapeutic agent cyclophosphamide, was used to induce further oxidative stress to the cells. We then measured cell viability following

incubation with either threshold concentration of C26:0 or acrolein or both. Oligodendrocytes incubated with low concentrations of C26:0 (25μM, 24hrs) or acrolein (25μM, 1hr) showed modest cell toxicity (84±1% and 81±1% cell survival respectively). However, pre-treatment with C26:0 and subsequent incubation with acrolein at the same conditions profoundly showed cell toxicity (56±1.5% cell survival), indicating a synergistic cytotoxic effect (Figure 5-7). Results verified the hypothesis that pre-treatment of C26:0 could increase the sensitivity to acrolein.

Next we evaluated the effects of NAC in protecting C26:0 treated cells from additional acrolein treatment. NAC at 500 μM was co-incubated with C26:0 for 24hrs before replacing with acrolein for 1hr. As a result, we found that addition of NAC increased the cell survival to 71±3%, presumably by its effect on replenishing mtGSH thereby desensitizing the cells to acrolein.

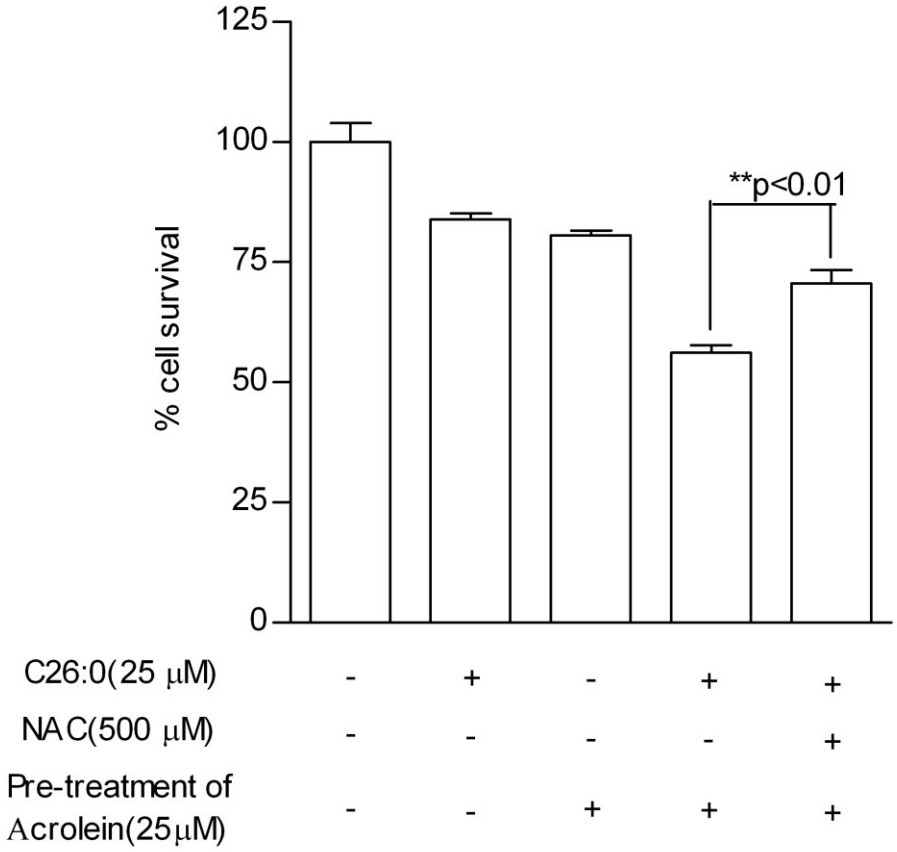

Figure 5-7 *C26:0 increased sensitivity to acrolein in 158N cells. Cell survival rates following treatments with C26 only (25 μM, 24hrs), acrolein only (25μM, 1hr), C26 (25 μM, 24hrs) and then acrolein (25μM, 1hr), as well as C26 (25 μM)-NAC (500 μM) co-incubation for 24 hrs and then acrolein (25μM, 1hr). Pre-treatment with C26:0 and subsequent incubation with acrolein at the same conditions profoundly decreased cell survival (56±1.5%) compared to C26:0 or acrolein treatment. Addition of NAC in pre-treatment procedure increased the cell survival to 71±3%, ** p<0.01, ANOVA followed by Bonferroni test.*

5.4 Discussion

Increased levels of VLCFAs in plasma and tissues and mutations in *Abcd1* gene are hallmarks of ALD. Mutated *Abcd1* gene causes impaired degradation of VLCFAs which come from either endogenous synthesis by microsomal elongation system or exogenous source of diet (Moser et al., 2005a). However, the detailed pathology regarding to how accumulation of VLCFAs leads to neurodegeneration in CCALD is still unclear. *In vitro* toxicity assays using VLCFAs such as C26:0 offer great insights into the pathology of ALD. Previous studies have investigated the toxicology of VLCFAs on fibroblasts from ALD patients (Fourcade et al., 2008, Fourcade et al., 2010, Galino et al., 2011), on rat hippocampal cell cultures of oligodendrocytes and astrocytes (Hein et al., 2008), as well as on established oligodendrocyte cell lines (Baarine et al., 2012a, Baarine et al., 2012b).

VLCFAs were found to impact total intracellular GSH levels and cell survival (Fourcade et al., 2008), reactive oxygen species (ROS) and nitrogen species (RNS) production (Baarine et al., 2012a), as well as mitochondrial and lysosomal functions (Baarine et al., 2012b) *in vitro*. A wide range of concentrations (1- 100 μM) of VLCFAs were investigated. Interestingly, there seemed to be a threshold level where VLCFAs induce detrimental toxicity in oligodendrocytes. At concentrations lower than the threshold, cell viability was minimally affected while elevated concentrations of VLCFAs decreased cell survival profoundly. Notably, the threshold concentrations of VLCFAs were within the range of reported values in plasma and tissue concentrations of ALD patients (Baarine et

al., 2012b). Thus VLCFAs might dispose the cells towards oxidative stress without affecting cell viability, becoming the first hit in the "three-hit hypothesis" (Singh and Pujol, 2010). Three-hit hypothesis assumed oxidative stress as the first hit in ALD disease pathology. Subsequently a second hit of inflammation or other stressors would then lead to loss of cell function and cell death as the final hit. The three hit hypothesis was quite helpful to explain the finding that the plasma concentrations of VLCFAs does not correlate with the disease severity or age of onset (Ofman et al., 2010) since a second hit is required for disease progression. We were interested to examine the effect of this "first hit" using threshold concentration of C26:0 *in vitro*.

Oxidative stress resulting from accumulation of VLCFAs was thought to highly associate with ALD disease progression (Powers et al., 2005). Evidence of oxidative stress as a hallmark of ALD has been shown in recent studies (Vargas et al., 2004, Fourcade et al., 2008) . Vargas et al., evaluated oxidative stress biomarkers in plasma, erythrocytes and fibroblasts from ALD patients. Results showed that biomarkers indicating free radicals and lipid peroxidation were elevated in ALD patients compared to control while total antioxidant capacity was decreased indicating a deficient capacity to rapidly handle oxidative stress (Vargas et al., 2004). Additionally, in *Abcd1*- murine models increased reactive oxygen species (ROS) formation and elevation of other oxidative stress markers were observed early on in disease progression (Fourcade et al., 2008).

As 95% of ROS is produced through the mitochondrial respiratory chain as byproducts of O_2 consumption and ATP generation (Emerit et al., 2004), oxidative stress is highly associated with mitochondrial function. It has been discussed widely whether VLCFAs could lead to mitochondrial dysfunction or not. And if it is true, the pathogenic pathways remain to be identified. Mitochondrial abnormalities and impaired cross-talk between mitochondria and peroxisome were observed in human and mouse *Abcd1*- fibroblast cells (McGuinness et al., 2003). Impaired mitochondrial oxidative phosphorylation and increased mtDNA oxidation was also observed in ALD patients' fibroblasts and *Abcd1*-mouse models (Lopez-Erauskin et al., 2013). Further, VLCFA affected the mitochondrial inner membrane potential, and was a likely mechanism for "mitochondrial-based cell death" (Hein et al., 2008). However, one report showed that mitochondrial abnormalities had no relationship with accumulation of VLCFAs based on Abcd1-mouse model and ALD patients' fibroblast cells (Oezen et al., 2005).

In our study, we were interested to investigate whether VLCFAs have any impact on mitochondrial function. Interestingly, we were able to show consistent results with previous publications that VLCFAs could cause decrease in ATP production and inner membrane potential, as well as increase in the superoxide species within mitochondria. Moreover, we were able to identify a new pathogenic effect of VLCFAs that it specifically depleted the mtGSH. In CCALD disorders with accumulation of VLCFAs, depletion of mtGSH could possibly cause mitochondria dysfunction and trigger further oxidative stress cascade. The imbalance between ROS and antioxidants within the

mitochondria might be one of the crucial pathways leading to mitochondrial dysfunction and can be the first hit on neurodegeneration.

To examine whether this pathogenic mechanism can be targeted, we performed experiments with NAC, which can potentially replenish the mtGSH depleted by VLCFAs. NAC is a precursor of cysteine, which is the rate-limiting endogenous substrate for generation of GSH, the crucial antioxidant in cells that protects against damage from free radicals. mtGSH has emerged as the major defense mechanism to maintain mitochondrial function (Mari et al., 2009). We were interested to know whether NAC could replenish the mtGSH levels which should be able to relieve the first hit of oxidative stress. With that in mind, we co-incubated NAC with VLCFAs to examine mitochondrial function parameters. Interestingly, NAC has an effect on reversing mitochondrial dysfunction caused by VLCFA accumulation.

The fact that pre-treatment with VLCFAs could increase the sensitivity to chemical oxidants further verified our hypothesis of first hit stress by VLCFAs (Figure 5-8). Depletion of mtGSH was thought to be the cause for increased sensitivity. In the disease pathology of CCALD, accumulation of VLCFAs could possibly increase the sensitivity of cells towards exogenous oxidative stimuli, pre-disposing the cells towards oxidative stress and resulting in irreversible cell death. NAC pre-treatment along with VLCFAs could replenish mitochondrial GSH thus sabotage the hypersensitivity. In our experiments, NAC has been shown to be a potential therapeutic agent in normalizing the

redox status in mitochondria. Also, these studies may lead to future clinical approaches wherein NAC can be combined with mitochondrial cofactors (Vitamin C, Vitamin E and Coenzyme Q) to enhance its therapeutic benefits.

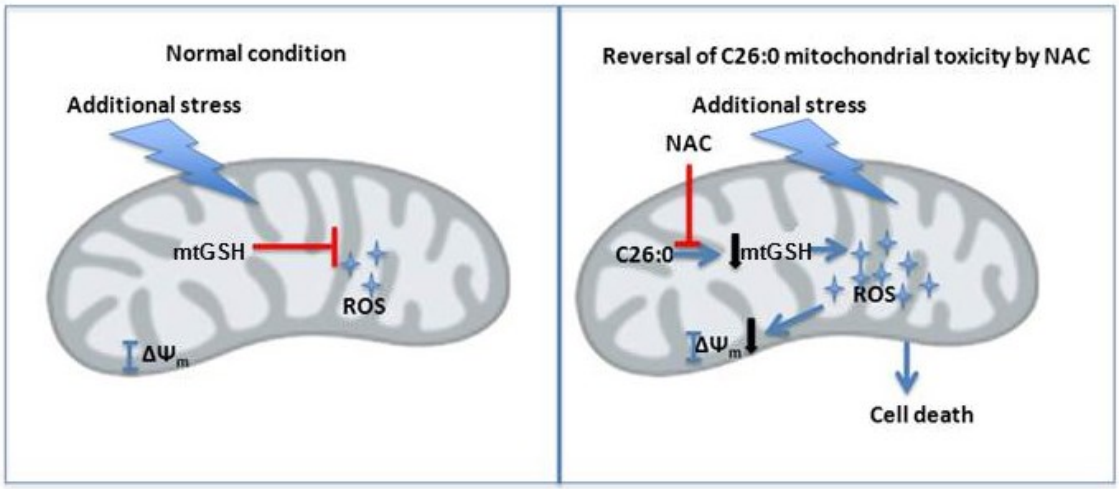

Figure 5-8 *Figure shows hypothesized model depicting first hit by C26:0 which depletes mtGSH. And loss of mtGSH subsequently pre-disposes the cells towards death in encountering additional stress such as oxidants. NAC reverses the mitochondrial toxicity of C26:0 by replenishing mtGSH, and thus protects against future oxidative insult. Figure adapted from (Mari et al., 2009).*

5.5 Conclusion

Accumulation of VLCFAs (C26:0) has been implicated in oxidative stress and consequent neurodegeneration [1]. The myelin-producing oligodendrocytes are particularly sensitive to VLCFAs. To further understand the toxic effects of VLCFAs, we exposed oligodendrocytes to hexacosanoic acid (C26:0) and analyzed cellular responses.

We observed significant mitochondrial toxicity of VLCFAs contributing to sensitivity towards further oxidative stimuli. We then examined if these mitochondria-specific effects of VLCFAs are reversed using antioxidants. We evaluated the effect of a well-known antioxidant NAC on the toxicity induced by VLCFAs in oligodendrocytes. Our data indicate that NAC has an effect on reversing mitochondrial dysfunction caused by VLCFAs accumulation, which is commonly observed in neurodegenerative diseases associated with peroxisomal defects.

Our future studies will target at further characterizing the precise mechanisms of NAC in restoring mitochondrial function and use various combinations of antioxidants to optimize and maximize the protective effects on mitochondria.

CHAPTER 6

A PHARMACOKINETIC AND PHARMACODYNAMIC STUDY OF N-ACETYLCYSTEINE TO UNDERSTAND ITS EFFECT ON BRAIN AND BLOOD GLUTATHIONE STATUS IN WILD-TYPE MICE

6.1 Introduction

NAC is a well-known antioxidant, indicated for mucolysis in cystic fibrosis and other respiratory conditions and as an antidote for acetaminophen overdose (Heard and Green, 2012a, Rushworth and Megson, 2013b). Recently, NAC has gained renewed attention as a potential therapy for a number of conditions including neurological(Adair et al., 2001, Berman et al., 2011), cardiac injury (Mahmoud and Ammar, 2011), metabolic (Badaloo et al., 2002, Atkuri et al., 2007) and HIV infection (De Rosa et al., 2000), due in part to its antioxidant properties as well as the capacity to replenish glutathione (GSH) levels.

GSH is a potent endogenous antioxidant which scavenges free radicals non-enzymatically. The depletion of GSH is often used as an indicator for oxidative stress (Wu et al., 2004b). For example, lower levels of GSH was found in brain of patients with multiple sclerosis (Choi et al., 2011a) and impaired GSH metabolism and imbalance is linked to Parkinson's disease (Zhou and Freed, 2005a, Choi et al., 2006a), Alzheimer's disease(Lovell et al., 1998), X-Aldrenoleukodystrophy (X-ALD) (Petrillo et al., 2013b) and Gaucher's disease (Roversi et al., 2006). The ratio of the reduced form (GSH) and oxidized form (GSSG) is defined as the redox ratio, which is used as another indicator for oxidative stress (Nemeth and Boda, 1994). Decreased redox ratios were reported to be associated with diabetes, autism in children and cancer (James et al., 2004, Bravi et al., 2006, Chauhan et al., 2012, Zitka et al., 2012).

NAC is widely investigated in conditions where GSH depletion and abnormal redox ratios are involved (De Rosa et al., 2000, Al-Tonbary et al., 2009, Dean et al., 2011b). Our research group showed that high doses of intravenous NAC can increase both blood and brain GSH levels in humans. In addition, this increase in GSH by administration of NAC is not only observed in patients with Parkinson's and Gaucher's disease, but also in healthy subjects who are assumed to have normal GSH levels (Holmay, et al. 2013). However, this study is lack of scientific rationale for dose selection. Moreover, high-dose intravenous administration is not likely feasible as long-term therapy. Quantitatively characterizing the relationship between NAC dosing and increased GSH levels/redox ratios is thus necessary and crucial for selection of dose, regimen, and route of administration.

NAC has long been considered to contribute to the maintenance of intracellular GSH levels by providing the rate-limiting substrate cysteine for GSH synthesis(van Zandwijk, 1995b). However, the precise mechanism by which this occurs is not well understood.

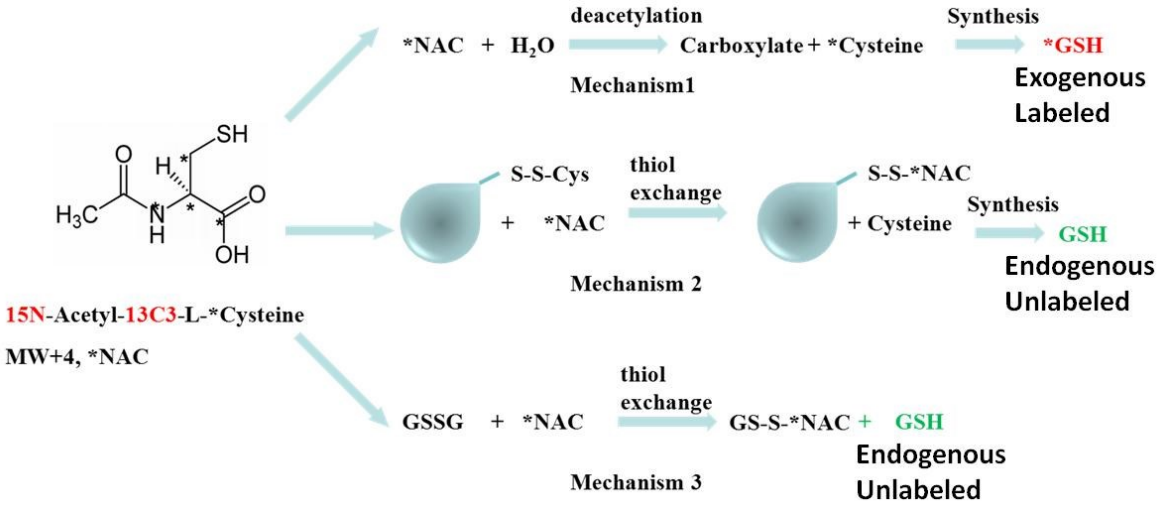

Figure 6-1 Structure of stable-labeled 15N-Acetyl(13C3) L-Cysteine, isotope atoms were shown with asterisk(*); Biotransformation pathways of NAC into GSH. Pathway A: cysteine is formed through deacetylation by acyclase I to form cysteine, and further used for GSH synthesis. Pathway B: NAC exchanges thiol with oxidized form of cysteine and releases free reduced form cysteine for GSH synthesis. Pathway C: NAC directly exchanges thiol with oxidized form of GSH and releases free reduced form GSH. In pathway A, the final product GSH carries the stable labels from labeled NAC but both pathway B and C do not carry the label.

NAC was reported to increase GSH levels by direct deacetylation to cysteine (Fig1, pathway A)(Nakagawa et al., 2013) or by indirectly modulating cysteine/GSH levels through thiol exchange (Fig1, pathway B&C)(Ventura et al., 1999, Raftos et al., 2007, Whillier et al., 2009, Radtke et al., 2012). Stable isotope labeled NAC (*15N-Acetyl (13C3) L-Cysteine*) was used in this study to differentiate exogenous source for synthesis

(labeled) from endogenous source of GSH (non-labeled), (Fig 1). In pathway A where deacetylated NAC contributes to the synthesis of GSH, GSH would also carry the stable labeled atoms, whereas in pathway B&C where NAC makes endogenous cysteine or GSH available, the final product GSH will not have isotope atoms. Mass spectrometry analysis can be used to differentiate the endogenous (non-labeled) GSH and exogenous (labeled) GSH based on their differences in molecular weight.

The objective of this study was to examine the biotransformation and disposition of NAC in blood and brain of mice following an intravenous dose of a stable-labeled NAC solution. Moreover, the therapeutic potential of NAC to increase GSH levels in RBCs/redox ratios in brains was also evaluated and PK/PD relationships between NAC concentrations and GSH concentration increases in RBCs developed.

6.2 Materials and Methods:

6.2.1 Materials

Phosphate buffered saline (PBS) was obtained from Life Technologies (CA, USA). Unlabeled NAC and glutathione (GSH) used as calibration standards were purchased from Sigma-Aldrich (MO, USA). 1M Dithioerythritol (DTE) solution in water was obtained from Sigma-Aldrich (MO, USA).

6.2.2 Subjects

Experimentally naïve, 12-week-old female C57BL/6NCr mice were obtained from National Cancer Institute (MD, USA). Mice were housed in rooms with a 12:12 light/dark cycle at 21.1-22.8 °C with water and food. Mice were acclimated in the UMN-TC facility for a minimum of one week.

All experiments were conducted under the approval of University of Minnesota Institutional Animal Care and Use Committee (IACUC).

6.2.3 NAC intravenous formulation

Stable isotope-labeled NAC (*15N-Acetyl 13C3 L-Cysteine*) was purchased from Cambridge isotope laboratories (Andover, MA). During manufacturing of the labeled NAC, three carbon-12s and one nitrogen-14 in the cysteine group were replaced with one carbon-13 each and with one nitrogen-15, respectively resulting in a compound with 4 mass units greater than the unlabeled NAC. Representative spectra of this compound are shown in Figure 6-2.

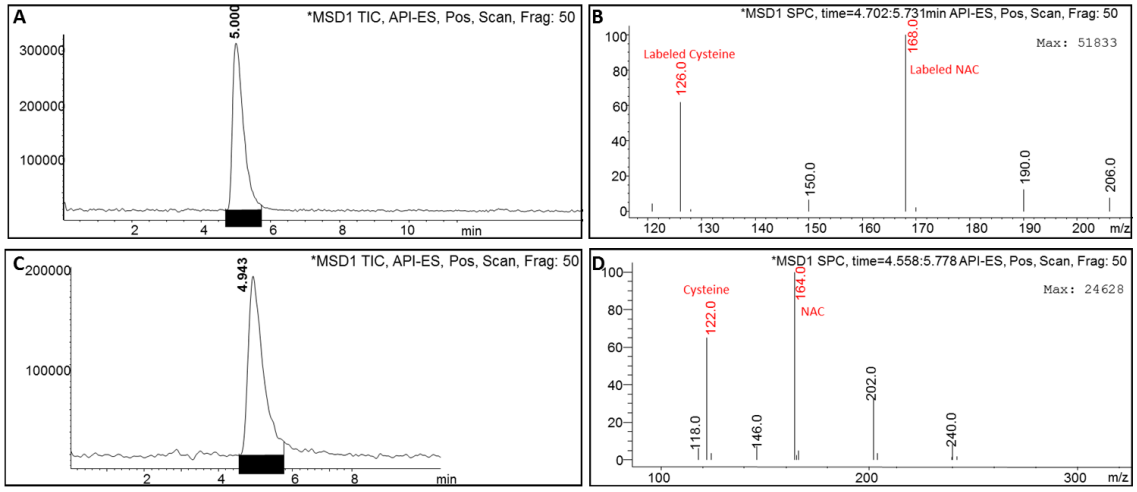

Figure 6-2 LC/MS chromatography of stable-labeled NAC (A , B) and unlabeled NAC (C, D). Isotope atoms were labeled on the cysteine group of the NAC molecule, resulting in increase of 4 mass units in molecular weight (m/z=168, positive mode, B) as shown on Mass Spectrometry (MS) compared to non-labeled NAC (m/z=164, positive mode, D), while peaking at the same location (approximately 5.0 min) as unlabeled NAC on liquid chromatography (HPLC) graph (A, C).

Stable-labeled NAC was dissolved in PBS at a concentration of 28g/L. Then the solution was adjusted to pH 7.0 and passed through a 220nm syringe filter on the day of experiment.

6.2.4 Drug administration

A single NAC dose of 150mg/kg was administered intravenously in the tail vein of each mouse. Sterile PBS solution was also prepared and administered to the mice assigned to the baseline group.

6.2.5 Sampling methods

A destructive sampling method was employed. 22 mice were randomized to 7 groups. At baseline (dosed with saline), 5min, 15min, 30min, 60min, 90min, and 150min post-dosing, one group of mice was anesthetized using carbon dioxide. Blood samples were collected using cardiac puncture afterwards at each specified time point. Whole blood was placed in tubes pre-treated with heparin. Fresh whole blood was centrifuged immediately at 1500g for 5 minutes to separate plasma and RBCs. Upper layer plasma and lower layer RBCs were immediately snap frozen in liquid nitrogen and subsequently stored at -80 °C for further analysis of NAC and its metabolites. Whole brain tissues were perfused with pre-heated PBS to clean blood, and subsequently snapped frozen in liquid nitrogen and stored at -80 °C, and weighed afterwards for further analysis.

6.2.6 Plasma/RBC/brain sample processing methods

In order to measure the total concentrations of NAC and GSH including both reduced and oxidized forms, plasma and RBCs were co-incubated with 1:2 volume ratio of 0.5mg/ml the reducing agent dithioerythritol (DTE) at 37 ^{o}C for 30minutes prior to analysis. Brain

tissue homogenates were prepared without reducing agent to measure both GSH and GSSG levels for redox ratio calculation. Bullet Blender storm from Next Advance (NY, USA) was used for brain tissue homogenization according to manufacturer's protocol under 4^{o} C.

6.2.7 Analytical methods

Total NAC concentrations in plasma, total GSH levels in RBCs and GSH/GSSG redox ratios in brain tissue homogenates were analyzed using liquid chromatography-mass spectrometry (HPLC-MS) (Agilent Technologies, CA, USA) with series 1100 system consisted of a G1322A degasser, a G1311A quaternary pump, and a G1313A autosampler. The electrospray interface is connected to a single quadrupole G1946A. The HPLC-MS system was controlled and data were processed using Chemstation software (Agilent Technologies, CA, USA).

Briefly, processed RBC and brain tissue samples were mixed with equal volume of RBC lysis solution (Qiagen, MD, USA) and gently votexed. 2 ml of methanol was added into 100 µL of obtained brain lysates/RBC lysates/plasma prior to vortexing. After centrifuging at 2500 rpm for 10 minutes at 4°C, the organic supernatant was transferred into glass tubes and evaporated under nitrogen gas at 37°C. Dried samples were reconstituted with mobile phase and filtered into HPLC vials using nylon acrodisc syringe filters (Pall Life Sciences, MI, USA). Separation of compounds was performed

using mobile phase consisting of 98% 20mM ammonium formate buffer (pH 3.0) and 2% acetonitrile through Agilent ZORBAX Eclipse XDB-C18 (3×150mm, 3.5µm) column. The flow rate was 0.35 ml and the total analytical period for each sample was 10 minutes. Finally, samples were analyzed using selective ion monitoring (SIM) mode, detecting positive ions for labeled NAC (m/z, 168), unlabeled GSH (m/z, 308), labeled GSH (m/z, 312) and oxidized GSSG (m/z, 614).

Calibration standards were prepared in plasma, red blood cells, and brain and analyzed with the corresponding samples. NAC calibration standards (1-200 µg/ml) were prepared daily and spiked into mouse plasma. Quality control NAC standard in plasma was also prepared with a final NAC concentration of 10ug/mL to run with every batch of samples. GSH calibration standards (250-1000 µg/ml) were prepared and spiked into RBC lysates from control mice. Quality control GSH standard in RBC lysates was prepared with a final GSH concentration of 500 µg/ml. GSH standards (1.25-50 µg/ml) and GSSG standards (1.25-50 µg/ml) were prepared and spiked into brain tissues homogenates from control mice. Quality controls were prepared at 10µg/ml for both GSH and GSSG in brain homogenates. All samples and standards were analyzed in duplicates.

The lower limit of quantitation (LLOQ) of the assay was 1µg/mL for NAC and 0.625 µg/mL for both GSH and GSSG. The average within-run precision was 5.0% for NAC in plasma. The between-run precision was 8.4% for NAC in plasma. The recovery rates for

GSH and GSSG in red blood cells and brain tissues were between 91% and 97% for standards ranging from 1.25 to 1000 μg/ml.

6.2.8 Treatment of NAC Plasma Concentrations below the Limit of Quantification (BLQ)

The rules for treating the reported NAC plasma concentrations below the BLQ were pre-defined as missing since there was only one sample per subject in destructive sampling.

6.2.9 Non-compartmental PK analysis

Area-under-the-curve (AUC), maximum concentration (Cmax), elimination half-life ($t_{1/2}$), clearance (CL) and Volume of distribution (Vd) were estimated in Phoenix WinNonlin (Version6.3, Pharsight Corp., NC,USA) using non-compartmental analysis (NCA) of sparse sampling method (Nedelman and Jia, 1998). In addition, two bootstrapping re-sampling methods (Mager and Goller, 1998), Pseudoprofile-based bootstrap (PpbB) and Pooled data bootstrap(PDB), designed specifically for destructive sampling, were also performed in R software (version 3.0.1, open source). PK analysis results were compared between the three different methods.

Area under the curve above baseline (AUCb) for unlabeled and labeled GSH was estimated in Phoenix WinNonlin (Version6.3, Pharsight Corp., NC, USA) by linear trapezoidal linear interpolation rule.

6.2.10 Population pharmacokinetic/pharmacodynamic analysis

Due to the nature of destructive sampling procedures, each animal contributed to only one data point. Thus, it is not possible to evaluate the inter-individual variability and residual random variability due to identifiability issues. Therefore, residual random variability in population PK analysis and population PK/PD analysis was fixed to reflect the magnitude of assay errors.

Compartmental population PK analysis was performed via nonlinear mixed effects modeling in Phoenix NLME (version 1.2, Pharsight Corp., NC, USA) using the first-order conditional estimation method with interaction.

An exponential variance model was used to describe the inter-individual variability of PK parameters:

$$Pi = TVP * EXP(\eta i),$$

where Pi is the estimated parameter for the i^{th} individual, TVP is the typical population mean of the parameter, and ηi is the deviation from population mean TVP for i^{th} individual, which is assumed to be distributed: $\eta \sim N(0, \omega^2)$. A two compartmental model was found to be the best-fit based on pre-defined goodness of fit criteria. Observed concentration Cobs was fitted into two-compartmental model where intra-individual variability (ηi) were modeled on volume (V1) and rate constants k12, k21 and k10 as shown in Figure 6-3.

Proportional, additive, and combined additive and proportional residual error models were investigated during the model selection. In the final model, residual error was described by exponential error model:

$$Cobs_{ij} = C_{ij} * EXP(\varepsilon_{ij}),$$

where $Cobs_{ij}$ is the observed plasma concentration for i^{th} individual at j^{th} time point, C_{ij} is the predicted concentration and ε_{ij} is the exponential error term under the assumption that $\varepsilon \sim N(0, \sigma^2)$, σ^2 were fixed to 0.01 to resolve the identifiability issue. The differential equations for population PK modeling can be expressed as following with X(1) as the central compartment and X(2) as the peripheral compartment.

$$dX(1)/dt = -K10*X(1) - K12*X(1) + K21*X(2)$$
$$dX(2)/dt = K12*X(1) - K21*X(2)$$

Models were selected based on following criteria: 1) successful minimization 2) visual goodness of fit of diagnostic plots and 3) precision of model parameters as measured by the percent standard error of the mean (RSE %) 4) decrease in objective function value (-2 * log-likelihood) for nested models or Akaike Information Criterion (AIC) and Schwarz Criterion(SBC).

Population PK/PD modeling were implemented using ADAPT5 (Biomedical Simulations Resource, USC, CA, USA) (D'Argenio, et al. 2009) and ADAPT5 Model Evaluation Graphical Toolkit (AMGET), an external package written in the open source R programming language (version 3.0.1) (Guiastrennec et al., 2013). Maximum likelihood solution via the expectation-maximization Algorithm (MLEM) program was selected in ADAPT5 to implement the PK/PD models. In the program run, the lognormal distribution option was selected for the model parameters. Finally, 3000 samples/EM iteration and 50 EM iterations were specified. AMGET package in R was used to generate diagnostic plots such as visual predictive check (VPC) based on ADAPT5 outputs.

PD models were established as a combination of indirect response model and Emax model as shown in Figure 6-3, where Kin is the rate of production of GSH in RBC, Kout is the first-order elimination rate constant of GSH in RBC. Plasma concentrations of NAC are assumed to correlate with Kin defined by Emax model. Similarly to population

PK models, the inter-individual variability of PK/PD parameters were defined using proportional variance model Pi =TVP+ TVP*(ηi), η~N(0, ω^2). And proportional residual error models were defined as $GSHobs_{ij}$ =GSH_{ij} + GSH_{ij}*(ε_{ij}), ε~N(0, 0.01). In addition, functions describing the process were expressed as:

GSH(t) = Kin*(1 + Emax*X(1)/V / (EC50+X(1)/V)) - Kin/GSH(0)*GSH(t)

$GSHobs_{ij}$ =GSH_{ij}*EXP(ε_{ij})

ε~ N(0, σ^2) and σ^2 =0.01

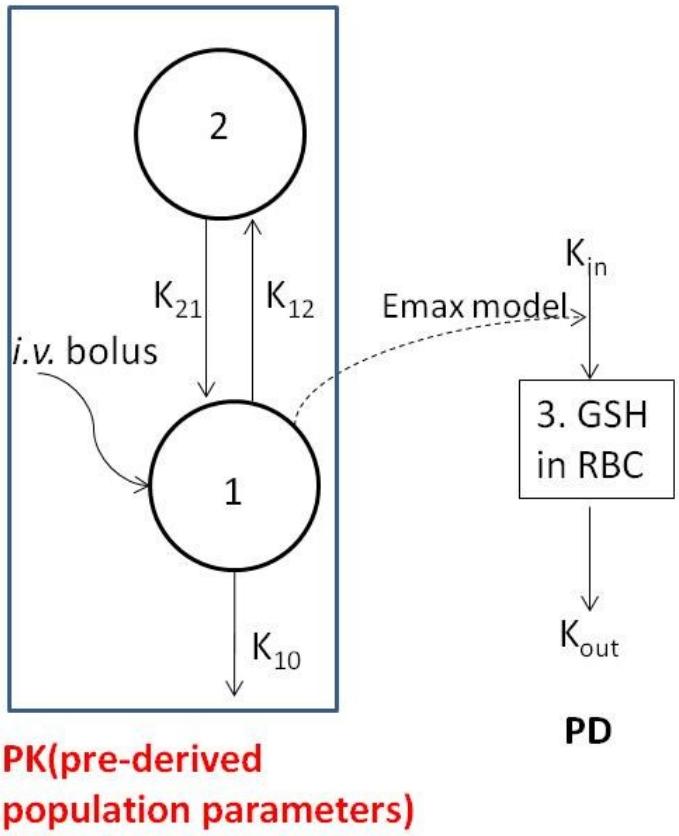

Figure 6-3 Structure of the PK-PD model for NAC-GSH. Simultaneous PK and PD analysis strategy was employed with fixed previously derived population PK parameters (population means, variance and covariance matrix).

6.2.11 Model evaluation

The predictive properties of the final model were evaluated by performing visual predictive check. 3000 individual Monte-Carlo simulation was implemented in Phoenix NLME or ADAPT5 based on model structure and final estimates. Medians and 95% confidence intervals for both simulated data and observed data were plotted. The performance of the model was assumed to be acceptable if the observed data were appropriately distributed within the 5% and 95% of the simulated data.

6.3 Results

6.3.1 Non-compartmental PK analysis of NAC in wild type (WT) mice

A total number of 22 female 12-week-old C57 WT mice received one single intravenous bolus dose of 150mg/kg NAC. The weight of mice was measured prior to dosing and was 20.5±1.2 g (±SD). The NAC plasma concentration time profile is shown in Figure 6-4. Non-compartmental analyses (NCA) were performed using three different methods: NCA sparse sampling, pseudoprofile-based bootstrap (PpbB) and Pooled data bootstrap (PDB). AUCinf (from time 0 to ∞), AUClast (from 0 to last measurable concentration), C0 (concentration at time 0), CL (clearance), $T_{1/2}$ (half-life), Vd (Volume of distribution) were also estimated and shown in Table 6-1 respectively. Estimated parameters were

quite consistent when calculated by the three different methods. For example, the $T_{1/2}$ was estimated to be 24.5 minutes in NCA sparse sampling, 22.9±1.2 minutes in PpbB, and 23.9 ±1.9 minutes in PDB. A half-life of 20-25 minutes indicates that NAC was eliminated rapidly in mice. In addition, CL and Vd were estimated to be 0.035ml/min/g and 1.22 ml/g respectively using NCA sparse sampling method.

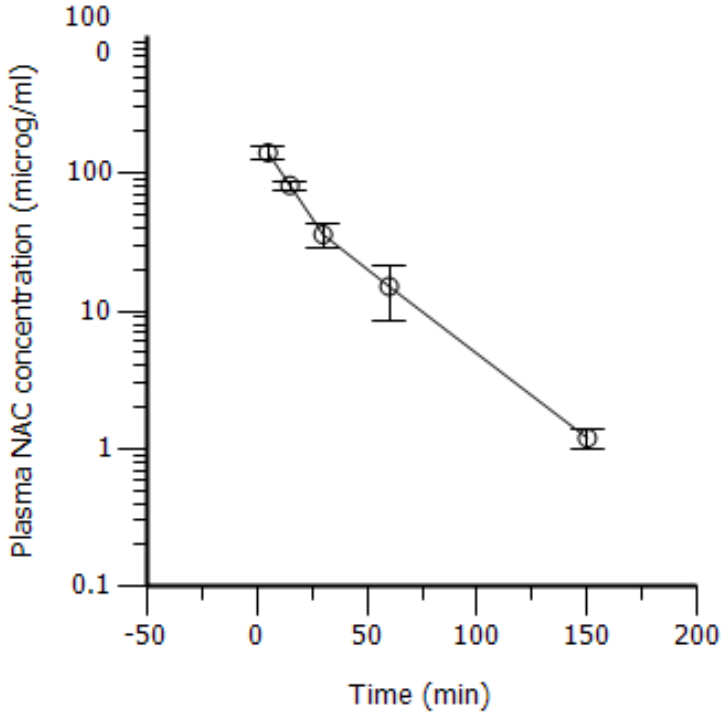

Figure 6-4 Plasma NAC concentration- time profile in WT mice after application of BLQ rules. Data represents the mean±standard error following 150mg/kg NAC intravenous administration.

Parameters	Units	NCA sparse sampling	PpbB	PDB
AUCinf	min·μg/ml	4351.2	4360.3 ± 377.8	4341.5 ± 377.3
AUClast	min·μg/ml	4308.8 ± 441.6	4326.6 ± 386.2	4300.0 ± 378.2
CL	ml/min/g	0.035	0.035 ± 0.003	0.035 ± 0.003
Vd	ml/g	1.22	1.16 ± 0.12	1.20 ± 0.16
$T_{1/2}$	min	24.5	23.2 ± 2.4	23.9 ± 1.9

Table 6-1 NAC PK parameters estimated by three different NCA methods in WT mice.

6.3.2 Compartmental population analysis of NAC in WT mice

Population PK analysis was also performed to characterize the disposition of NAC in plasma. A 2-compartmental model (intravenous bolus dose) was selected as the best fit model according to previous defined criteria and parameterized with elimination rate constant from central compartment (K10), distribution rate constant from central compartment to peripheral compartment (K12), distribution rate constant from peripheral compartment to central compartment (K21) and volume of distribution of the central compartment (V1). No covariates were incorporated into the model. 1-compartmental PK model was also evaluated which deviated at the terminal phase.

The final PK parameter estimates obtained from this model were shown in Table 6-2. Secondary parameters of α, β were also derived from estimated rate constants as 0.053 min^{-1} and 0.0086 min^{-1} respectively. Most parameters showed a reasonable amount of inter-individual variability (≤40%) except K21. Goodness of fit plots of observed versus population and individual predicted concentrations were shown in Figure 6-5. The

observed versus population-predicted/individual-predicted plots showed a uniform distribution of the data points across the line of unity. Visual predictive check was also implemented and shown in Figure 6-6. The observed values were found to distribute appropriately within the (5-95%) range of the simulated data.

2 compartmental model (iv.)		
$Pi = TVP * EXP(\eta i)$		
$Cobs_{ij} = C_{ij} * EXP(\varepsilon_{ij})$, $\varepsilon \sim N(0, 0.01)$		
Parameter	**Population estimate(%SE)**	**Between subject variability (%)**
V1 (ml)	16.8753 (0.6364)	9.2
K10 (1/min)	0.0454 (0.0706)	19.3
K12 (1/min)	0.0065 (0.1583)	36.4
K21 (1/min)	0.0101 (0.2464)	80.2
Secondary parameters		
α (1/min)	0.053	
β (1/min)	0.086	

Table 6-2 Final PK parameter estimates obtained from 2-compartmental model for intravenous NAC in WT mice; secondary parameters of α and β were also calculated.

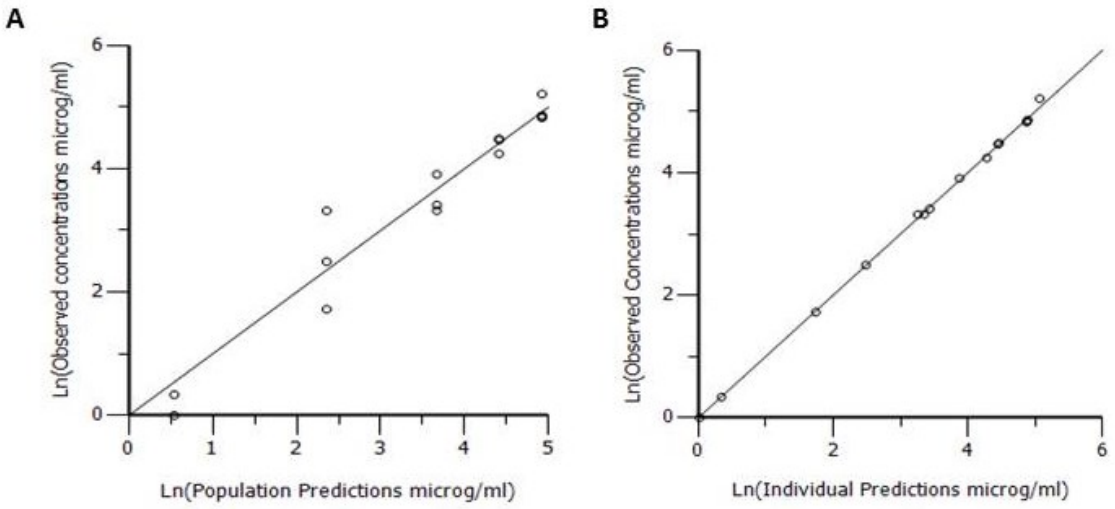

Figure 6-5 Goodness-of-fit graphics for NAC plasma concentration fitted with 2-compartmental PK model. All values were transformed with natural log. (A), the observed concentrations versus the population predictions, (B) the observed concentrations versus the individual predictions. The line of identity is included in Figure 3 (A) and (B).

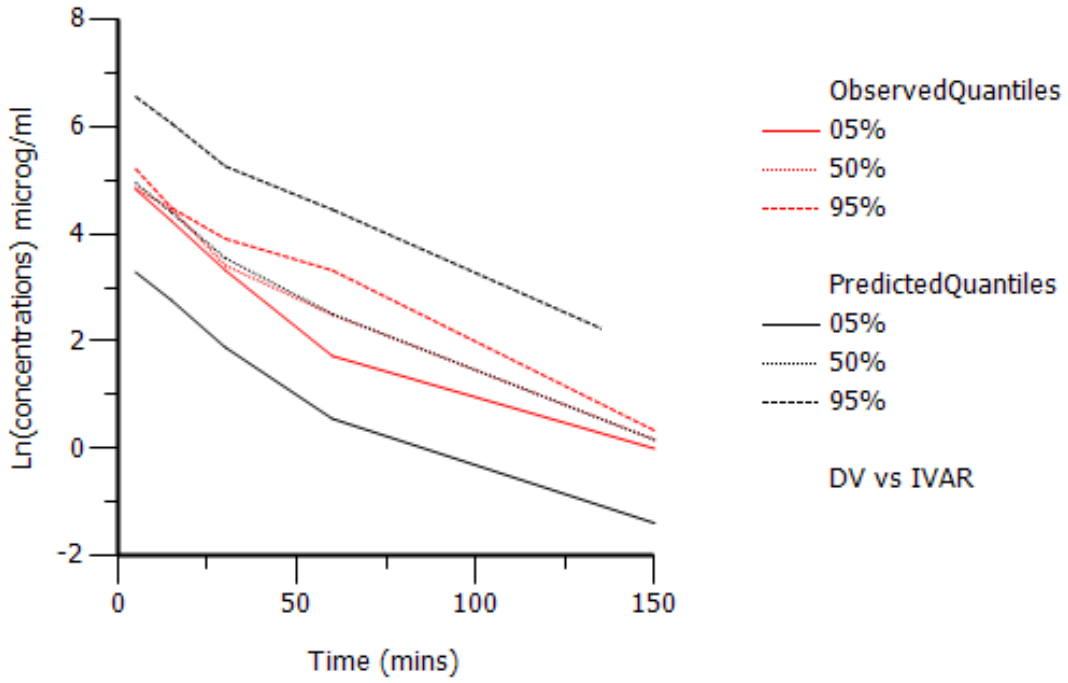

Figure 6-6 Visual predictive check (VPC) for NAC plasma concentration fitted with 2-compartmental PK model. Red lines: 5, 50 and 95th percentile for observed concentrations; black lines: 5, 50 and 95th percentile for simulated concentrations. Ideally, 90% of the observations should fall inside the 90% prediction interval.

6.3.3 Labeled NAC boosts unlabeled GSH rather than labeled GSH in RBC

The concentration of GSH in the plasma has been reported to be much lower than the concentrations in RBC (Pendyala and Creaven, 1995). To better investigate the change of GSH, we chose RBC as our target matrix to measure the change in total GSH because RBC is where the predominant GSH is stored. As proposed in Figure 6-1, there are

several hypotheses of how NAC boosts GSH concentrations. In order to differentiate these different pathways, we used stable-labeled NAC to track the labeled cysteine group of NAC in its biotransformation and disposition.

In RBC lysates, total GSH, both unlabeled and labeled, reduced and oxidized, was detected simultaneously using our established LC/MS method. As shown in Figure 6-7, the baseline total unlabeled GSH was 1289±196 μg/ml and total labeled GSH was undetectable. Following dosing with NAC, the total unlabeled GSH was increased. The maximal concentration was 1579±86 μg/ml, with corresponding Tmax of 150 minutes post-dosing. It was a quite interesting finding that the unlabeled GSH was increased up to ~290μg/ml (22.5% of baseline) following the administration of labeled NAC. The results indicated that NAC could boost the GSH levels through other pathways in addition to acting as cysteine prodrug for GSH synthesis.

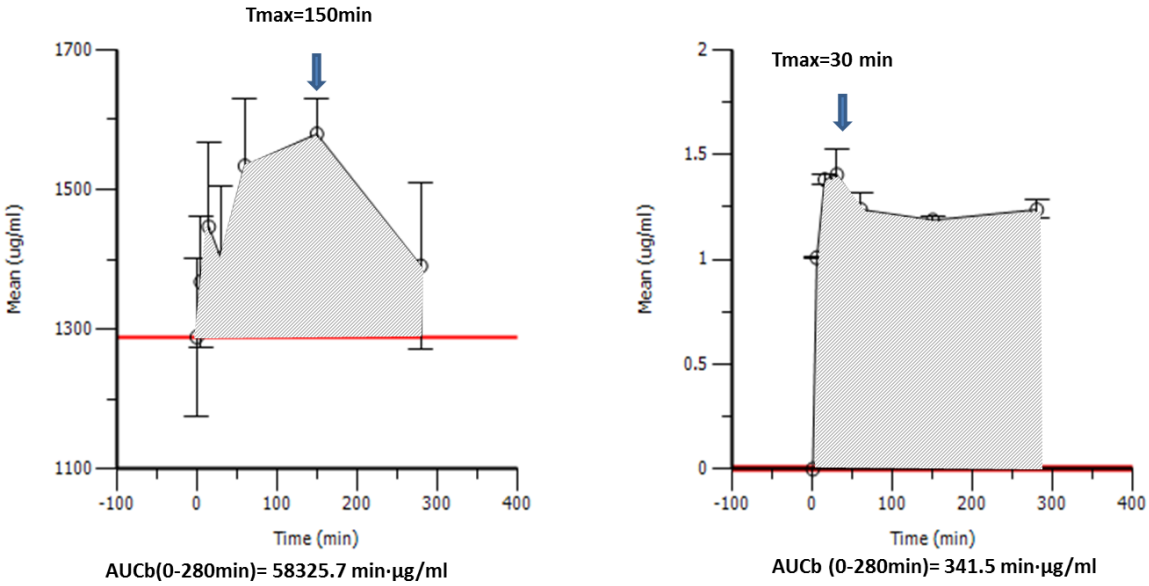

Figure 6-7 Unlabeled(A) and labeled total GSH(B) levels detected in the RBC following NAC dosing in WT mice. Baseline levels prior to NAC dosing was presented by the red lines; Area under the curve above the baseline (AUCb) from 0-280 minutes were calculated and shown as well as the time for maximal concentration (Tmax).

The baseline level for labeled GSH was found to be 0 µg/ml, since there was lack of stable labeled atoms endogenously. Following the administration of labeled NAC, labeled GSH was found to be increased (Figure 6-7) with a maximal concentration of 1.4±0.2 µg/ml with corresponding Tmax of 30 minutes post-dosing. The concentration of labeled GSH quickly decreased to concentrations around the BLQ. The maximal increase in the labeled GSH was minimal (1.4 µg/ml) compared to the increase in unlabeled GSH (290 µg/ml). Moreover, when we compared the area under the curve and above the baseline (AUCb) from 0 to 280 minute, the AUCb of labeled GSH was 341.5 µg· min·ml^{-1} and that of unlabeled GSH was 58325.7 µg· min·ml^{-1}. The results indicated that boosting the

unlabeled GSH was the major pathway for NAC mechanisms of action. In the following studies, we used the unlabeled GSH as the major PD endpoint and correlated the plasma concentrations of NAC with the unlabeled GSH.

6.3.4 Population PK/PD analysis of NAC in plasma and total GSH in RBC

Simultaneous PK and PD modeling on NAC/GSH were implemented with fixed population means, variance and covariance matrix of NAC PK parameters, which were previously derived from the population PK analysis. The PD model described in Figure 6-3 was fitted using total GSH in RBC. A population PK/PD analysis was performed where the population means, variance and covariance matrix of V1, K10, K12, and K21 were fixed (Table 6-2). The population PD parameters estimates are listed in Table 3. Of note, the population mean for efficacy (Emax) was estimated to be 22.6% increase in the rate of GSH production. Between-subject variability for all parameters were estimated and found to be lower than 40.0%. The coefficient of variation for the random residual constant was fixed to be 10% based on assay variability to resolve the identifiability issue. The VPC revealed that the full model provided a reliable description of the data with good precision of structural model and variance parameter estimates. Figure 6-9 shows the observed GSH in RBCs concentrations versus time, with the observed median (solid line) and the observed 5th and 95th percentiles (blue shaded area) overlaid. The plot also shows results from the VPC as the simulated median (dashed line) and 5th and 95th

percentiles (lighter blue shaded area) overlaid. Overall, simulated distributions were similar to the observed NAC concentrations.

Parameters	Estimates	BSV%	Units	Indication
Kin	26.10	37.9	µg·min/ml	Rate of production
EC50	0.64	39.4	µg/ml	Concentration for 50% efficacy
Emax	22.6%	24.4	%	% increase in Rate of Synthesis
GSH(0)	1309	5.18	µg/ml	Baseline

Table 6-3 NAC-GSH population PD parameters in WT mice estimated in ADAPT5. PK parameters were the same as in Table2.

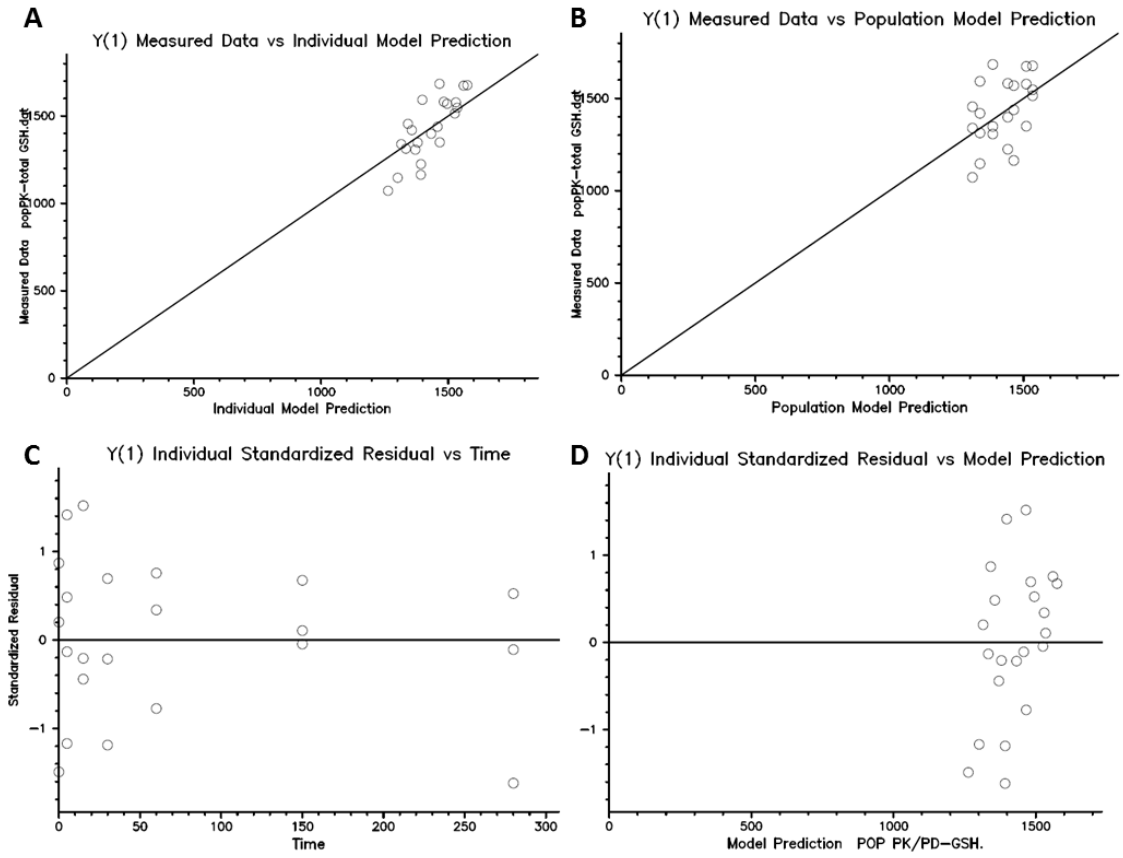

Figure 6-8 Goodness-of-fit graphics for PD output (GSH in RBC) of NAC-GSH PK/PD modeling. Population PK parameters were fixed. (A), the observed concentrations versus the individual predictions; (B), the observed concentrations versus the population predictions; (C), standardized residuals versus the time after dosing; (D) standardized residuals versus the individual predictions; the line of identity is included in both (A) and (B).

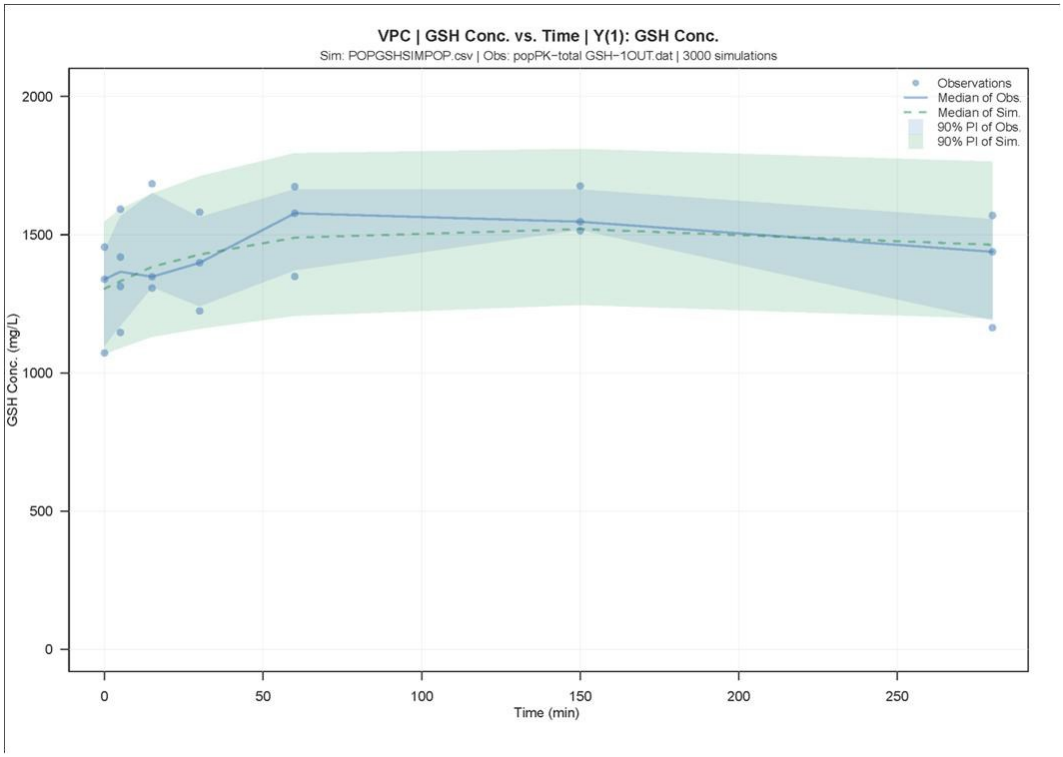

Figure 6-9 Visual predictive check (VPC) plots for NAC-GSH PK-PD model evaluation (total GSH levels were simulated). Observed data is similar to the simulated data in a reasonable way.

6.3.5 Labeled NAC boosts redox ratios of unlabeled GSH/GSSG in brain

In brain homogenates, NAC, unlabeled and labeled (on one cysteine residual) GSH, unlabeled and labeled GSSG were detected simultaneously using our established LC/MS method. Interestingly, no NAC was detected in brain homogenates which was consistent with previous findings that very limited amount of radio-labeled NAC could cross the brain-blood barrier (BBB) (Farr et al., 2003). In addition, we were not able to detect any

labeled GSH and GSSG products in brain homogenates (data not shown). Redox ratios of unlabeled GSH/GSSG in brain tissue homogenates were found to be increased after the administration of single intravenous bolus NAC (Figure 6-10). The baseline redox ratios (GSH/GSSG) in control group dosed with saline were 11.2± 0.9. Redox ratios were found be higher than the baseline levels at all sampling times post-dosing (5min -280 min) and the maximal redox ratio was found to be 19.5± 2.9 at 150 minutes post-dosing. Two peaks appeared over the sampling interval with a fast peak appeared at 15 min and a slow peak appeared at 150 min. These results indicated that intravenous bolus NAC increases the redox ratios in the brain for a sustained period of time and possibly via multiple mechanisms.

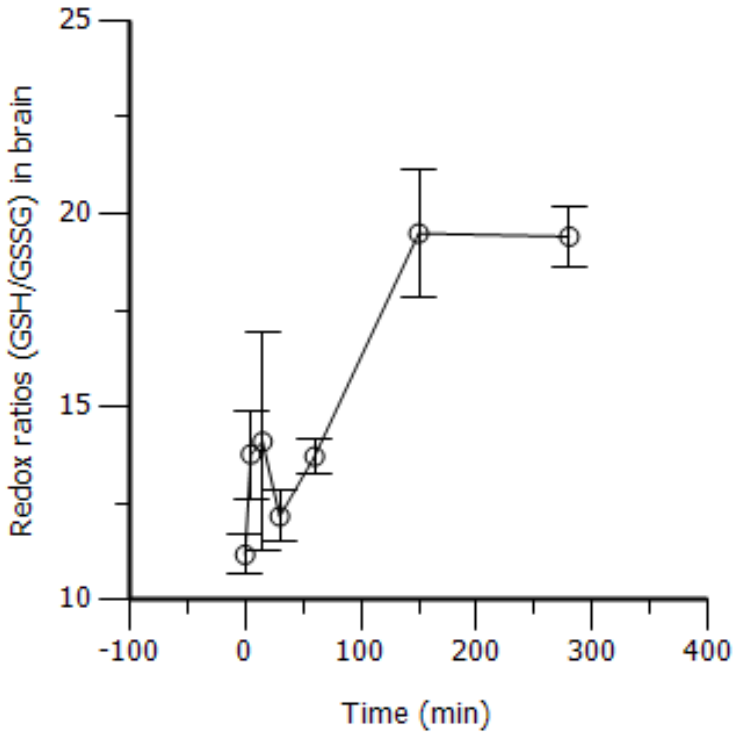

Figure 6-10 Redox ratios (GSH/GSSG) in the brain post NAC dosing in WT mice.

6.4 Discussion

NAC has long been considered as a potent antioxidant in eliminating free radicals or oxidative stress in clinical studies and this effect is thought to be related to its contribution towards the biosynthesis of GSH, which plays a key role in antioxidant defense system of cells. However, the precise mechanisms of action for the biotransformation of NAC into GSH are not clear. The present study was designed to identify the mechanisms of action of NAC in wild type (WT) mice using stable-labeled technology where the cysteine group on NAC molecule is labeled with non-radioactive isotopes so as to track its fate in biotransformation. As shown in Figure 6-7, the labeled GSH concentrations increased much less than the unlabeled GSH concentrations following a single intravenous NAC dose. The AUCb (0-280 min) of labeled GSH was found to be less than 0.1% of unlabeled AUCb. These data suggest that only minimal GSH synthesis is the result of direct deacetylation of NAC to cysteine. Based on these data, increased availability of free cysteine (Figure 6-1, pathway B) or increased free GSH (Figure 6-1, pathway C) might describe the role of NAC in GSH synthesis better compared to direct synthesis (Figure 6-1, pathway A). However, this conclusion may only be valid in WT mice without GSH depletion. In in-*vivo* disease models with GSH depletion, endogenously- and exogenously-produced GSH may both play key roles in the antioxidative defense.

Despite the wide investigation of NAC's effects on total GSH and redox ratios, the PK/PD parameters of NAC and GSH have not been well characterized. The fact that NAC and GSH are present in both the reduced and oxidized forms makes the analytical methods quite complicated (Olsson et al., 1988).Olsson *et al.* showed that the PK parameters of reduced form NAC were quite different from total (reduced and oxidized) forms of NAC. Thus the method of analysis for NAC and GSH varied and might influence the PK study results (Cotgreave and Moldeus, 1987, Ercal et al., 1996, Zinellu et al., 2009). Our lab has established a standard LC/MS assay protocol to simultaneously measure the reduced, oxidized or total forms of NAC or GSH which was crucial for this study.

We also characterized the PK parameters of NAC in WT mice. Consistent with previous results, the $T_{1/2}$ was estimated to be around 20 minutes using radio-labeled techniques (Farr et al., 2003) in mice. This $T_{1/2}$ in mice was found to be much shorter than in cat (1.3 hrs) (Buur et al., 2013), dog (4.0 hrs) (Shen et al., 2008) and human (2.3 hrs) (Borgstrom et al., 1986) which indicated that NAC was eliminated in mice very quickly. In addition, we also found out that a 2-compartmental model fitted the data pretty well, consistent with previous modeling work of NAC in dog (Shen et al., 2008) and cat (Buur et al., 2013). In humans, 2-compartment and 3-compartment PK models were both implemented for intravenous NAC (Brown et al., 2004). However, the validity of the PK model is restricted by limited sampling time points in our study, especially at the terminal phase. Current NAC studies in murine disease models, such as ALD mouse model

(Lopez-Erauskin et al., 2011a), Parkinson's mouse model (Park et al., 2004) and Alzheimer's mouse model (Farr et al., 2003), lack PK analysis which would better characterize the therapeutic potential of NAC. Results from this study would greatly facilitate the PK/PD modeling of NAC in these disease models.

NAC was reported to increase the intracellular GSH levels in RBCs in rats (De Flora et al., 1985) and peripheral blood lymphocyte in human (Pendyala and Creaven, 1995). The elevations in GSH was assumed to shed beneficial effects on various oxidative stress related disease conditions such as cancer patients receiving chemotherapy (Pendyala and Creaven, 1995) , or neurodegenerative disorders of Parkinson's disease (Guo et al., 2013) and Alzheimer's disease (Lasierra-Cirujeda et al., 2013). However, there is no PK/PD model established to describe the relationship between NAC and GSH as to our knowledge. In this study, we found out the indirect response model (or turnover model, Figure 6-11) (Dayneka et al., 1993) could be rationally used to describe the production process of intracellular GSH where NAC concentration was linked to stimulate the rate of GSH production through an Emax model (Figure 6-3). Our results indicated that the maximal increase in the rate of GSH production (Emax) was 22.6%. Given this result be extended to human due to similar pathways of mechanisms of action and enzyme properties, it could well explain previous published results that most human subjects were observed to have around 20% increase in GSH levels in peripheral blood lymphocyte post NAC dosing (Pendyala and Creaven, 1995).

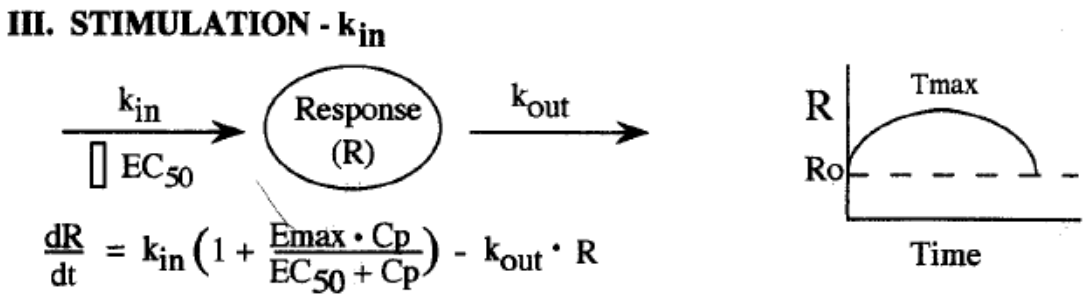

Figure 6-11, basic indirect response model structure (left) and representative response variable time profile (right). Figure from (Dayneka et al., 1993).

In addition, we also investigated the redox ratio changes in brain tissues as exploratory specific aim for this study. Redox ratios in the brain were reported as crucial indicator for oxidative stress (Escobar et al., 2013, Mishra and Srivastava, 2013). Using magnetic resonance spectroscopy (MRS) in Parkinson's and Gaucher's patients and healthy volunteers, Holmay et al. discovered that brain GSH was boosted in all tested subjects following a single intravenous administration of 150mg/kg NAC (Holmay et al., 2013). In this study, we further tested the redox ratios in the brain tissues following the same dose of NAC in mice. Redox ratios were found to be greatly increased. Although the $T_{1/2}$ of NAC in plasma was 24.5 minutes as shown in Table1, the redox ratios were sustained for the later time points when NAC was undetectable in plasma. The results indicated delayed and sustained effect of intravenous bolus NAC to boost brain redox ratios. The fact that there was very limited NAC, if any, crossed the blood-brain-barrier indicated that NAC may not need to be taken up into the brain to boost redox ratios. It is well-known that the amount of cysteine is highly correlated with the GSH/GSSG redox ratios (Dayneka et al., 1993), and that NAC could release free cysteine quickly and significantly

(Radtke et al., 2012). Thus it is highly possible that NAC increases GSH/GSSG redox ratios by increasing free cysteine available in the brain.

However, due to the limitations in experimental design with destructive sampling techniques, as well as limited animals per group and lack of sampling time points after 3 hours, large amount of variability was observed in both PK and PK/PD modeling studies. Further studies using large animals with more intensive sampling time points could greatly improve the PK/PD model and generate better understanding of the mechanisms of action of NAC.

In the current study, ~20g C57 mice were administered with a single dose of 150 mg/kg NAC intravenously. The plasma NAC concentration immediately following dosing (maximal) was estimated to be180 μg/ml, and the $T_{1/2}$ was estimated to be 25 minutes. Previously, our lab had collected PK data in CCALD patients dosed with 70mg/kg every 6 hrs intravenous NAC (Holmay et al., 2012). The maximal concentration for plasma NAC was found to be ~100 μg/ml and the $T_{1/2}$ was estimated to be 1.5hrs in patients. The plasma concentrations studied in mice and CCALD patients are comparable except that NAC is eliminated more quickly in mice than in patients. Conclusions from this mice study can be also applicable to CCALD patients.

6.5 Conclusion

In summary, the present study characterized the PK properties of NAC in mice, established the PK/PD model between plasma concentration of NAC and GSH levels in RBCs, and explored the effect of NAC administration on redox ratios in the brain. Further, this study investigated the biotransformation of NAC and proved that increased GSH mainly came from endogenous source instead of exogenous source using stable-labeled NAC.

Our long-term research goal is to understand, develop, and refine dosing strategies for NAC in oxidative stress related CNS disorders such as Parkinson's and Gaucher's disease. Our understanding of the mechanisms of action of NAC and results from this study provide target concentrations that will inform the design of NAC dosing strategies in future studies in disease mouse models and clinical studies.

CHAPTER 7

CONCLUSIONS AND FUTURE STUDIES

7.1 Summary and conclusions

CCALD is one type of neurodegenerative disorders and assumed to be highly associated with oxidative stress in recent studies. The successful application of NAC in CCALD patients during HSCT is the main drive for design of experiments in current research. The main goal of this study is to investigate *in vitro*, *in vivo* and clinical pharmacology of NAC in mitigating oxidative stress in CCALD patients. Projects in the thesis include a clinical study to find out the downstream antioxidant proteins induced by NAC in CCALD patients (Chapter 3), an *in-vitro* cell study to examine the mechanisms of action of NAC in promoting cell survival under oxidative stress (Chapter 4), an *in-vitro* cell study to investigate the roles of NAC in reversing the mitochondrial toxicity induced by VLCFAs associated with CCALD disorders (Chapter 5), and an *in-vivo* mice study to characterize the PK/PD properties of NAC as well as its transformation pathways into GSH (Chapter 6).

Major conclusions from all studies above are summarized below:

a) The clinical and *in-vitro* studies (Chapter 3 and 4) led us to conclude that HO-1 is a potential mediator for NAC cytoprotective action in addition to the well-known GSH.

b) HO-1 and ferritin induced by NAC are highly correlated in plasma of CCALD patients (Chapter 3).

c) NAC promotes cell survival under oxidative stress through HO-1 and GSH (Chapter 4).

d) VLCFAs, which are thought to be the primary cause for CCALD disease, cause mitochondrial dysfunction in oligodendrocytes. In particular, VLCFAs deplete mtGSH and therefore increase levels of superoxide anions in mitochondria (Chapter 5).

e) NAC restores mtGSH depleted by VLCFAs and reverses the mitochondrial toxicity caused by VLCFAs (Chapter 5).

f) PK/PD studies in mice showed that intravenous administration of NAC could increase the total GSH in RBCs and redox ratios in brain (Chapter 6).

g) Tracking the biotransformation of stable-labeled NAC revealed that NAC increases GSH levels through increasing the availability of endogenous cysteine or releasing GSH from oxidized forms, rather than providing the exogenous cysteine as substrates for GSH synthesis (Chapter 6).

In summary, we investigated the pharmacology of NAC using different biological systems including mitochondria, cells, mice and human patients. NAC was shown to mitigate oxidative stress in CCALD associated models by supplementing GSH and increasing the expression of HO-1. In addition, NAC was also shown to be effective at the site of brain which is extremely meaningful to neurodegenerative disorders with CNS dysfunction such as CCALD.

7.2 Significance

NAC has been investigated extensively in various disease conditions. The current studies target to provide more information for the application of NAC in the treatment of CCALD. Although NAC has become the standard of care for late-stage CCALD patients during HSCT, the application of NAC in the early-stage of CCALD or in other clinical phenotypes of ALD such as AMN has not been validated and studied extensively. In addition, NAC may also benefit other types of neurodegenerative disorders associated with oxidative stress. Full understanding of the mechanisms of action of NAC is therefore quite meaningful in promoting the use of NAC into neurodegenerative disorders sharing similar pathologies such as Gaucher's disease, Multiple Sclerosis, Alzheimer's disease etc.

Significance of studies performed in this thesis is summarized below:

a) Studies indicate HO-1 as the newly discovered downstream mediator for NAC's mechanisms of action (Chapter 3 and 4).

b) Results from the thesis show for the first time that depletion of mtGSH is one of the pathological mechanisms in CCALD and that targeting mitochondrial dysfunction may be a potential intervention strategy for CCALD patients (Chapter 5).

c) PK/PD models are generated for the first time to describe the role of NAC *in vivo.* And that the biotransformation of NAC is clarified (Chapter 6).

d) Characterization of NAC mechanisms of action can help to optimize therapy in late-stage CCALD patients. GSH levels, redox ratio, HO-1 and ferritin levels can serve as new biomarkers assessing NAC therapy. These biomarkers can guide dosing regiments including dose and route of administration.

e) The information generated from my study on the efficacy of NAC in CCALD is also applicable to other neurodegenerative disorders sharing similar pathologies such as Gaucher's disease, Multiple Sclerosis, Alzheimer's disease etc.

In summary, results from this thesis will advance the use of NAC by providing a clearer understanding of its pharmacology. Information from the studies will help to explain the results of past clinical trials and, prospectively, be used to design studies aimed at determining optimal NAC dosage regimens.

7.3 Future studies

The fact that NAC improves the survival in late-stage CCALD patients makes the use of NAC promising. Understanding of its mechanisms of action can greatly facilitate its use in other disease conditions. From conclusions drawn from current research, use of NAC in early-stage CCALD is possibly beneficial, as well as in other types of neurodegenerative disorders. However, clinical trial is the golden standard to verify and extend conclusions from *in-vitro* and *in-vivo* studies to patients. Future studies will be required to examine the efficacy of NAC on mitigating oxidative stress in different stages

of CCALD, other types of ALD, and other neurodegenerative disorders associated with oxidative stress.

In addition, there are still unanswered questions on the use of NAC in neurodegenerative disorders, e.g., whether oral NAC is as equivalent as intravenous NAC in mitigating oxidative stress in neurodegeneration. And if it is true, substitution of intravenous formulation with oral formulation could greatly reduce the cost given the fact that cheaper NAC tablet is available on market. In addition, NAC could be used in combination with other antioxidants, which could possibly generate synergistic beneficial effects due to various mechanisms of antioxidant action.

References

Abraham NG, Asija A, Drummond G, Peterson S (2007) Heme oxygenase -1 gene therapy: recent advances and therapeutic applications. Curr Gene Ther 7:89-108.

Abraham NG, Kappas A (2008) Pharmacological and clinical aspects of heme oxygenase. Pharmacol Rev 60:79-127.

Adair JC, Knoefel JE, Morgan N (2001) Controlled trial of N-acetylcysteine for patients with probable Alzheimer's disease. Neurology 57:1515-1517.

Ahmad S, Khan MB, Hoda MN, Bhatia K, Haque R, Fazili IS, Jamal A, Khan JS, Katare DP (2012) Neuroprotective effect of sesame seed oil in 6-hydroxydopamine induced neurotoxicity in mice model: cellular, biochemical and neurochemical evidence. Neurochem Res 37:516-526.

Ahola T, Fellman V, Laaksonen R, Laitila J, Lapatto R, Neuvonen PJ, Raivio KO (1999) Pharmacokinetics of intravenous N-acetylcysteine in pre-term new-born infants. Eur J Clin Pharmacol 55:645-650.

Al-Tonbary Y, Al-Haggar M, El-Ashry R, El-Dakroory S, Azzam H, Fouda A (2009) Vitamin e and N-acetylcysteine as antioxidant adjuvant therapy in children with acute lymphoblastic leukemia. Adv Hematol 2009:689639.

Andersen JK (2004) Oxidative stress in neurodegeneration: cause or consequence? Nat Med 10 Suppl:S18-25.

Anderson MF, Sims NR (2002) The effects of focal ischemia and reperfusion on the glutathione content of mitochondria from rat brain subregions. J Neurochem 81:541-549.

Aoyama K, Nakaki T (2013) Impaired glutathione synthesis in neurodegeneration. Int J Mol Sci 14:21021-21044.

Appelboam AV, Dargan PI, Knighton J (2002) Fatal anaphylactoid reaction to N-acetylcysteine: caution in patients with asthma. Emerg Med J 19:594-595.

Appleton SD, Chretien ML, McLaughlin BE, Vreman HJ, Stevenson DK, Brien JF, Nakatsu K, Maurice DH, Marks GS (1999) Selective inhibition of heme oxygenase, without inhibition of nitric oxide synthase or soluble guanylyl cyclase, by metalloporphyrins at low concentrations. Drug metabolism and disposition: the biological fate of chemicals 27:1214-1219.

Arakawa M, Ushimaru N, Osada N, Oda T, Ishige K, Ito Y (2006) N-acetylcysteine selectively protects cerebellar granule cells from 4-hydroxynonenal-induced cell death. Neurosci Res 55:255-263.

Arfsten DP, Johnson EW, Wilfong ER, Jung AE, Bobb AJ (2007) Distribution of radio-labeled N-Acetyl-L-Cysteine in Sprague-Dawley rats and its effect on glutathione metabolism following single and repeat dosing by oral gavage. Cutan Ocul Toxicol 26:113-134.

Aruoma OI, Halliwell B, Hoey BM, Butler J (1989) The antioxidant action of N-acetylcysteine: its reaction with hydrogen peroxide, hydroxyl radical, superoxide, and hypochlorous acid. Free radical biology & medicine 6:593-597.

Asheuer M, Bieche I, Laurendeau I, Moser A, Hainque B, Vidaud M, Aubourg P (2005) Decreased expression of ABCD4 and BG1 genes early in the pathogenesis of X-linked adrenoleukodystrophy. Hum Mol Genet 14:1293-1303.

Atkuri KR, Mantovani JJ, Herzenberg LA (2007) N-Acetylcysteine--a safe antidote for cysteine/glutathione deficiency. Curr Opin Pharmacol 7:355-359.

Aubourg P, Adamsbaum C, Lavallard-Rousseau MC, Rocchiccioli F, Cartier N, Jambaque I, Jakobezak C, Lemaitre A, Boureau F, Wolf C, et al. (1993) A two-year trial of oleic and erucic acids ("Lorenzo's oil") as treatment for adrenomyeloneuropathy. N Engl J Med 329:745-752.

Baarine M, Andreoletti P, Athias A, Nury T, Zarrouk A, Ragot K, Vejux A, Riedinger JM, Kattan Z, Bessede G, Trompier D, Savary S, Cherkaoui-Malki M, Lizard G (2012a) Evidence of oxidative stress in very long chain fatty acid--treated oligodendrocytes and potentialization of ROS production using RNA interference-directed knockdown of ABCD1 and ACOX1 peroxisomal proteins. Neuroscience 213:1-18.

Baarine M, Ragot K, Athias A, Nury T, Kattan Z, Genin EC, Andreoletti P, Menetrier F, Riedinger JM, Bardou M, Lizard G (2012b) Incidence of Abcd1 level on the induction of cell death and organelle dysfunctions triggered by very long chain fatty acids and TNF-alpha on oligodendrocytes and astrocytes. Neurotoxicology 33:212-228.

Baarine M, Ragot K, Genin EC, El Hajj H, Trompier D, Andreoletti P, Ghandour MS, Menetrier F, Cherkaoui-Malki M, Savary S, Lizard G (2009a) Peroxisomal and mitochondrial status of two murine oligodendrocytic cell lines (158N, 158JP): potential models for the study of peroxisomal disorders associated with dysmyelination processes. J Neurochem 111:119-131.

Baarine M, Ragot K, Genin EC, El Hajj H, Trompier D, Andreoletti P, Ghandour MS, Menetrier F, Cherkaoui-Malki M, Savary S, Lizard G (2009b) Peroxisomal and mitochondrial status of two murine oligodendrocytic cell lines (158N, 158JP): potential models for the study of peroxisomal disorders associated with dysmyelination processes. Journal of neurochemistry 111:119-131.

Badaloo A, Reid M, Forrester T, Heird WC, Jahoor F (2002) Cysteine supplementation improves the erythrocyte glutathione synthesis rate in children with severe edematous malnutrition. Am J Clin Nutr 76:646-652.

Badisa RB, Goodman CB, Fitch-Pye CA (2013) Attenuating effect of N-acetyl-L-cysteine against acute cocaine toxicity in rat C6 astroglial cells. International journal of molecular medicine 32:497-502.

Bagh MB, Maiti AK, Jana S, Banerjee K, Roy A, Chakrabarti S (2008) Quinone and oxyradical scavenging properties of N-acetylcysteine prevent dopamine mediated inhibition of Na+, K+-ATPase and mitochondrial electron transport chain activity in rat brain: implications in the neuroprotective therapy of Parkinson's disease. Free Radic Res 42:574-581.

Bao W, Rong S, Zhang M, Yu X, Zhao Y, Xiao X, Yang W, Wang D, Yao P, Hu FB, Liu L (2012) Plasma heme oxygenase-1 concentration in relation to impaired glucose regulation in a non-diabetic Chinese population. PLoS One 7:e32223.

Bao W, Song F, Li X, Rong S, Yang W, Zhang M, Yao P, Hao L, Yang N, Hu FB, Liu L (2010) Plasma heme oxygenase-1 concentration is elevated in individuals with type 2 diabetes mellitus. PLoS One 5:e12371.

Barone E, Di Domenico F, Mancuso C, Butterfield DA (2013) The Janus face of the heme oxygenase/biliverdin reductase system in Alzheimer disease: It's time for reconciliation. Neurobiol Dis 62C:144-159.

Barone E, Di Domenico F, Sultana R, Coccia R, Mancuso C, Perluigi M, Butterfield DA (2012) Heme oxygenase-1 posttranslational modifications in the brain of subjects with Alzheimer disease and mild cognitive impairment. Free radical biology & medicine 52:2292-2301.

Bebarta VS, Kao L, Froberg B, Clark RF, Lavonas E, Qi M, Delgado J, McDonagh J, Arnold T, Odujebe O, O'Malley G, Lares C, Aguilera E, Dart R, Heard K, Stanford C, Kokko J, Bogdan G, Mendoza C, Mlynarchek S, Rhyee S, Hoppe J, Haur W, Tan HH, Tran NN, Varney S, Zosel A, Buchanan J, Al-Helial M (2010) A multicenter comparison of the safety of oral versus intravenous acetylcysteine for treatment of acetaminophen overdose. Clin Toxicol (Phila) 48:424-430.

Bennett LL, Mohan D (2013) Gaucher disease and its treatment options. Ann Pharmacother 47:1182-1193.

Berger J, Forss-Petter S, Eichler FS (2013) Pathophysiology of X-linked adrenoleukodystrophy. Biochimie.

Berman AE, Chan WY, Brennan AM, Reyes RC, Adler BL, Suh SW, Kauppinen TM, Edling Y, Swanson RA (2011) N-acetylcysteine prevents loss of dopaminergic neurons in the EAAC1-/- mouse. Ann Neurol 69:509-520.

Biffi A, Aubourg P, Cartier N (2011) Gene therapy for leukodystrophies. Hum Mol Genet 20:R42-53.

Biomarkers-Definitions-Working-Group (2001) Biomarkers and surrogate endpoints: preferred definitions and conceptual framework. Clin Pharmacol Ther 69:89-95.

Borgstrom L, Kagedal B, Paulsen O (1986) Pharmacokinetics of N-acetylcysteine in man. Eur J Clin Pharmacol 31:217-222.

Bravi MC, Armiento A, Laurenti O, Cassone-Faldetta M, De Luca O, Moretti A, De Mattia G (2006) Insulin decreases intracellular oxidative stress in patients with type 2 diabetes mellitus. Metabolism 55:691-695.

Brouard S, Otterbein LE, Anrather J, Tobiasch E, Bach FH, Choi AM, Soares MP (2000) Carbon monoxide generated by heme oxygenase 1 suppresses endothelial cell apoptosis. J Exp Med 192:1015-1026.

Brown M, Bjorksten A, Medved I, McKenna M (2004) Pharmacokinetics of intravenous N-acetylcysteine in men at rest and during exercise. Eur J Clin Pharmacol 60:717-723.

Brown RC, Lockwood AH, Sonawane BR (2005) Neurodegenerative diseases: an overview of environmental risk factors. Environ Health Perspect 113:1250-1256.

Buckley NA, Whyte IM, O'Connell DL, Dawson AH (1999) Oral or intravenous N-acetylcysteine: which is the treatment of choice for acetaminophen (paracetamol) poisoning? J Toxicol Clin Toxicol 37:759-767.

Butterfield DA, Castegna A, Lauderback CM, Drake J (2002) Evidence that amyloid beta-peptide-induced lipid peroxidation and its sequelae in Alzheimer's disease brain contribute to neuronal death. Neurobiol Aging 23:655-664.
Buur JL, Diniz PP, Roderick KV, KuKanich B, Tegzes JH (2013) Pharmacokinetics of N-acetylcysteine after oral and intravenous administration to healthy cats. Am J Vet Res 74:290-293.
Calabrese V, Lodi R, Tonon C, D'Agata V, Sapienza M, Scapagnini G, Mangiameli A, Pennisi G, Stella AM, Butterfield DA (2005) Oxidative stress, mitochondrial dysfunction and cellular stress response in Friedreich's ataxia. J Neurol Sci 233:145-162.
Cartier N, Aubourg P (2010) Hematopoietic stem cell transplantation and hematopoietic stem cell gene therapy in X-linked adrenoleukodystrophy. Brain Pathol 20:857-862.
Cartier N, Hacein-Bey-Abina S, Von Kalle C, Bougneres P, Fischer A, Cavazzana-Calvo M, Aubourg P (2010) [Gene therapy of x-linked adrenoleukodystrophy using hematopoietic stem cells and a lentiviral vector]. Bull Acad Natl Med 194:255-264; discussion 264-258.
Cassidy N, Tracey JA, Drew SA (2008) Cardiac arrest following therapeutic administration of N-acetylcysteine for paracetamol overdose. Clin Toxicol (Phila) 46:921.
Cella M, Kloprogge F, Danhof M, Della Pasqua O (2012) Dosing rationale for fixed-dose combinations in children: shooting from the hip? Clin Pharmacol Ther 91:718-725.
Chauhan A, Audhya T, Chauhan V (2012) Brain region-specific glutathione redox imbalance in autism. Neurochem Res 37:1681-1689.
Chien WL, Lee TR, Hung SY, Kang KH, Lee MJ, Fu WM (2011) Impairment of oxidative stress-induced heme oxygenase-1 expression by the defect of Parkinson-related gene of PINK1. Journal of neurochemistry 117:643-653.
Chinta SJ, Kumar MJ, Hsu M, Rajagopalan S, Kaur D, Rane A, Nicholls DG, Choi J, Andersen JK (2007) Inducible alterations of glutathione levels in adult dopaminergic midbrain neurons result in nigrostriatal degeneration. J Neurosci 27:13997-14006.
Choi AM, Alam J (1996) Heme oxygenase-1: function, regulation, and implication of a novel stress-inducible protein in oxidant-induced lung injury. Am J Respir Cell Mol Biol 15:9-19.
Choi IY, Lee SP, Denney DR, Lynch SG (2011a) Lower levels of glutathione in the brains of secondary progressive multiple sclerosis patients measured by 1H magnetic resonance chemical shift imaging at 3 T. Mult Scler 17:289-296.
Choi IY, Lee SP, Denney DR, Lynch SG (2011b) Lower levels of glutathione in the brains of secondary progressive multiple sclerosis patients measured by 1H magnetic resonance chemical shift imaging at 3 T. Multiple sclerosis 17:289-296.
Choi J, Sullards MC, Olzmann JA, Rees HD, Weintraub ST, Bostwick DE, Gearing M, Levey AI, Chin LS, Li L (2006a) Oxidative damage of DJ-1 is linked to sporadic

Parkinson and Alzheimer diseases. The Journal of biological chemistry 281:10816-10824.
Choi J, Sullards MC, Olzmann JA, Rees HD, Weintraub ST, Bostwick DE, Gearing M, Levey AI, Chin LS, Li L (2006b) Oxidative damage of DJ-1 is linked to sporadic Parkinson and Alzheimer diseases. J Biol Chem 281:10816-10824.
Colin-Gonzalez AL, Orozco-Ibarra M, Chanez-Cardenas ME, Rangel-Lopez E, Santamaria A, Pedraza-Chaverri J, Barrera-Oviedo D, Maldonado PD (2013) Heme oxygenase-1 (HO-1) upregulation delays morphological and oxidative damage induced in an excitotoxic/pro-oxidant model in the rat striatum. Neuroscience 231:91-101.
Cornford EM, Braun LD, Crane PD, Oldendorf WH (1978) Blood-brain barrier restriction of peptides and the low uptake of enkephalins. Endocrinology 103:1297-1303.
Cotgreave IA (1997) N-acetylcysteine: pharmacological considerations and experimental and clinical applications. Adv Pharmacol 38:205-227.
Cotgreave IA, Moldeus P (1987) Methodologies for the analysis of reduced and oxidized N-acetylcysteine in biological systems. Biopharm Drug Dispos 8:365-375.
Cuadrado A, Rojo AI (2008) Heme oxygenase-1 as a therapeutic target in neurodegenerative diseases and brain infections. Curr Pharm Des 14:429-442.
Dayneka NL, Garg V, Jusko WJ (1993) Comparison of four basic models of indirect pharmacodynamic responses. J Pharmacokinet Biopharm 21:457-478.
D'Argenio, D.Z., A. Schumitzky and X. Wang. ADAPT 5 User's Guide:Pharmacokinetic/Pharmacodynamic Systems Analysis Software. BiomedicalSimulations Resource, Los Angeles, 2009.
De Flora S, Bennicelli C, Camoirano A, Serra D, Romano M, Rossi GA, Morelli A, De Flora A (1985) In vivo effects of N-acetylcysteine on glutathione metabolism and on the biotransformation of carcinogenic and/or mutagenic compounds. Carcinogenesis 6:1735-1745.
De Rosa SC, Zaretsky MD, Dubs JG, Roederer M, Anderson M, Green A, Mitra D, Watanabe N, Nakamura H, Tjioe I, Deresinski SC, Moore WA, Ela SW, Parks D, Herzenberg LA (2000) N-acetylcysteine replenishes glutathione in HIV infection. Eur J Clin Invest 30:915-929.
Dean O, Giorlando F, Berk M (2011a) N-acetylcysteine in psychiatry: current therapeutic evidence and potential mechanisms of action. J Psychiatry Neurosci 36:78-86.
Dean OM, van den Buuse M, Berk M, Copolov DL, Mavros C, Bush AI (2011b) N-acetyl cysteine restores brain glutathione loss in combined 2-cyclohexene-1-one and d-amphetamine-treated rats: relevance to schizophrenia and bipolar disorder. Neurosci Lett 499:149-153.
Decramer M, Rutten-van Molken M, Dekhuijzen PN, Troosters T, van Herwaarden C, Pellegrino R, van Schayck CP, Olivieri D, Del Donno M, De Backer W, Lankhorst I, Ardia A (2005) Effects of N-acetylcysteine on outcomes in chronic obstructive pulmonary disease (Bronchitis Randomized on NAC Cost-Utility Study, BRONCUS): a randomised placebo-controlled trial. Lancet 365:1552-1560.

Deon M, Sitta A, Barschak AG, Coelho DM, Pigatto M, Schmitt GO, Jardim LB, Giugliani R, Wajner M, Vargas CR (2007) Induction of lipid peroxidation and decrease of antioxidant defenses in symptomatic and asymptomatic patients with X-linked adrenoleukodystrophy. Int J Dev Neurosci 25:441-444.

Deon M, Sitta A, Barschak AG, Coelho DM, Terroso T, Schmitt GO, Wanderley HY, Jardim LB, Giugliani R, Wajner M, Vargas CR (2008) Oxidative stress is induced in female carriers of X-linked adrenoleukodystrophy. J Neurol Sci 266:79-83.

Desai BS, Monahan AJ, Carvey PM, Hendey B (2007) Blood-brain barrier pathology in Alzheimer's and Parkinson's disease: implications for drug therapy. Cell Transplant 16:285-299.

Dexter DT, Carter CJ, Wells FR, Javoy-Agid F, Agid Y, Lees A, Jenner P, Marsden CD (1989) Basal lipid peroxidation in substantia nigra is increased in Parkinson's disease. J Neurochem 52:381-389.

Dodd S, Dean O, Copolov DL, Malhi GS, Berk M (2008) N-acetylcysteine for antioxidant therapy: pharmacology and clinical utility. Expert Opin Biol Ther 8:1955-1962.

Drew R, Miners JO (1984) The effects of buthionine sulphoximine (BSO) on glutathione depletion and xenobiotic biotransformation. Biochem Pharmacol 33:2989-2994.

Dringen R, Hamprecht B (1999) N-acetylcysteine, but not methionine or 2-oxothiazolidine-4-carboxylate, serves as cysteine donor for the synthesis of glutathione in cultured neurons derived from embryonal rat brain. Neurosci Lett 259:79-82.

Duchesne N, Dufour M, Bouchard G, Grondin P, Lemieux B (1995) Adrenoleukodystrophy: magnetic resonance follow-up after Lorenzo's oil therapy. Can Assoc Radiol J 46:386-391.

Dulak J, Jozkowicz A (2003) Carbon monoxide -- a "new" gaseous modulator of gene expression. Acta Biochim Pol 50:31-47.

Dusre L, Mimnaugh EG, Myers CE, Sinha BK (1989) Potentiation of doxorubicin cytotoxicity by buthionine sulfoximine in multidrug-resistant human breast tumor cells. Cancer research 49:511-515.

Eisenstein RS, Garcia-Mayol D, Pettingell W, Munro HN (1991) Regulation of ferritin and heme oxygenase synthesis in rat fibroblasts by different forms of iron. Proc Natl Acad Sci U S A 88:688-692.

Elmore S (2007) Apoptosis: a review of programmed cell death. Toxicol Pathol 35:495-516.

Emerit J, Edeas M, Bricaire F (2004) Neurodegenerative diseases and oxidative stress. Biomed Pharmacother 58:39-46.

Engelen M, Kemp S, van Geel BM (2008) [From gene to disease; X-linked adrenoleukodystrophy]. Ned Tijdschr Geneeskd 152:804-808.

Ercal N, Oztezcan S, Hammond TC, Matthews RH, Spitz DR (1996) High-performance liquid chromatography assay for N-acetylcysteine in biological samples following derivatization with N-(1-pyrenyl)maleimide. J Chromatogr B Biomed Appl 685:329-334.

Erdmann K, Cheung BW, Immenschuh S, Schroder H (2008) Heme oxygenase-1 is a novel target and antioxidant mediator of S-adenosylmethionine. Biochem Biophys Res Commun 368:937-941.
Erdmann K, Grosser N, Schroder H (2005) L-methionine reduces oxidant stress in endothelial cells: role of heme oxygenase-1, ferritin, and nitric oxide. Aaps J 7:E195-200.
Erickson MA, Hansen K, Banks WA (2012) Inflammation-induced dysfunction of the low-density lipoprotein receptor-related protein-1 at the blood-brain barrier: protection by the antioxidant N-acetylcysteine. Brain Behav Immun 26:1085-1094.
Escobar J, Cubells E, Enomoto M, Quintas G, Kuligowski J, Fernandez CM, Torres-Cuevas I, Sastre J, Belik J, Vento M (2013) Prolonging in utero-like oxygenation after birth diminishes oxidative stress in the lung and brain of mice pups. Redox Biol 1:297-303.
Ewing P, Hildebrandt GC, Planke S, Andreesen R, Holler E, Gerbitz A (2007) Cobalt protoporphyrine IX-mediated heme oxygenase-I induction alters the inflammatory cytokine response, but not antigen presentation after experimental allogeneic bone marrow transplantation. Int J Mol Med 20:301-308.
Farr SA, Poon HF, Dogrukol-Ak D, Drake J, Banks WA, Eyerman E, Butterfield DA, Morley JE (2003) The antioxidants alpha-lipoic acid and N-acetylcysteine reverse memory impairment and brain oxidative stress in aged SAMP8 mice. J Neurochem 84:1173-1183.
Fedotcheva NI, Teplova VV, Beloborodova NV (2012) [The role of thiol antioxidants in restoring mitochondrial functions, modified by microbial metabolites]. Biofizika 57:820-826.
Feigin A (2004) Evidence from biomarkers and surrogate endpoints. NeuroRx 1:323-330.
Fernandez-Checa JC, Kaplowitz N, Garcia-Ruiz C, Colell A (1998) Mitochondrial glutathione: importance and transport. Semin Liver Dis 18:389-401.
Fourcade S, Lopez-Erauskin J, Galino J, Duval C, Naudi A, Jove M, Kemp S, Villarroya F, Ferrer I, Pamplona R, Portero-Otin M, Pujol A (2008) Early oxidative damage underlying neurodegeneration in X-adrenoleukodystrophy. Hum Mol Genet 17:1762-1773.
Fourcade S, Lopez-Erauskin J, Ruiz M, Ferrer I, Pujol A (2013) Mitochondrial dysfunction and oxidative damage cooperatively fuel axonal degeneration in X-linked adrenoleukodystrophy. Biochimie.
Fourcade S, Ruiz M, Guilera C, Hahnen E, Brichta L, Naudi A, Portero-Otin M, Dacremont G, Cartier N, Wanders R, Kemp S, Mandel JL, Wirth B, Pamplona R, Aubourg P, Pujol A (2010) Valproic acid induces antioxidant effects in X-linked adrenoleukodystrophy. Hum Mol Genet 19:2005-2014.
Frank-Cannon TC, Alto LT, McAlpine FE, Tansey MG (2009) Does neuroinflammation fan the flame in neurodegenerative diseases? Mol Neurodegener 4:47.
French HM, Reid M, Mamontov P, Simmons RA, Grinspan JB (2009) Oxidative stress disrupts oligodendrocyte maturation. J Neurosci Res 87:3076-3087.

Galea E, Launay N, Portero-Otin M, Ruiz M, Pamplona R, Aubourg P, Ferrer I, Pujol A (2012) Oxidative stress underlying axonal degeneration in adrenoleukodystrophy: a paradigm for multifactorial neurodegenerative diseases? Biochim Biophys Acta 1822:1475-1488.

Galino J, Ruiz M, Fourcade S, Schluter A, Lopez-Erauskin J, Guilera C, Jove M, Naudi A, Garcia-Arumi E, Andreu AL, Starkov AA, Pamplona R, Ferrer I, Portero-Otin M, Pujol A (2011) Oxidative damage compromises energy metabolism in the axonal degeneration mouse model of X-adrenoleukodystrophy. Antioxid Redox Signal 15:2095-2107.

Gerbitz A, Ewing P, Wilke A, Schubert T, Eissner G, Dietl B, Andreesen R, Cooke KR, Holler E (2004) Induction of heme oxygenase-1 before conditioning results in improved survival and reduced graft-versus-host disease after experimental allogeneic bone marrow transplantation. Biol Blood Marrow Transplant 10:461-472.

Gilgun-Sherki Y, Melamed E, Offen D (2004) The role of oxidative stress in the pathogenesis of multiple sclerosis: the need for effective antioxidant therapy. J Neurol 251:261-268.

Goes AT, Souza LC, Filho CB, Del Fabbro L, De Gomes MG, Boeira SP, Jesse CR (2013) Neuroprotective effects of swimming training in a mouse model of Parkinson's disease induced by 6-hydroxydopamine. Neuroscience 256C:61-71.

Grosser N, Abate A, Oberle S, Vreman HJ, Dennery PA, Becker JC, Pohle T, Seidman DS, Schroder H (2003) Heme oxygenase-1 induction may explain the antioxidant profile of aspirin. Biochem Biophys Res Commun 308:956-960.

Grosser N, Hemmerle A, Berndt G, Erdmann K, Hinkelmann U, Schurger S, Wijayanti N, Immenschuh S, Schroder H (2004) The antioxidant defense protein heme oxygenase 1 is a novel target for statins in endothelial cells. Free radical biology & medicine 37:2064-2071.

Guiastrennec B, Wollenberg L, Forrest A, Ait-Oudhia S (2013) AMGET, an R-Based Postprocessing Tool for ADAPT 5. CPT Pharmacometrics Syst Pharmacol 2:e61.

Guo B, Xu D, Duan H, Du J, Zhang Z, Lee SM, Wang Y (2013) Therapeutic effects of multifunctional tetramethylpyrazine nitrone on models of Parkinson's disease in vitro and in vivo. Biol Pharm Bull.

Halliwell B (2001) Role of free radicals in the neurodegenerative diseases: therapeutic implications for antioxidant treatment. Drugs Aging 18:685-716.

Harauz G, Ishiyama N, Hill CM, Bates IR, Libich DS, Fares C (2004) Myelin basic protein-diverse conformational states of an intrinsically unstructured protein and its roles in myelin assembly and multiple sclerosis. Micron 35:503-542.

Hashimoto T, Fujita T, Usuda N, Cook W, Qi C, Peters JM, Gonzalez FJ, Yeldandi AV, Rao MS, Reddy JK (1999) Peroxisomal and mitochondrial fatty acid beta-oxidation in mice nullizygous for both peroxisome proliferator-activated receptor alpha and peroxisomal fatty acyl-CoA oxidase. Genotype correlation with fatty liver phenotype. J Biol Chem 274:19228-19236.

Heard K, Green J (2012a) Acetylcysteine therapy for acetaminophen poisoning. Curr Pharm Biotechnol 13:1917-1923.

Heard K, Green J (2012b) Acetylcysteine therapy for acetaminophen poisoning. Curr Pharm Biotechnol 13:1917-1923.
Hegazy SK, Tolba OA, Mostafa TM, Eid MA, El-Afify DR (2013) Alpha-lipoic Acid improves subclinical left ventricular dysfunction in asymptomatic patients with type 1 diabetes. Rev Diabet Stud 10:58-67.
Hein S, Schonfeld P, Kahlert S, Reiser G (2008) Toxic effects of X-linked adrenoleukodystrophy-associated, very long chain fatty acids on glial cells and neurons from rat hippocampus in culture. Hum Mol Genet 17:1750-1761.
Hildebrandt TM, Grieshaber MK (2008) Three enzymatic activities catalyze the oxidation of sulfide to thiosulfate in mammalian and invertebrate mitochondria. FEBS J 275:3352-3361.
Hinkelmann U, Grosser N, Erdmann K, Schroder H, Immenschuh S (2010) Simvastatin-dependent up-regulation of heme oxygenase-1 via mRNA stabilization in human endothelial cells. Eur J Pharm Sci 41:118-124.
Holdiness MR (1991) Clinical pharmacokinetics of N-acetylcysteine. Clin Pharmacokinet 20:123-134.
Holmay MJ, Terpstra M, Coles LD, Mishra U, Ahlskog M, Oz G, Cloyd JC, Tuite PJ (2013) N-acetylcysteine boosts brain and blood glutathione in Gaucher and Parkinson diseases. Clin Neuropharmacol 36:103-106.
Holmay M., Zhou J., Coles L., Kartha RV, Radtke K., Mishra U., Basso L., Orchard PJ, Schroeder H., Cloyd JC.. N-acetylcysteine Therapy in Children with Cerebral Adrenoleukodystrophy undergoing Hematopoietic Stem Cell Transplantation. 3rd Conference on Clinical Research for Rare Diseases. (Rockville, MD, Oct. 2012)
Horowitz RS, Dart RC, Jarvie DR, Bearer CF, Gupta U (1997) Placental transfer of N-acetylcysteine following human maternal acetaminophen toxicity. J Toxicol Clin Toxicol 35:447-451.
Hu LF, Lu M, Hon Wong PT, Bian JS (2011) Hydrogen sulfide: neurophysiology and neuropathology. Antioxid Redox Signal 15:405-419.
Igarashi M, Schaumburg HH, Powers J, Kishmoto Y, Kolodny E, Suzuki K (1976) Fatty acid abnormality in adrenoleukodystrophy. J Neurochem 26:851-860.
Ishaq GM, Saidu Y, Bilbis LS, Muhammad SA, Jinjir N, Shehu BB (2013) Effects of alpha-tocopherol and ascorbic acid in the severity and management of traumatic brain injury in albino rats. J Neurosci Rural Pract 4:292-297.
James SJ, Cutler P, Melnyk S, Jernigan S, Janak L, Gaylor DW, Neubrander JA (2004) Metabolic biomarkers of increased oxidative stress and impaired methylation capacity in children with autism. Am J Clin Nutr 80:1611-1617.
Jana A, Pahan K (2007) Oxidative stress kills human primary oligodendrocytes via neutral sphingomyelinase: implications for multiple sclerosis. J Neuroimmune Pharmacol 2:184-193.
Jazwa A, Cuadrado A (2010) Targeting heme oxygenase-1 for neuroprotection and neuroinflammation in neurodegenerative diseases. Curr Drug Targets 11:1517-1531.

Jin H, Kanthasamy A, Ghosh A, Anantharam V, Kalyanaraman B, Kanthasamy AG (2013) Mitochondria-targeted antioxidants for treatment of Parkinson's disease: Preclinical and clinical outcomes. Biochimica et biophysica acta.
Johnson WM, Wilson-Delfosse AL, Mieyal JJ (2012) Dysregulation of glutathione homeostasis in neurodegenerative diseases. Nutrients 4:1399-1440.
Juckett MB, Balla J, Balla G, Jessurun J, Jacob HS, Vercellotti GM (1995) Ferritin protects endothelial cells from oxidized low density lipoprotein in vitro. Am J Pathol 147:782-789.
Jusko WJ, Ko HC, Ebling WF (1995) Convergence of direct and indirect pharmacodynamic response models. J Pharmacokinet Biopharm 23:5-8; discussion 9-10.
Kannan R, Chakrabarti R, Tang D, Kim KJ, Kaplowitz N (2000) GSH transport in human cerebrovascular endothelial cells and human astrocytes: evidence for luminal localization of Na+-dependent GSH transport in HCEC. Brain Res 852:374-382.
Kannan R, Kuhlenkamp JF, Jeandidier E, Trinh H, Ookhtens M, Kaplowitz N (1990) Evidence for carrier-mediated transport of glutathione across the blood-brain barrier in the rat. J Clin Invest 85:2009-2013.
Kartha RV, Zhou J, Hovde LB, Cheung BW, Schroder H (2012) Enhanced detection of hydrogen sulfide generated in cell culture using an agar trap method. Anal Biochem 423:102-108.
Kassmann CM, Lappe-Siefke C, Baes M, Brugger B, Mildner A, Werner HB, Natt O, Michaelis T, Prinz M, Frahm J, Nave KA (2007) Axonal loss and neuroinflammation caused by peroxisome-deficient oligodendrocytes. Nat Genet 39:969-976.
Kemp S, Berger J, Aubourg P (2012) X-linked adrenoleukodystrophy: clinical, metabolic, genetic and pathophysiological aspects. Biochim Biophys Acta 1822:1465-1474.
Kemp S, Pujol A, Waterham HR, van Geel BM, Boehm CD, Raymond GV, Cutting GR, Wanders RJ, Moser HW (2001) ABCD1 mutations and the X-linked adrenoleukodystrophy mutation database: role in diagnosis and clinical correlations. Hum Mutat 18:499-515.
Kim KJ, Kim KS, Kim NR, Chin HS (2012) Effects of simvastatin on the expression of heme oxygenase-1 in human RPE cells. Invest Ophthalmol Vis Sci 53:6456-6464.
Kim N, Hwangbo C, Lee S, Lee JH (2013) Eupatolide Inhibits PDGF-induced Proliferation and Migration of Aortic Smooth Muscle Cells Through ROS-dependent Heme Oxygenase-1 Induction. Phytother Res 27:1700-1707.
Kirkinezos IG, Moraes CT (2001) Reactive oxygen species and mitochondrial diseases. Semin Cell Dev Biol 12:449-457.
Knapp PE, Adjan VV, Hauser KF (2009) Cell-specific loss of kappa-opioid receptors in oligodendrocytes of the dysmyelinating jimpy mouse. Neuroscience letters 451:114-118.
Kociancic T, Reed MD (2003) Acetaminophen intoxication and length of treatment: how long is long enough? Pharmacotherapy 23:1052-1059.

Kweon MH, Jung MJ, Sung HC (2004) Cytoprotective effects of heme oxygenase-1 induction by 3-O-caffeoyl-1-methylquinic acid. Free radical biology & medicine 36:40-52.
Lasierra-Cirujeda J, Coronel P, Aza M, Gimeno M (2013) Beta-amyloidolysis and glutathione in Alzheimer's disease. J Blood Med 4:31-38.
Lave T, Parrott N, Grimm HP, Fleury A, Reddy M (2007) Challenges and opportunities with modelling and simulation in drug discovery and drug development. Xenobiotica 37:1295-1310.
Le WD, Xie WJ, Appel SH (1999) Protective role of heme oxygenase-1 in oxidative stress-induced neuronal injury. J Neurosci Res 56:652-658.
Lee YJ, Im JH, Lee DM, Park JS, Won SY, Cho MK, Nam HS, Lee SH (2012) Synergistic inhibition of mesothelioma cell growth by the combination of clofarabine and resveratrol involves Nrf2 downregulation. BMB Rep 45:647-652.
Li M, Liu Y, Shi H, Zhang Y, Wang G, Xu J, Lu J, Zhang D, Xie X, Han D, Wu Y, Li S (2012) Statins inhibit pulmonary artery smooth muscle cell proliferation by upregulation of HO-1 and p21WAF1. Naunyn Schmiedebergs Arch Pharmacol 385:961-968.
Lin MT, Beal MF (2006) Mitochondrial dysfunction and oxidative stress in neurodegenerative diseases. Nature 443:787-795.
Lin YC, Lai YS, Chou TC (2013) The protective effect of alpha-lipoic Acid in lipopolysaccharide-induced acute lung injury is mediated by heme oxygenase-1. Evid Based Complement Alternat Med 2013:590363.
Lluis JM, Morales A, Blasco C, Colell A, Mari M, Garcia-Ruiz C, Fernandez-Checa JC (2005) Critical role of mitochondrial glutathione in the survival of hepatocytes during hypoxia. J Biol Chem 280:3224-3232.
Loes DJ, Fatemi A, Melhem ER, Gupte N, Bezman L, Moser HW, Raymond GV (2003) Analysis of MRI patterns aids prediction of progression in X-linked adrenoleukodystrophy. Neurology 61:369-374.
Loes DJ, Hite S, Moser H, Stillman AE, Shapiro E, Lockman L, Latchaw RE, Krivit W (1994) Adrenoleukodystrophy: a scoring method for brain MR observations. AJNR Am J Neuroradiol 15:1761-1766.
Lopez-Erauskin J, Fourcade S, Galino J, Ruiz M, Schluter A, Naudi A, Jove M, Portero-Otin M, Pamplona R, Ferrer I, Pujol A (2011a) Antioxidants halt axonal degeneration in a mouse model of X-adrenoleukodystrophy. Ann Neurol 70:84-92.
Lopez-Erauskin J, Fourcade S, Galino J, Ruiz M, Schluter A, Naudi A, Jove M, Portero-Otin M, Pamplona R, Ferrer I, Pujol A (2011b) Antioxidants halt axonal degeneration in a mouse model of X-adrenoleukodystrophy. Annals of neurology 70:84-92.
Lopez-Erauskin J, Galino J, Ruiz M, Cuezva JM, Fabregat I, Cacabelos D, Boada J, Martinez J, Ferrer I, Pamplona R, Villarroya F, Portero-Otin M, Fourcade S, Pujol A (2013) Impaired mitochondrial oxidative phosphorylation in the peroxisomal disease X-linked adrenoleukodystrophy. Hum Mol Genet 22:3296-3305.

Lovell MA, Xie C, Markesbery WR (1998) Decreased glutathione transferase activity in brain and ventricular fluid in Alzheimer's disease. Neurology 51:1562-1566.
Lynch RM, Robertson R (2004) Anaphylactoid reactions to intravenous N-acetylcysteine: a prospective case controlled study. Accid Emerg Nurs 12:10-15.
Mager DE, Wyska E, Jusko WJ (2003) Diversity of mechanism-based pharmacodynamic models. Drug Metab Dispos 31:510-518.
Mager H, Goller G (1998) Resampling methods in sparse sampling situations in preclinical pharmacokinetic studies. J Pharm Sci 87:372-378.
Mahmoud KM, Ammar AS (2011) Effect of N-acetylcysteine on cardiac injury and oxidative stress after abdominal aortic aneurysm repair: a randomized controlled trial. Acta Anaesthesiol Scand 55:1015-1021.
Majid AS, Yin ZQ, Ji D (2013) Sulphur antioxidants inhibit oxidative stress induced retinal ganglion cell death by scavenging reactive oxygen species but influence nuclear factor (erythroid-derived 2)-like 2 signalling pathway differently. Biol Pharm Bull 36:1095-1110.
Maltsev AV, Santockyte R, Bystryak S, Galzitskaya OV (2013) Activation of Neuronal Defense Mechanisms in Response to Pathogenic Factors Triggering Induction of Amyloidosis in Alzheimer's Disease. J Alzheimers Dis.
Mao X, Wang T, Liu Y, Irwin MG, Ou JS, Liao XL, Gao X, Xu Y, Ng KF, Vanhoutte PM, Xia Z (2013) N-acetylcysteine and allopurinol confer synergy in attenuating myocardial ischemia injury via restoring HIF-1alpha/HO-1 signaling in diabetic rats. PloS one 8:e68949.
Mardikian PN, LaRowe SD, Hedden S, Kalivas PW, Malcolm RJ (2007) An open-label trial of N-acetylcysteine for the treatment of cocaine dependence: a pilot study. Prog Neuropsychopharmacol Biol Psychiatry 31:389-394.
Mari M, Morales A, Colell A, Garcia-Ruiz C, Fernandez-Checa JC (2009) Mitochondrial glutathione, a key survival antioxidant. Antioxid Redox Signal 11:2685-2700.
Marian AJ, Senthil V, Chen SN, Lombardi R (2006) Antifibrotic effects of antioxidant N-acetylcysteine in a mouse model of human hypertrophic cardiomyopathy mutation. J Am Coll Cardiol 47:827-834.
Matsuzawa D, Obata T, Shirayama Y, Nonaka H, Kanazawa Y, Yoshitome E, Takanashi J, Matsuda T, Shimizu E, Ikehira H, Iyo M, Hashimoto K (2008) Negative correlation between brain glutathione level and negative symptoms in schizophrenia: a 3T 1H-MRS study. PLoS One 3:e1944.
McGuinness MC, Lu JF, Zhang HP, Dong GX, Heinzer AK, Watkins PA, Powers J, Smith KD (2003) Role of ALDP (ABCD1) and mitochondria in X-linked adrenoleukodystrophy. Mol Cell Biol 23:744-753.
Meek PD, McKeithan K, Schumock GT (1998) Economic considerations in Alzheimer's disease. Pharmacotherapy 18:68-73; discussion 79-82.
Meibohm B, Derendorf H (1997) Basic concepts of pharmacokinetic/pharmacodynamic (PK/PD) modelling. Int J Clin Pharmacol Ther 35:401-413.
Miller NJ, Rice-Evans C, Davies MJ, Gopinathan V, Milner A (1993) A novel method for measuring antioxidant capacity and its application to monitoring the antioxidant status in premature neonates. Clin Sci (Lond) 84:407-412.

Miller WP, Rothman SM, Nascene D, Kivisto T, DeFor TE, Ziegler RS, Eisengart J, Leiser K, Raymond G, Lund TC, Tolar J, Orchard PJ (2011) Outcomes after allogeneic hematopoietic cell transplantation for childhood cerebral adrenoleukodystrophy: the largest single-institution cohort report. Blood 118:1971-1978.

Mishra V, Srivastava N (2013) Organophosphate pesticides-induced changes in the redox status of rat tissues and protective effects of antioxidant vitamins. Environ Toxicol.

Moser HW (2006) Therapy of X-linked adrenoleukodystrophy. NeuroRx 3:246-253.

Moser HW, Raymond GV, Dubey P (2005a) Adrenoleukodystrophy: new approaches to a neurodegenerative disease. JAMA 294:3131-3134.

Moser HW, Raymond GV, Lu SE, Muenz LR, Moser AB, Xu J, Jones RO, Loes DJ, Melhem ER, Dubey P, Bezman L, Brereton NH, Odone A (2005b) Follow-up of 89 asymptomatic patients with adrenoleukodystrophy treated with Lorenzo's oil. Arch Neurol 62:1073-1080.

Mould DR, Upton RN (2013) Basic concepts in population modeling, simulation, and model-based drug development-part 2: introduction to pharmacokinetic modeling methods. CPT Pharmacometrics Syst Pharmacol 2:e38.

Nakagawa Y, Suzuki T, Nakajima K, Inomata A, Ogata A, Nakae D (2013) Effects of N-acetyl-L-cysteine on target sites of hydroxylated fullerene-induced cytotoxicity in isolated rat hepatocytes. Arch Toxicol.

Nedelman JR, Jia X (1998) An extension of Satterthwaite's approximation applied to pharmacokinetics. J Biopharm Stat 8:317-328.

Nemeth I, Boda D (1994) Blood glutathione redox ratio as a parameter of oxidative stress in premature infants with IRDS. Free Radic Biol Med 16:347-353.

Neuwelt EA, Pagel MA, Hasler BP, Deloughery TG, Muldoon LL (2001) Therapeutic efficacy of aortic administration of N-acetylcysteine as a chemoprotectant against bone marrow toxicity after intracarotid administration of alkylators, with or without glutathione depletion in a rat model. Cancer Res 61:7868-7874.

Nguyen D, Samson SL, Reddy VT, Gonzalez EV, Sekhar RV (2013) Impaired mitochondrial fatty acid oxidation and insulin resistance in aging: novel protective role of glutathione. Aging Cell 12:415-425.

Oezen I, Rossmanith W, Forss-Petter S, Kemp S, Voigtlander T, Moser-Thier K, Wanders RJ, Bittner RE, Berger J (2005) Accumulation of very long-chain fatty acids does not affect mitochondrial function in adrenoleukodystrophy protein deficiency. Hum Mol Genet 14:1127-1137.

Ofman R, Dijkstra IM, van Roermund CW, Burger N, Turkenburg M, van Cruchten A, van Engen CE, Wanders RJ, Kemp S (2010) The role of ELOVL1 in very long-chain fatty acid homeostasis and X-linked adrenoleukodystrophy. EMBO Mol Med 2:90-97.

Ogborne RM, Rushworth SA, O'Connell MA (2005) Alpha-lipoic acid-induced heme oxygenase-1 expression is mediated by nuclear factor erythroid 2-related factor 2 and p38 mitogen-activated protein kinase in human monocytic cells. Arterioscler Thromb Vasc Biol 25:2100-2105.

Olsson B, Johansson M, Gabrielsson J, Bolme P (1988) Pharmacokinetics and bioavailability of reduced and oxidized N-acetylcysteine. Eur J Clin Pharmacol 34:77-82.
Or R, Matzner Y, Konijn AM (1987) Serum ferritin in patients undergoing bone marrow transplantation. Cancer 60:1127-1131.
Orchard PJ, Lund T, Miller W, Rothman SM, Raymond G, Nascene D, Basso L, Cloyd J, Tolar J (2011) Chitotriosidase as a biomarker of cerebral adrenoleukodystrophy. J Neuroinflammation 8:144.
Otterbein LE, Bach FH, Alam J, Soares M, Tao Lu H, Wysk M, Davis RJ, Flavell RA, Choi AM (2000) Carbon monoxide has anti-inflammatory effects involving the mitogen-activated protein kinase pathway. Nat Med 6:422-428.
Panahian N, Yoshiura M, Maines MD (1999) Overexpression of heme oxygenase-1 is neuroprotective in a model of permanent middle cerebral artery occlusion in transgenic mice. Journal of neurochemistry 72:1187-1203.
Pardridge WM, Boado RJ, Farrell CR (1990) Brain-type glucose transporter (GLUT-1) is selectively localized to the blood-brain barrier. Studies with quantitative western blotting and in situ hybridization. J Biol Chem 265:18035-18040.
Park SW, Kim SH, Park KH, Kim SD, Kim JY, Baek SY, Chung BS, Kang CD (2004) Preventive effect of antioxidants in MPTP-induced mouse model of Parkinson's disease. Neurosci Lett 363:243-246.
Parkinson-study-group (1993) Effects of tocopherol and deprenyl on the progression of disability in early Parkinson's disease. N Engl J Med 328:176-183.
Pendyala L, Creaven PJ (1995) Pharmacokinetic and pharmacodynamic studies of N-acetylcysteine, a potential chemopreventive agent during a phase I trial. Cancer Epidemiol Biomarkers Prev 4:245-251.
Peng J, Oo ML, Andersen JK (2010) Synergistic effects of environmental risk factors and gene mutations in Parkinson's disease accelerate age-related neurodegeneration. J Neurochem 115:1363-1373.
Peters C, Charnas LR, Tan Y, Ziegler RS, Shapiro EG, DeFor T, Grewal SS, Orchard PJ, Abel SL, Goldman AI, Ramsay NK, Dusenbery KE, Loes DJ, Lockman LA, Kato S, Aubourg PR, Moser HW, Krivit W (2004) Cerebral X-linked adrenoleukodystrophy: the international hematopoietic cell transplantation experience from 1982 to 1999. Blood 104:881-888.
Petrillo S, Piemonte F, Pastore A, Tozzi G, Aiello C, Pujol A, Cappa M, Bertini E (2013a) Glutathione imbalance in patients with X-linked adrenoleukodystrophy. Molecular genetics and metabolism 109:366-370.
Petrillo S, Piemonte F, Pastore A, Tozzi G, Aiello C, Pujol A, Cappa M, Bertini E (2013b) Glutathione imbalance in patients with X-linked adrenoleukodystrophy. Mol Genet Metab 109:366-370.
Powers JM, Pei Z, Heinzer AK, Deering R, Moser AB, Moser HW, Watkins PA, Smith KD (2005) Adreno-leukodystrophy: oxidative stress of mice and men. J Neuropathol Exp Neurol 64:1067-1079.
PPMI (2011) The Parkinson Progression Marker Initiative (PPMI). Prog Neurobiol 95:629-635.

Radtke KK, Coles LD, Mishra U, Orchard PJ, Holmay M, Cloyd JC (2012) Interaction of N-acetylcysteine and cysteine in human plasma. J Pharm Sci 101:4653-4659.
Raftos JE, Whillier S, Chapman BE, Kuchel PW (2007) Kinetics of uptake and deacetylation of N-acetylcysteine by human erythrocytes. Int J Biochem Cell Biol 39:1698-1706.
Reitz C, Mayeux R (2010) Use of genetic variation as biomarkers for mild cognitive impairment and progression of mild cognitive impairment to dementia. J Alzheimers Dis 19:229-251.
Rensing H, Bauer I, Peters I, Wein T, Silomon M, Jaeschke H, Bauer M (1999) Role of reactive oxygen species for hepatocellular injury and heme oxygenase-1 gene expression after hemorrhage and resuscitation. Shock 12:300-308.
Riederer P, Sofic E, Rausch WD, Schmidt B, Reynolds GP, Jellinger K, Youdim MB (1989) Transition metals, ferritin, glutathione, and ascorbic acid in parkinsonian brains. J Neurochem 52:515-520.
Robinson RA, Joshi G, Huang Q, Sultana R, Baker AS, Cai J, Pierce W, St Clair DK, Markesbery WR, Butterfield DA (2011) Proteomic analysis of brain proteins in APP/PS-1 human double mutant knock-in mice with increasing amyloid beta-peptide deposition: insights into the effects of in vivo treatment with N-acetylcysteine as a potential therapeutic intervention in mild cognitive impairment and Alzheimer's disease. Proteomics 11:4243-4256.
Roversi FM, Galdieri LC, Grego BH, Souza FG, Micheletti C, Martins AM, D'Almeida V (2006) Blood oxidative stress markers in Gaucher disease patients. Clin Chim Acta 364:316-320.
Rushworth GF, Megson IL (2013a) Existing and potential therapeutic uses for N-acetylcysteine: The need for conversion to intracellular glutathione for antioxidant benefits. Pharmacol Ther.
Rushworth GF, Megson IL (2013b) Existing and potential therapeutic uses for N-acetylcysteine: The need for conversion to intracellular glutathione for antioxidant benefits. Pharmacol Ther.
Ryter SW, Choi AM (2005) Heme oxygenase-1: redox regulation of a stress protein in lung and cell culture models. Antioxidants & redox signaling 7:80-91.
Sadowska AM, Verbraecken J, Darquennes K, De Backer WA (2006) Role of N-acetylcysteine in the management of COPD. Int J Chron Obstruct Pulmon Dis 1:425-434.
Sandilands EA, Bateman DN (2009) Adverse reactions associated with acetylcysteine. Clin Toxicol (Phila) 47:81-88.
Sano M, Ernesto C, Thomas RG, Klauber MR, Schafer K, Grundman M, Woodbury P, Growdon J, Cotman CW, Pfeiffer E, Schneider LS, Thal LJ (1997) A controlled trial of selegiline, alpha-tocopherol, or both as treatment for Alzheimer's disease. The Alzheimer's Disease Cooperative Study. N Engl J Med 336:1216-1222.
Satpute RM, Hariharakrishnan J, Bhattacharya R (2010) Effect of alpha-ketoglutarate and N-acetyl cysteine on cyanide-induced oxidative stress mediated cell death in PC12 cells. Toxicol Ind Health 26:297-308.

Scandalios JG (2005) Oxidative stress: molecular perception and transduction of signals triggering antioxidant gene defenses. Braz J Med Biol Res 38:995-1014.
Schallner N, Romao CC, Biermann J, Lagreze WA, Otterbein LE, Buerkle H, Loop T, Goebel U (2013) Carbon monoxide abrogates ischemic insult to neuronal cells via the soluble guanylate cyclase-cGMP pathway. PLoS One 8:e60672.
Schipper HM (2004) Heme oxygenase expression in human central nervous system disorders. Free Radic Biol Med 37:1995-2011.
Schipper HM, Gupta A, Szarek WA (2009a) Suppression of glial HO-1 activity as a potential neurotherapeutic intervention in AD. Curr Alzheimer Res 6:424-430.
Schipper HM, Song W, Zukor H, Hascalovici JR, Zeligman D (2009b) Heme oxygenase-1 and neurodegeneration: expanding frontiers of engagement. J Neurochem 110:469-485.
Schrader M, Yoon Y (2007) Mitochondria and peroxisomes: are the 'big brother' and the 'little sister' closer than assumed? Bioessays 29:1105-1114.
Schroder H, Warren S, Bargetzi MJ, Torti SV, Torti FM (1993) N-acetyl-L-cysteine protects endothelial cells but not L929 tumor cells from tumor necrosis factor-alpha-mediated cytotoxicity. Naunyn Schmiedebergs Arch Pharmacol 347:664-666.
Sechi G, Deledda MG, Bua G, Satta WM, Deiana GA, Pes GM, Rosati G (1996) Reduced intravenous glutathione in the treatment of early Parkinson's disease. Prog Neuropsychopharmacol Biol Psychiatry 20:1159-1170.
Shukla V, Mishra SK, Pant HC (2011a) Oxidative stress in neurodegeneration. Adv Pharmacol Sci 2011:572634.
Shukla V, Mishra SK, Pant HC (2011b) Oxidative stress in neurodegeneration. Adv Pharmacol Sci 2011:572634.
Shults CW, Beal MF, Fontaine D, Nakano K, Haas RH (1998) Absorption, tolerability, and effects on mitochondrial activity of oral coenzyme Q10 in parkinsonian patients. Neurology 50:793-795.
Sian J, Dexter DT, Lees AJ, Daniel S, Agid Y, Javoy-Agid F, Jenner P, Marsden CD (1994) Alterations in glutathione levels in Parkinson's disease and other neurodegenerative disorders affecting basal ganglia. Ann Neurol 36:348-355.
Singh I, Pujol A (2010) Pathomechanisms underlying X-adrenoleukodystrophy: a three-hit hypothesis. Brain Pathol 20:838-844.
Singh K, Malviya A, Bhori M, Marar T (2012) An in vitro study of the ameliorative role of alpha-tocopherol on methotrexate-induced oxidative stress in rat heart mitochondria. J Basic Clin Physiol Pharmacol 23:163-168.
Skovronsky DM, Lee VM, Trojanowski JQ (2006) Neurodegenerative diseases: new concepts of pathogenesis and their therapeutic implications. Annu Rev Pathol 1:151-170.
Smith KJ, Kapoor R, Felts PA (1999) Demyelination: the role of reactive oxygen and nitrogen species. Brain pathology 9:69-92.
Smith RA, Murphy MP (2011) Mitochondria-targeted antioxidants as therapies. Discov Med 11:106-114.

Son Y, Lee JH, Chung HT, Pae HO (2013) Therapeutic Roles of Heme Oxygenase-1 in Metabolic Diseases: Curcumin and Resveratrol Analogues as Possible Inducers of Heme Oxygenase-1. Oxid Med Cell Longev 2013:639541.

Sparatore A, Perrino E, Tazzari V, Giustarini D, Rossi R, Rossoni G, Erdmann K, Schroder H, Del Soldato P (2009) Pharmacological profile of a novel H(2)S-releasing aspirin. Free radical biology & medicine 46:586-592.

Steinberg SJ, Moser AB, Raymond GV (1993) X-Linked Adrenoleukodystrophy.

Stocchi F, Olanow CW (2013) Obstacles to the development of a neuroprotective therapy for Parkinson's disease. Mov Disord 28:3-7.

Suzuki K, Mori M, Kugawa F, Ishihara H (2002) Whole-body X-irradiation induces acute and transient expression of heme oxygenase-1 in rat liver. J Radiat Res 43:205-210.

Shen, L. (2008). preclinical pharmacokinetics and bioavailability studies of S-carboxymethylcysteine, Nacetylcysteine and (-)-carbodine (Unpublished doctoral dissertation). University of Georgia, Athens, Georgia.

Sultana, R., Cenini, G. and Butterfield, D. A. (2013) Biomarkers of Oxidative Stress in Neurodegenerative Diseases, in Molecular Basis of Oxidative Stress: Chemistry, Mechanisms, and Disease Pathogenesis (ed F. A. Villamena), John Wiley & Sons, Inc., Hoboken, NJ, USA. doi: 10.1002/9781118355886.ch14

Teng D, Lu Y, Gao R, Xin Y, Cao G, Li X, Wang L, Wang J, Li Y (2006) Conversion from cyclosporine to mycophenolate mofetil improves expression of A20 in the rat kidney allografts undergoing chronic rejection. Transplant Proc 38:2164-2167.

Tenhunen R, Marver HS, Schmid R (1968) The enzymatic conversion of heme to bilirubin by microsomal heme oxygenase. Proc Natl Acad Sci U S A 61:748-755.

Tolar J, Orchard PJ, Bjoraker KJ, Ziegler RS, Shapiro EG, Charnas L (2007) N-acetyl-L-cysteine improves outcome of advanced cerebral adrenoleukodystrophy. Bone Marrow Transplant 39:211-215.

U.S. Food and Drug Administration (2004), Center for Drug Evaluation and Research. Acetadote NDA 021539 package insert. Retrieved Dec.27th, 2013, from http://www.accessdata.fda.gov/drugsatfda_docs/label/2004/21539_N-acetylcysteine_lbl.pdf

Valianpour F, Selhorst JJ, van Lint LE, van Gennip AH, Wanders RJ, Kemp S (2003) Analysis of very long-chain fatty acids using electrospray ionization mass spectrometry. Mol Genet Metab 79:189-196.

Van Den Eeden SK, Tanner CM, Bernstein AL, Fross RD, Leimpeter A, Bloch DA, Nelson LM (2003) Incidence of Parkinson's disease: variation by age, gender, and race/ethnicity. Am J Epidemiol 157:1015-1022.

van Zandwijk N (1995a) N-acetylcysteine (NAC) and glutathione (GSH): antioxidant and chemopreventive properties, with special reference to lung cancer. J Cell Biochem Suppl 22:24-32.

van Zandwijk N (1995b) N-acetylcysteine (NAC) and glutathione (GSH): antioxidant and chemopreventive properties, with special reference to lung cancer. J Cell Biochem Suppl 22:24-32.

Vargas CR, Wajner M, Sirtori LR, Goulart L, Chiochetta M, Coelho D, Latini A, Llesuy S, Bello-Klein A, Giugliani R, Deon M, Mello CF (2004) Evidence that oxidative stress is increased in patients with X-linked adrenoleukodystrophy. Biochim Biophys Acta 1688:26-32.

Ventura P, Panini R, Pasini MC, Scarpetta G, Salvioli G (1999) N -Acetyl-cysteine reduces homocysteine plasma levels after single intravenous administration by increasing thiols urinary excretion. Pharmacol Res 40:345-350.

Wang C, Youle RJ (2009) The role of mitochondria in apoptosis*. Annu Rev Genet 43:95-118.

Waring WS, Stephen AF, Robinson OD, Dow MA, Pettie JM (2008) Lower incidence of anaphylactoid reactions to N-acetylcysteine in patients with high acetaminophen concentrations after overdose. Clin Toxicol (Phila) 46:496-500.

Wengenack TM, Curran GL, Poduslo JF (1997) Postischemic, systemic administration of polyamine-modified superoxide dismutase reduces hippocampal CA1 neurodegeneration in rat global cerebral ischemia. Brain Res 754:46-54.

Whillier S, Raftos JE, Chapman B, Kuchel PW (2009) Role of N-acetylcysteine and cystine in glutathione synthesis in human erythrocytes. Redox Rep 14:115-124.

Whyte IM, Francis B, Dawson AH (2007) Safety and efficacy of intravenous N-acetylcysteine for acetaminophen overdose: analysis of the Hunter Area Toxicology Service (HATS) database. Curr Med Res Opin 23:2359-2368.

Wu G, Fang YZ, Yang S, Lupton JR, Turner ND (2004a) Glutathione metabolism and its implications for health. J Nutr 134:489-492.

Wu G, Fang YZ, Yang S, Lupton JR, Turner ND (2004b) Glutathione metabolism and its implications for health. J Nutr 134:489-492.

Xu J, Lei S, Liu Y, Gao X, Irwin MG, Xia ZY, Hei Z, Gan X, Wang T, Xia Z (2013) Antioxidant N-acetylcysteine attenuates the reduction of Brg1 protein expression in the myocardium of type 1 diabetic rats. J Diabetes Res 2013:716219.

Zafarullah M, Li WQ, Sylvester J, Ahmad M (2003) Molecular mechanisms of N-acetylcysteine actions. Cell Mol Life Sci 60:6-20.

Zager RA, Johnson AC, Becker K (2012) Plasma and urinary heme oxygenase-1 in AKI. J Am Soc Nephrol 23:1048-1057.

Zaman GJ, Lankelma J, van Tellingen O, Beijnen J, Dekker H, Paulusma C, Oude Elferink RP, Baas F, Borst P (1995) Role of glutathione in the export of compounds from cells by the multidrug-resistance-associated protein. Proceedings of the National Academy of Sciences of the United States of America 92:7690-7694.

Zhang F, Yao SY, Whetsell WO, Jr., Sriram S (2013) Astrogliopathy and oligodendrogliopathy are early events in CNS demyelination. Glia 61:1261-1273.

Zhou J*, Kartha RV*, Basso L, Orchard PJ, Schröder H, Cloyd JC. Heme oxygenase-1 (HO-1) is a possible mediator of cytoprotective effects by N-acetyl cysteine (NAC) in CCALD patients. Clin Pharmacol Ther, 2012; 91 (suppl 1) : S17 (* equal contribution)

Zhou W, Freed CR (2005a) DJ-1 up-regulates glutathione synthesis during oxidative stress and inhibits A53T alpha-synuclein toxicity. J Biol Chem 280:43150-43158.

Zhou W, Freed CR (2005b) DJ-1 up-regulates glutathione synthesis during oxidative stress and inhibits A53T alpha-synuclein toxicity. The Journal of biological chemistry 280:43150-43158.
Zhu X, Lee HG, Perry G, Smith MA (2007) Alzheimer disease, the two-hit hypothesis: an update. Biochim Biophys Acta 1772:494-502.
Zinellu A, Sotgia S, Scanu B, Usai MF, Fois AG, Spada V, Deledda A, Deiana L, Pirina P, Carru C (2009) Simultaneous detection of N-acetyl-L-cysteine and physiological low molecular mass thiols in plasma by capillary electrophoresis. Amino Acids 37:395-400.
Zitka O, Skalickova S, Gumulec J, Masarik M, Adam V, Hubalek J, Trnkova L, Kruseova J, Eckschlager T, Kizek R (2012) Redox status expressed as GSH:GSSG ratio as a marker for oxidative stress in paediatric tumour patients. Oncol Lett 4:1247-1253.